Leveraging homologous recombination to generate clone-less *in vivo* assembly and integration of DNA to genetically modify *Saccharomyces cerevisiae* using CRISPR-Cas9

Yara Khalil

Thesis submitted to the University of Ottawa in partial fulfillment of the requirements for the Master of Science degree in Cellular and Molecular Medicine

Department of Cellular and Molecular Medicine

Faculty of Medicine

University of Ottawa

Table of Contents

List of Tables

List of Figures

List of Abbreviations

Assembly junction (AJ)

Autonomous replication sequences (ARS)

Cargo linker (CL)

Chromosomal homology region (cHR)

Clustered Regularly Interspaced Short Palindromic Repeats (CRISPR)

Colony-forming Units (CFU)

CRISPR-associated protein (Cas)

Deoxyribonucleic acid (DNA)

Deoxynucleotide triphosphate (dNTP)

Double-stranded DNA (dsDNA)

Double-stranded DNA breaks (DSBs)

EasyClone (EC)

EasyClone Expansion Pack (EC EP)

Gene of interest (GOI)

Green fluorescent protein (GFP)

Guide RNA (gRNA)

Homologous recombination (HR)

Homology-directed repair (HDR)

In vivo Imaging System (IVIS)

Insertions or deletions (indels)

Luria-Bertani (LB)

Melting temperature (Tm)

Non-homologous end joining (NHEJ)

Origin of replication (ori)

Polymerase Chain Reaction (PCR)

Protospacer Adjacent Motif (PAM)

Terminator Insulator Spacer (TINS)

Terminator Insulator spacer Adaptor (TINA)

Transcription Activator-Like Effector Nucleases (TALENs)

Versatile Genetic Assembly System (VEGAS)

Yeast Artificial Chromosome (YAC)

Yeast Centromere plasmid (YCp)

Yeast Episomal plasmid (YEp)

Yeast extract Peptone Dextrose (YPD)

Yeast Integrating plasmid (YIp)

Yeast Replicating plasmid (YRp)

Yeast two-hybrid (Y2H)

Zinc Finger Nucleases (ZFNs)

Abstract

Saccharomyces cerevisiae's well-characterized genome and efficient homologous recombination capabilities make it a powerful model organism for genetic engineering, enabling the development of precise genome modification techniques. However, simultaneous multi-locus gene integration (multiplexing) remains challenging, often requiring extensive and tedious *in vitro* cloning. This thesis hypothesizes that a novel yeast integrating plasmid, envisioned as an EasyClone Expansion Pack, can be designed to enable two-step multiplexing leveraging homologous recombination and bypassing *in vitro* cloning. To accomplish this, we developed a clone-less *in vivo* DNA assembly method, demonstrating a 20-fold increase in transformation efficiency with CRISPR-Cas9-mediated DNA breaks. A cost-effective multiplexing workflow was established using 200 bp chromosomal homology regions and 30 bp overhangs on transgenes. The foundational design of the expansion pack plasmid, including one-step linearizability and unique homology regions, was validated. This research offers a cost-effective and streamlined approach for strain engineering for use in diverse bioproduction and biomanufacturing applications.

Acknowledgments

I wish to extend my sincere gratitude to my co-supervisors, Dr. Mads Kaern and Dr. Will Costain, for providing invaluable opportunities to learn, grow, and develop my scientific interests and understanding throughout my master's journey. Their guidance and support have been instrumental in shaping my thesis research.

I also thank my Thesis Advisory Committee, Dr. Michael Downey and Dr. Scott McComb, for their guidance and constructive feedback, which significantly contributed to the progression of my research. In addition, I am grateful to the Ottawa Institute of Systems Biology for granting me an OISB-NRC Graduate Scholarship.

I would like to acknowledge and express my appreciation to the members of the Kaern lab, particularly Léa Montminy-Bergeron for her assistance and company in the lab, and Roy Hwang for his mentorship and guidance with DNA construct and experimental designs, troubleshooting, writing, and data analysis. I would also like to thank the Downey lab members for their help and the resources they generously shared. Additionally, I would like to thank NRC personnel, Dongling Zhang and Dorothy Fatehi, for recommending the use of an *in vivo* imaging system for yeast whole-plate fluorescent imaging.

Lastly, I want to thank my family and friends for their continuous support and encouragement throughout this process.

Chapter 1: Introduction

1.1 Background and Context

Genetic engineering is revolutionizing research by driving breakthroughs in understanding cellular processes, developing targeted therapies, advancing personalized medicine, and uncovering disease mechanisms and metabolic pathways [1]. These significant advancements in cellular and molecular medicine have been made possible through the development of genome editing tools that enable precise and targeted genetic modifications to engineer organisms [2]. The process of homologous recombination (HR) is at the basis of these genome editing tools [3].

When a double-stranded DNA break (DSB) occurs in a cell, typically due to exposure to DNA-damaging agents or errors during replication, DNA repair pathways, primarily HR and non-homologous end joining (NHEJ), are activated to maintain genomic integrity [4]. HR is a naturally occurring, evolutionarily conserved process that enables the error-free repair of DSBs and facilitates the precise integration of foreign DNA through exchanging matching nucleotide sequences between homologous regions [5], [6]. In eukaryotic cells, HR is predominantly active during the S and G2 phases of the cell cycle [7]. HR begins with the MRN complex binding to the ends of the DSB followed by DNA end resection to produce 3' single-stranded DNA overhangs that are then bound by the recombinase RAD51, which facilitates strand invasion into a homologous DNA template for template-dependent DNA synthesis [8]. In contrast, the alternative pathway of non-homologous end joining (NHEJ) is often error-prone, frequently introducing insertions or deletions (indels) at DSBs, which can lead to gene inactivation [9]. NHEJ repairs DSBs without a homologous template and, in eukaryotic cells, is active throughout the cell cycle but is prevalent in the G1 phase [7]. This process is characterized by the Ku

complex (Ku70/Ku80 heterodimer) binding to the DSB ends, followed by the recruitment of the core NHEJ machinery, including DNA-PKcs and DNA Ligase IV, to process and ligate the DNA ends [10].

By building on the foundational knowledge gained by observing and characterizing HR in the simple model systems of bacteria and yeast, early-stage genetic engineering tools harboring HR were developed [11]. Recombination-mediated genetic engineering (recombineering) [12] in *Escherichia coli* uses phage-derived systems, such as the Lambda Red system, for precise DSBs free DNA modifications via HR [13]. However, the reliance on the host's HR machinery to assemble DNA with short regions of homology limits recombineering efficiency and increases off-target effects, while its application beyond *E. coli* is further constrained by the need for specific phage proteins and variable HR efficiency across organisms [13], [14].

To overcome the limitations of *in vivo* HR-dependent approaches and enhance genome editing capabilities, subsequent tools focused on inducing targeted DSBs [2]. Notably, Zinc Finger Nucleases (ZFNs) are engineered proteins that function as artificial restriction enzymes, creating a targeted DSB in various organisms, including mammalian cells, via customizable zinc finger DNA-binding domains (targeting 9-18 bp) fused to the FokI nuclease, which requires dimerization for cleavage [15]. Following ZFNs, researchers developed Transcription Activator-Like Effector Nucleases (TALENs) as engineered nucleases that create DSBs by using transcription activator-like effector domains for sequence-specific DNA binding and a FokI nuclease requiring dimerization for cleavage [16]. The DSBs induced by ZFNs and TALENs are primarily repaired by the cell's endogenous pathways of NHEJ, often resulting in indels, or by homology-directed repair (HDR) if a homologous DNA template is provided [17]. The key limitations of using ZFNs and TALENs as robust genome editing tools are the complex and time-

consuming protein engineering required to target new DNA sequences and the difficulty in multiplexing, which is the simultaneous editing of multiple genomic locations [2], [17].

1.1.1 CRISPR Bioengineering

In contrast, the Nobel Prize-winning Clustered Regularly Interspaced Short Palindromic Repeats (CRISPR) system that originates from bacteria and archaea's adaptive immune system, offers a more efficient and versatile approach to targeted genome editing [18]. CRISPR employs a ribonucleoprotein (RNP) complex comprising a CRISPR-associated (Cas) protein, commonly Cas9 endonuclease from *Streptococcus pyogenes* (SpCas9), guided by a customizable guide RNA (gRNA) with a short targeting sequence (20-26 bp) to induce a targeted DSB at a specific genomic location containing a necessary Protospacer Adjacent Motif (PAM) sequence, such as 5'-NGG-3' for SpCas9, downstream of the target site [18].

CRISPR-induced double-strand breaks (DSBs) are primarily repaired by NHEJ, which uses short homologous sequences (microhomologies) to ligate DNA [19]. While microhomologies can ensure accurate repair when the single-stranded overhangs present on the ends of the dsDNA break are perfectly compatible, NHEJ is prone to errors, often leading to nucleotide loss, mutations, and challenges in using this pathway for precise gene editing techniques [19]. Consequently, researchers favour the HDR pathway for CRISPR-induced DSBs repair since designed DNA templates can be introduced to create targeted integrations, deletions, insertions and mutations [20].

CRISPR has transformed genome editing across numerous fields of research. In agriculture, CRISPR facilitates crop improvement by enhancing biomass production and grain yield, nutrition, and resistance to pests and environmental stresses [21]. In bacteria, CRISPR has led to innovations in antimicrobial development, pathogen diagnostic tools, and microbial

metabolic engineering for sustainable bioproducts [22]. Moreover, in medicine, CRISPR-Cas9-based gene therapy for sickle cell disease is advancing in clinical trials, demonstrating the potential for durable remission through targeted editing of hematopoietic stem cells [23]. CRISPR bioengineering has also advanced the development of cancer immunotherapies by enabling precise genetic engineering of immune cells, such as enhancing CAR-T cells via targeted gene knock-in or knockout to improve anti-tumour responses [24].

1.1.2 Yeast as a Model Organism

Despite the significant promise of CRISPR-based human health therapeutics for precision medicine, the development of these gene editing tools faces considerable challenges when relying solely on mammalian cell models [25], [26]. A significant hurdle is the high cost and complexity associated with mammalian cell cultures because of the need for specialized growth media, controlled growth environments, and time-consuming efforts to maintain cell cultures to assess gene editing outcomes [25]. Another considerable challenge is the difficulty in obtaining stable and predictable expression of transgenes within mammalian cells with the widely used transient transfection methods of which modifying can be laborious and time-consuming [26]. Furthermore, in mammalian cells, NHEJ functions as the primary DNA repair pathway and is active throughout the cell cycle, while HR, which is essential for precise gene editing, is limited to the S and G2 phases and is suppressed by NHEJ [27], [28].

Recognizing the limitations of mammalian cell models for the efficient study and high-throughput development of genome editing tools, researchers widely adopt alternative systems to enhance throughput and streamline progress. The budding yeast, *Saccharomyces cerevisiae*, is frequently employed as a model eukaryotic organism for investigating fundamental cell biology and genetics, developing genetic engineering tools, and rapidly prototyping and optimizing

genome editing strategies [29]. This unicellular eukaryote, commonly known as Baker's or Brewer's yeast, is favoured due to its rapid 90-minute life cycle, facilitating quick genetic analysis and its simple, cost-effective cultivation [30]. Furthermore, *S. cerevisiae* exhibits a high frequency of HR throughout all phases of its cell cycle, making it an ideal system for studying and implementing homology-based DNA manipulation techniques [31], [32]. Its fully sequenced and well-characterized genome, the first complete eukaryotic genome (1996) [33], combined with the conservation of fundamental cellular mechanisms and genes with mammalian cells, renders yeast an invaluable platform for developing and testing genetic engineering technologies applicable to higher eukaryotes [34].

1.1.3 Significance of Yeast Research

The ability to genetically modify *S. cerevisiae* enabled revolutionary discoveries in transcriptional regulation, cell cycle control, and DNA repair [35], [36]. Nobel Prizes were awarded to researchers that, through precise manipulation of yeast, identified key cell cycle regulators such as CDC28 (a cyclin-dependent kinase crucial for the G1 phase), introduced the concept of cell cycle checkpoints, and advanced understanding of processes like eukaryotic transcription, telomere maintenance, vesicle transport, and autophagy [35]. Moreover, the ability to delete, replace, mutate, or overexpress genes within the mating-type (*MAT*) locus of *S. cerevisiae* provided a powerful tool for dissecting specific mechanisms of DNA repair [35], [36]. Similar to other fungi, *S. cerevisiae* propagates vegetatively through budding; however, its mating type is determined by the *MAT* locus, a region on chromosome III that contains either the *MATa* or *MATα* allele, dictating the haploid cell's ability to produce specific pheromones (a-factor or α-factor) and receptors (Ste2 or Ste3) that facilitate mating with a cell of the opposite type [37]. By targeting the *MAT* locus, researchers observed phenotypic changes linked to mating

type switching, using these experimental outcomes to evaluate DNA repair efficiency following specific gene manipulations [37], [38].

Another robust yeast-specific cell process that has significantly advanced scientific discovery is the yeast two-hybrid (Y2H) system, an *in vivo* genetic engineering technique for studying protein-protein interactions [39]. The Y2H system is comprised of two fusion proteins: a "bait" fused to a DNA-binding domain and a "prey" fused to a transcriptional activation domain, expressed in a yeast, primarily, *S. cerevisiae*, reporter strain [40]. Physical interaction between bait and prey proteins reconstitutes a functional transcription factor, activating a reporter gene to signal protein-protein interaction [39], [40]. The Y2H system has been pivotal in mapping intricate protein interaction networks [41] and has contributed significantly to drug development for viral diseases by identifying critical host-pathogen interactions, such as those between HIV-1 and host transcription factors that regulate viral replication [42]. Y2H-based assays have also been used to map interaction networks in viruses like dengue and SARS-CoV-2 to pinpoint therapeutic targets and facilitate the discovery of potential inhibitors for key interactions [43], [44].

Additionally, yeast is a vital and versatile cell factory for the sustainable and cost-effective production of various biomolecules because of its well-characterized and easily modifiable metabolic pathways, coupled with its capacity for large-scale cultivation [45]. Building upon Louis Pasteur's foundational 19th-century discovery of yeast's anaerobic fermentation of sugars into ethanol, modern metabolic engineering has significantly expanded yeast's biomanufacturing capabilities [46]. This has enabled the industrial production of advanced biofuels like butanol and cellulosic ethanol using engineered *S. cerevisiae* strains and biodiesel precursors through lipid overaccumulation in *Yarrowia lipolytica* (an oleaginous yeast

species), presenting sustainable alternatives to fossil fuel-derived energy sources [47]. Another notable industrial application of yeast is its role in food production, where *S. cerevisiae'*s metabolic versatility extends beyond traditional fermentation in bread, wine, and beer to engineered production of specific flavour compounds and vitamins for food enhancement [48]. Yeast research has also been instrumental in increasing the accessibility of medicine to developing countries by offering a low-cost alternative to the production of recombinant protein-based vaccines against Hepatitis B and COVID-19 [49], [50].

In summary, while only a few examples have been highlighted, the remarkable versatility of yeast in scientific research is truly boundless. The overarching theme remains that there is always room for enhancement, whether through incremental refinements or groundbreaking advances.

1.2 Yeast Genetic Engineering

Genetic engineering of yeast has profoundly advanced scientific research and innovation. Throughout the 21st century, significant strides have been made in manipulating genes, pathways, and cellular processes [29], [39], [45], [46], [49], [50]. These breakthroughs were enabled by foundational molecular biology tools for DNA amplification and assembly [25], [34]. Furthermore, the development of yeast-specific integration methods and the creation of specialized toolkits have greatly enhanced precision and efficiency in yeast genetic modification [51].

1.2.1 DNA Manipulation Tools and Techniques

The ability to manipulate DNA in a test tube, *in vitro*, or in an organism, *in vivo*, forms the basis of cloning (creating identical copies) and recombinant DNA technology (combining

DNA fragments from different sources to generate novel genetic combinations) [52]. Accordingly, a wide array of tools and techniques have been developed to amplify, linearize, and assemble DNA for the purpose of genetically modifying organisms following basic molecular biology principles.

For DNA linearization and amplification, restriction enzyme digestion and Polymerase Chain Reaction (PCR) are among the most widely used techniques [53], [55]. Developed in the early 1970s, restriction enzyme digestion fundamentally advanced molecular biology by providing a method for precise DNA manipulation through sequence-specific cleavage [53]. Restriction enzyme digestion involves the use of specific endonucleases to cleave double-stranded DNA (dsDNA) at defined recognition sequences, generating linear DNA fragments with either “sticky” (overhanging) or “blunt” (straight) ends, depending on the enzyme and site [54]. In 1985, PCR was introduced to enable precise amplification of specific DNA sequences through cycles of denaturation (strand separation), primer annealing (binding of short single-stranded oligonucleotides to complementary sequences), and extension (DNA synthesis by a polymerase) [55]. To perform PCR, researchers combine the DNA template with essential components in a reaction tube: primers (18–24 nucleotides long) designed to flank the target region with considerations for melting temperature (Tm), specificity, and minimal self-complementarity to avoid primer-dimer formation; deoxynucleotide triphosphates (dNTPs); a heat-stable polymerase for strand synthesis; and a buffer, including magnesium ions, for optimal enzyme activity and fidelity [55], [56].

Numerous DNA assembly methods and tools are employed in research, each providing specialized approaches for the precise joining of DNA fragments. Restriction enzyme ligation, the first widely adopted DNA assembly method, joins compatibly digested linear DNA fragments

and plasmid vectors using a DNA ligase (typically T4 ligase) to form covalent phosphodiester bonds, creating recombinant DNA molecules [57]. However, this approach is limited by the necessity of suitable restriction sites and often introduces scar sequences (restriction site remnants) at the ligation junctions [58]. Moving towards modularity in designing plasmids and DNA fragments, the BioBrick standard (initially RFC10) was developed on the principle of flanking genetic parts with standardized prefix and suffix sequences containing specific restriction sites for ordered ligation [58], [59]. Consequently, this standardization inherently introduces scar sequences at each junction and restricts the internal use of those same restriction sites within the DNA fragments [58], [59].

Notable scarless DNA assembly alternatives include Golden Gate cloning, which uses Type IIS enzymes to enable the ordered assembly of multiple fragments by simultaneously digesting and ligating DNA fragments, creating seamless junctions [60], and USER cloning, a ligase-free method employing uracil-DNA glycosylase and endonuclease VIII to generate single-stranded overhangs at uracil-containing PCR sites [61]. Limitations include the need for precise fusion site design and the risk of off-target cleavage with Type IIS enzymes in Golden Gate [60], as well as primer design with uracil incorporation and sensitivity to PCR conditions in USER cloning [61].

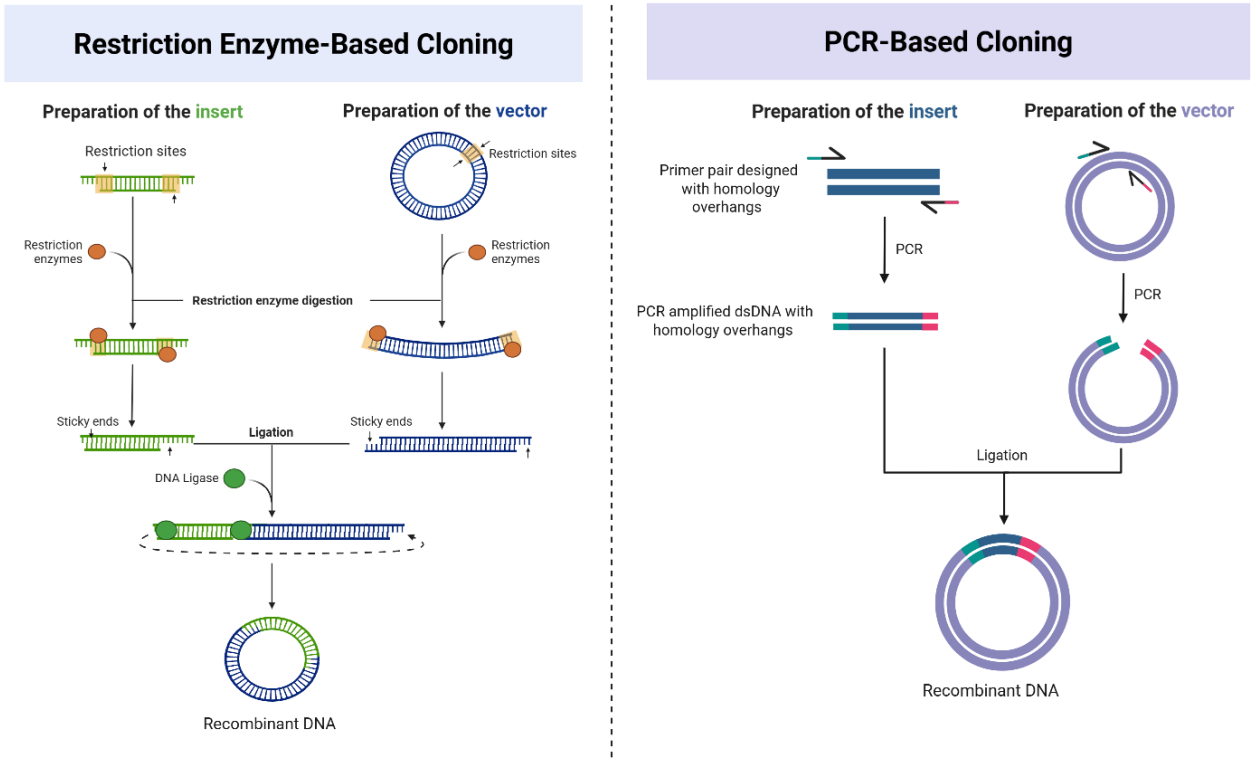

Figure 1. Generalized workflows for restriction enzyme and PCR-based cloning. Restriction enzyme-based cloning methods (such as BioBricks and Golden Gate Assembly) involve enzymatic digestion at specific sites to create compatible ends for ligation. PCR-based cloning uses user-designed primers to introduce homologous overhangs between double-stranded DNA for seamless assembly. Examples include overhang-extension PCR, USER cloning, and Gibson Assembly. Figure created with BioRender.com.

In contrast, the popular Gibson Assembly method overcomes the constraint of restriction enzyme sites and offers flexibility in experimental design by using HR to join several DNA fragments with overlapping ends made by user-designed PCR primers in a single isothermal reaction with a 5' exonuclease, DNA polymerase, and DNA ligase [57]. Beyond enzymatic cleavage and ligation, overhang extension PCR presents a distinct approach to DNA assembly, relying on specifically designed primers with 5' extensions to introduce overlapping sequences between the fragments to be assembled, facilitating seamless annealing and subsequent extension during PCR cycles for precise DNA fragment joining [62].

1.2.2 Yeast Integration Strategies

To stably introduce recombinant DNA and modify *S. cerevisiae* traits, researchers have developed a range of yeast-specific integration strategies using linear or circular DNA vectors that rely on HR. Based on their mode of replication in yeast, the classic strategies can be grouped into five classes: Yeast Replicating plasmids (YRp), Yeast Centromere plasmids (YCp), Yeast Episomal plasmids (YEp), Yeast Integrating plasmids (YIp), and Yeast Artificial Chromosome (YAC) [63], [64].

Classified as shuttle vectors for their dual-host replication in *E. coli* and yeast, YRp, YCp, and YEp exhibit distinct characteristics for maintenance in *S. cerevisiae* [65]. YRps contain a chromosomal Autonomously Replicating Sequence (ARS) for replication in yeast but are extremely mitotically unstable, making them better suited for high-frequency transformations and unsuitable for metabolic engineering applications [66]. YCps, characterized by having both a centromere sequence and an ARS, are low-copy plasmids that allow for enhanced replication stability (persist episomally in yeast cells) during mitosis and meiosis [67]. YEps possess a 2-micron circle origin of replication, allowing for high-copy number gene expression and often resulting in high transformation efficiency, although their mitotic stability can be variable depending on the specific vector [67].

In contrast, YIps contain only an *E. coli* origin of replication (ori), preventing autonomous replication in yeast [63], [67]. YIps require genomic integration to be maintained, which is achieved by linearizing the plasmids at sequences homologous to targeted sites in the yeast chromosome, enabling stable HR-mediated integration of DNA [67]. YACs also integrate as linear DNA, have a bacterial ori, and replicate in yeast by mimicking chromosomes, with essential elements of a centromere, telomeres, and ARS [66]. YACs were famously used in the

Human Genome Project for cloning large DNA fragments, making them essential for genome mapping and sequencing, but faced limitations such as high chimerism rates, instability, low transformation efficiency, and challenges in handling and purifying large DNA [66] [64], [68].

1.2.3 Yeast Toolkits

Building on the diverse yeast integration strategies provided by vectors such as YACs, YIps, YRps, YEps, and YCps, the development of sophisticated yeast toolkits has further streamlined and enhanced the ability to manipulate the yeast genome. Yeast toolkits have revolutionized genomic engineering by providing a framework for modular assembly, significantly enhancing sharing and collaboration among researchers [51]. Table 1 details the specifics of some of the many toolkits available for yeast genetic engineering.

Table 1. Overview of notable yeast genetic engineering toolkits. This table summarizes key features of prominent toolkits used for yeast genetic engineering. Toolkit descriptions are derived from cited references, and the availability section outlines how each toolkit can be accessed.

ToolKit	Description and Components	Availability	References
MoClo Yeast Toolkit (MYT)	• Based on Modular Cloning (MoClo), MYT provides a standardized library of genetic parts (promoters, coding sequences, terminators) for assembling constructs. • Uses Type IIS restriction enzymes in a Golden Gate-based system. DNA constructs are assembled in *E. coli* shuttle vectors, linearized via restriction digest, and integrated into *S. cerevisiae* at ten chromosomal loci. • Compatible with CRISPR-Cas9 for multiplex genome editing.	Toolkit is available from Addgene (http://www.addgene.org), Kit 1000000229	Original MoClo [69]. MYT [70].
Assembly and CRISPR-targeted *in vivo* Editing (ACtivE)	• Uses linear DNA fragments instead of plasmids for CRISPR-Cas9 genome editing in *S. cerevisiae*. • Offers a repository of PCR-verified, ready-to-use fragments for direct integration of Cas9, gRNA, and donor DNA via HR. Each linear fragment includes terminal synthetic connectors for modular part exchange. • Eliminates the need for *in vitro* DNA assembly by enabling *in vivo* integration directly within yeast cells. • Targets eight ARS-proximal intergenic regions.	Toolkit is available from authors of the study at the LeoRios Lab.	[71]

Versatile Genetic Assembly System (VEGAS)	• Designed for assembling genetic pathways in *S. cerevisiae*. Genes within a pathway are organized into transcriptional units containing a promoter, gene of interest, terminator, and VEGAS adaptor sequences. • The transcriptional units are initially assembled via Golden Gate cloning, followed by assembly into a yeast vector (that contains a selectable marker, centromere sequence, and ARS to ensure mitotic stability in yeast). • The vectors are then linearized via restriction digest before integration into designated yeast genomic sites.	Toolkit is available from authors of the study at the Boeke Lab.	[72]
EasyClone System	• Developed by the Borodina Lab (2012), iterated into EasyClone 2.0 and MarkerFree toolkits. • These systems enable stable and neutral DNA integration into eleven pre-characterized intergenic loci in the *S. cerevisiae* genome, ensuring consistent gene expression. • These toolkits offer YIps with BioBrick standards, where, by USER cloning, plasmids are assembled *in vitro*, needing to be linearized by restriction enzyme digest prior to integrating into yeast. • The 2.0 toolkit uses HR for DNA integration. It includes yeast selection markers (antibiotic and auxotrophic), which can be removed through Cre-mediated marker rescue. • The MarkerFree toolkit employs CRISPR-Cas9 for enhanced integration efficiency, supports single and multi-locus integration (up to three loci simultaneously), and offers YIps without selection markers. Includes YEps (gRNA helper vectors) and YRps (SpCas9 vector) featuring antibiotic selection, with gRNA vector removal via non-selective media culture.	Available from Addgene (http://www.addgene.org). The 2.0 kit # is 1000000073 and the MarkerFree kit # is 1000000098	Characterization of genomic loci [73]. Cloning procedure followed to generate EacyClone system [74]. EasyClone 2.0 [75]. EasyClone MarkerFree [76].

1.3 Project Rationale

As demonstrated in Table 1, a common strategy among synthetic biologists developing *S. cerevisiae*-specific toolkits involves plasmid-based systems with standardized parts [51]. Several toolkits are available to streamline and enhance genetic manipulation in yeast, with the EasyClone system being one of the most accessible.

The EasyClone system stands out as a versatile tool, enabling flexible manipulation of integrative vectors and offering eleven well-characterized integration sites [74], [75]. Its capabilities have been further expanded to incorporate CRISPR-mediated DSBs using HDR and

multiplexing [76]. Widely recognized for its robustness and predictable outcomes, the EasyClone system has been successfully implemented in diverse applications. These include a teaching protocol for the metabolic engineering of industrially relevant yeast strains (*S. cerevisiae* and *Y. lipolytica*) to produce β-carotene [77], development of yeast cell factories for vanillin-glucoside production [78], and treatment modelling for murine colitis [79], among many more.

The broad applicability of the EasyClone system is further exemplified by its adoption at Canada's first and only Genome Foundry, established at Concordia University in 2018, which uses automated systems for the construction of synthetic genomes [80]. The director, Dr. Vincent Martin, published a paper in 2022 detailing the development of a Markerless Yeast Localization and Overexpression (MyLO) CRISPR-Cas9 toolkit that uses EasyClone-derived integrative vectors and sequences for the rapid introduction of tagged genes and compartmental markers (GFP/RFP for 15 subcellular locations) [81].

Given its valuable attributes and significant impact across various research areas, the EasyClone system has influenced the direction of my thesis research. However, upon examining the EasyClone system and considering the overview of other toolkits in Table 1, it is evident that yeast genomic integrations can be streamlined by eliminating the requirement for *in vitro* cloning. Avoiding the usual prerequisite of *in vitro* cloning, which involves multiple rounds of DNA amplification, assembly using costly and specific techniques, bacterial transformation, colony inoculation, and plasmid purification and validation, is especially useful when developing simplified multiplexing experimental workflows.

1.3.1 Hypothesis

The hypothesis of my research is that a novel YIp can be designed to contain short regions of homology to enable one-step, simultaneous gene integrations into multiple *S. cerevisiae* genomic loci by leveraging yeast's HR capabilities.

To evaluate this hypothesis, my research employed iterative design, build, and test cycles. These stages focused on determining the most streamlined approach by characterizing the capabilities and limitations of the EasyClone system, demonstrating CRISPR-Cas9-mediated multiplexing, understanding yeast's HR capabilities, and designing unique YIps and homology regions.

1.3.2 Research Objectives

The EasyClone system integrates genes of interest (GOIs) into specified chromosomal sites using YIps, either with selection markers (EasyClone 2.0 system [75]) or without them (EasyClone MarkerFree [76]). Figure 2a describes EasyClone 2.0's workflow to integrate a GOI cassette into the X-4 site with a *hphMX6* marker for hygromycin selection. This involves the *in vitro* cloning of the GOI cassette, which includes a promoter, terminator, and assembly junctions (AJs) as standardized homology overhangs into an EasyClone YIp (pCFB2194 in this example). The assembled vector is then linearized with a restriction enzyme (NotI), removing the bacterial backbone and yielding a linear DNA fragment containing the GOI cassette and chromosomal homology regions (cHRs) to enable integration into the X-4 chromosomal site in *S. cerevisiae* via HR (Figure 2c). As evident in Figure 2a, using the EasyClone system requires multiple experimental steps for the *in vitro* addition of cHRs and selection marker to GOIs, which is time-

consuming and unnecessarily laborious compared to *in vivo* DNA assembly in yeast using PCR products with homology overhangs [82], [83].

First Objective: Clone-less *in vivo* Assembly and Integration

Therefore, the first objective of my research is to establish an efficient clone-less *in vivo* DNA assembly and integration method leveraging yeast's endogenous HR ability. Figure 2b demonstrates a PCR-based approach for the amplification of two linear DNA fragments from the EasyClone YIp. The first fragment contains the upstream X-4 cHR and assembly junction (AJ), and the second fragment contains the downstream AJ, *hphMX6* cassette, and downstream X-4 cHR. These linear DNA fragments are then transformed into a commonly used yeast lab strain, BY4741, with a GOI cassette, resulting in the *in vivo* assembly and integration of these linear DNA fragments into the X-4 site of the yeast genome (Figure 2c). This clone-less *in vivo* assembly design results in a two-step method to obtain the same product as the EasyClone system's multi-step approach (Figure 2c).

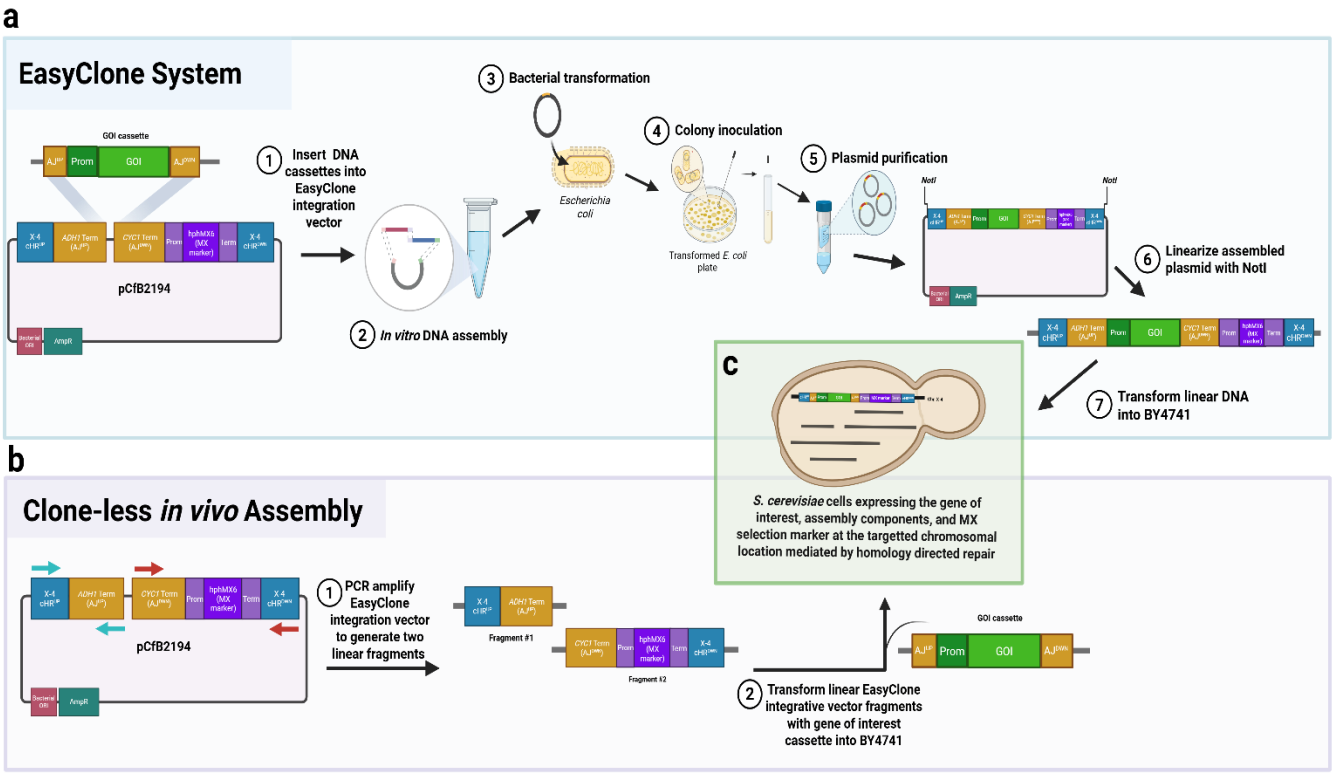

Figure 2. Workflow comparison of EasyClone 2.0 and a streamlined clone-less *in vivo* assembly method for genomic integration in *S. cerevisiae*. (a) The EasyClone 2.0 system integrates a gene of interest (GOI) and a hygromycin resistance marker (hphMX6) into the X-4 locus using a yeast integrating plasmid (YIp) with chromosomal homology (cHR) and assembly junctions (AJs). **(b)** A clone-less *in vivo* assembly approach using PCR to amplify the EasyClone 2.0 YIp. **(c)** Both methods result in the integration of the GOI and *hphMX6* cassettes at the X-4 site. Figure created with BioRender.com; EasyClone 2.0 protocol from [75].

As previously highlighted, the advent of CRISPR-Cas9 technology has revolutionized eukaryotic research through its precise gene editing capabilities. The Borodina lab leveraged this in their EasyClone system by expanding their toolkit to enable targeted DSBs for efficient integration of linearized YIp constructs [75], [76]. This advancement allows for the insertion of a single linearized YIp into a validated genomic locus, or the simultaneous integration of up to three linearized YIps at distinct sites, facilitated by specifically designed gRNAs [76]. This capacity for multiplexing gene editing holds significant potential for complex genetic engineering. Building upon this foundation, the second aim of my first research objective is to integrate CRISPR-Cas9-mediated DSBs into our existing clone-less *in vivo* DNA assembly and

integration approach. Figure 3 depicts how this can be achieved by the addition of an X-4 targeting gRNA (pCfB3042 from the EasyClone MarkerFree toolkit) when transforming the linear fragments described in Figure 2b via HR into a yeast strain expressing Cas9. This integration is anticipated to significantly enhance transformation efficiency, since, as previously discussed, the increased tendency for HDR because of CRISPR makes genomic edits based on HR significantly more efficient. Ultimately, this objective will highlight the capabilities and limitations of *in vitro* cloning-dependent approaches while providing a baseline transformation efficiency to benchmark our clone-less systems.

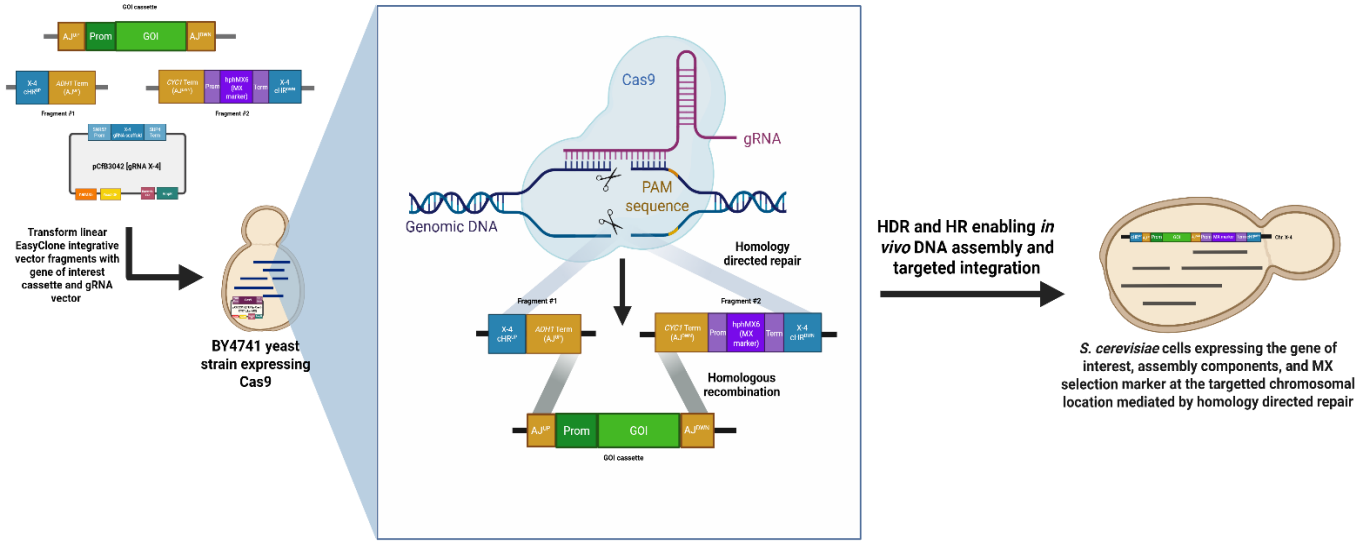

Figure 3. CRISPR-Cas9 assisted clone-less *in vivo* DNA assembly and genomic integration at the X-4 locus in *S. cerevisiae*. PCR-amplified fragments #1 and 2 from an EasyClone 2.0 YIp that enable the integration of a linear gene of interest (GOI) cassette into the X-4 locus are co-transformed with an EasyClone MarkerFree toolkit single guide RNA (gRNA) into a Cas9-expressing yeast BY4741 strain. This gRNA (pCfB3042) contains a scaffold that directs the Cas9 endonuclease (pCfB2312 from the EasyClone MarkerFree toolkit) to cut at a validated site in the X-4 locus. The assembly of the transformed linear DNA occur *in vivo* via homology-directed repair (HDR) and homologous recombination (HR), resulting in *S. cerevisiae* cells expressing the assembled fragments. Figure created with BioRender.com.

Second Objective: Characterizing Multiplexing

The EasyClone system enables stable DNA integration into eleven pre-selected intergenic regions of the *S. cerevisiae* genome. These sites were characterized and validated for efficient and predictable integration, aiming to minimize adverse effects on the host cell's growth and physiology, making these loci ideal for stable genetic engineering in yeast [73], [75], [76]. Therefore, the first aim of my second research objective is to determine which integration sites available by the EasyClone system are compatible with our clone-less *in vivo* DNA assembly and integration approach. The second aim is to characterize the EasyClone system's capability for multiplexing by simultaneously integrating different GOIs into three chromosomal loci with the help of CRISPR-Cas9. This research objective will provide a valuable understanding of the abilities and limitations of the EasyClone system for the development of a simplified multiplexing workflow.

Third Objective: Leveraging Homologous Recombination

Yeast's robust endogenous HR machinery efficiently assembles introduced DNA fragments *in vivo* by recognizing and combining regions of sequence similarity [31], [32]. Decades of research have aimed to define the minimal homology length required for successful integration. A well-cited study from 1997 demonstrated that just 30 bp of homologous regions at each end of a DNA fragment enable yeast-based *in vivo* cloning, with higher efficiency achieved with regions longer than 60 bp or if there is an asymmetric arrangement such as 20 bp at one end and 80 bp at the other [84]. While designing short homologies is desirable for streamlining cloning (for example, by adding overlaps via PCR primers) and reducing DNA synthesis costs, a caveat is the potential for higher error rates due to insufficient overlap for robust HR [85], [86].

Therefore, my third research objective is to leverage yeast HR to determine the optimal, shortest homologous overlap length for efficient and accurate DNA assembly and integration following our CRISPR-mediated clone-less approach. As depicted in Figure 4, I am using CRISPR-Cas9 to target and disrupt the *ADE2* locus to test the efficiency of integrating DNA fragments with varying lengths of cHR (30-400 bp) and AJ (30-200 bp). This can be achieved using a designed gRNA to target an *ADE2* open reading frame, allowing for site-specific insertion of the GOI and *hphmX6* selection marker. Targeting the *ADE2* locus in the XV chromosome results in a disruption of the adenine synthesis pathway, resulting in the buildup of an intermediate, AIR (5-aminoimidazole ribotide), whose oxidation during cellular respiratory growth causes an accumulation of a red pigment, imparting a pink colour on the yeast cell [87]. This system provides a direct visual readout of successful HDR at the targeted DSB.

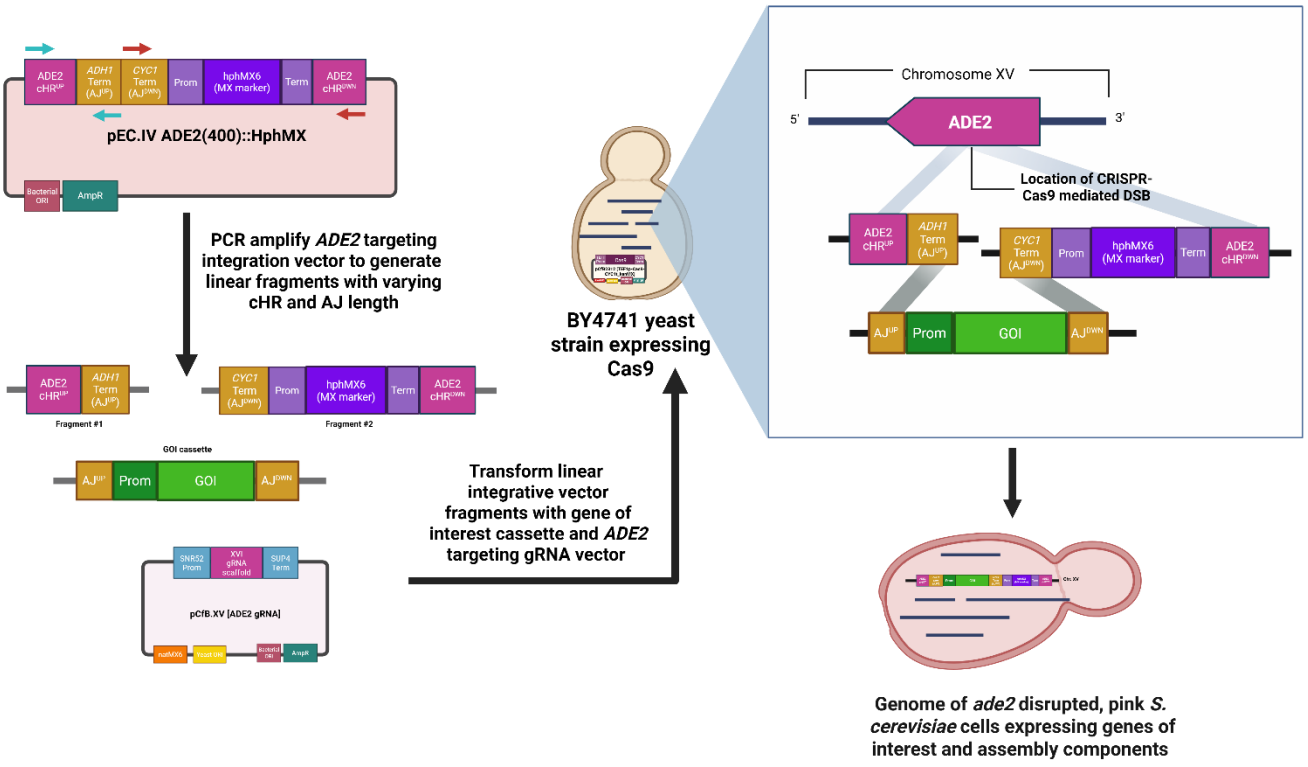

Figure 4. CRISPR-Cas9 assisted clone-less *in vivo* integration at the *ADE2* locus yields pink *S. cerevisiae* colonies. Our pEC.IV ade2(400)::HphMX YIp is designed to integrate a GOI interest with a *hphMX6* selection

marker at an open reading frame in the *ADE2* locus on chromosome XV. This YIp can be amplified by PCR to create fragments #1 and #2 with varying chromosomal homology region (cHR) and assembly junction (AJ) lengths. CRISPR-Cas9, guided by an *ADE2*-specific gRNA (pCfB.XV), induces a DSB at the *ADE2* locus on chromosome XV, leading to gene disruption and pink colonies as a visual readout. Figure created with BioRender.com.

Fourth Objective: Designing a Simplified Multiplexing System

To simplify multiplexing, I will expand the capabilities of our clone-less *in vivo* HR-based DNA assembly and integration approach in a two-step process: first, obtaining linear DNA fragments, and second, simultaneously transforming them into yeast. To achieve this, I have two experimental aims.

Current multiplexing with the EasyClone system requires multiple *in vitro* steps to generate three YIps with the genes of interest (GOIs) integrated. This process is time-consuming and needs streamlining, which leads to my first experimental aim of designing a one-step linearizable YIp that allows the integration of two gene cassettes into a single locus. Figure 5 illustrates a proof-of-concept design targeting the *ADE2* locus to provide a direct visual readout of successful transformation. This design includes a YIp of pEC.IV (XV.CL.MX) that can be linearized in one restriction digest reaction to release the assembly fragments of cargo linkers (CLs) required for the integration of a GOI cassette and an MX marker cassette.

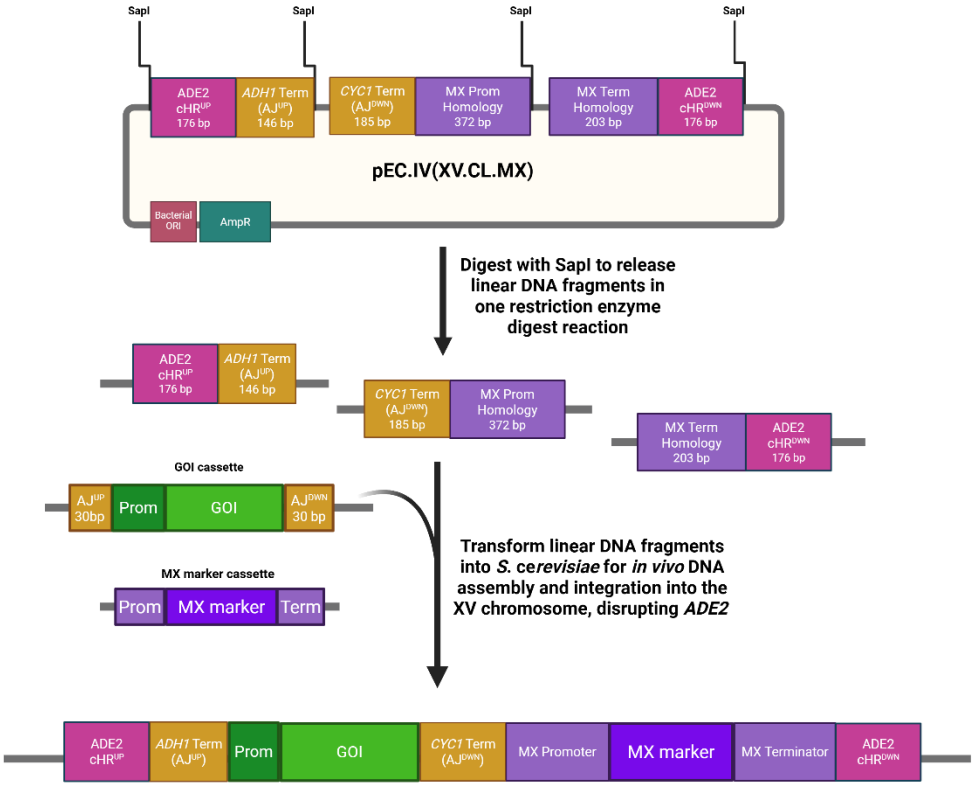

Figure 5. One-step linearizable yeast integrative vector for the clone-less *in vivo* assembly and integration of two gene cassettes into the *ADE2* locus. The YIp, pEC.IV (XV.CL.MX) is designed to be linearized by one restriction enzyme, SapI, to liberate the assembly fragments and enable the integration of GOI and MX marker cassettes into *S. cerevisiae*'s *ADE2* locus. Figure created with BioRender.com.

The next step is to scale up the linearizable plasmid from aim 1 to enable the simultaneous targeting of multiple genomic loci and the integration of multiple GOIs using a two-step experimental method. To achieve this, I can no longer rely on the EasyClone system's AJs, as these are identical across their YIps. Specifically, the EasyClone system's YIps all contain an upstream AJ that encodes the *ADH1* terminator, and a downstream AJ encoding the *CYC1* terminator [74], [75], [76]. Both the *ADH1* (Alcohol Dehydrogenase 1) and *CYC1* (Cytochrome c isoform 1) terminators are well-characterized for their efficient and reliable termination of transcription by RNA polymerase II in yeast [88]. Therefore, the second aim of this objective is to create AJs, which will contain unique regions of homology to facilitate my

clone-less *in vivo* DNA assembly and integration, that perform at a similar standard to the EasyClone system's AJs.

To design our unique AJs, we explored the Voigt lab's study on creating gene circuits for yeast using their design automation software, Cello 2.0 [89]. In this paper, sequences to genetic parts are provided to build insulated gates, which are genetic logic components that regulate gene expression in engineered yeast circuits [89]. These gates contain short synthetic promoters to initiate transcription, strong terminators to repress RNA polymerase read-through, insulators constructed using ribozymes and terminators to block transcriptional interference, and spacer sequences to prevent unwanted HR [89]. Drawing inspiration from the Voigt lab's work, we have designed terminator insulator spacer (TINS) sets to serve as unique AJs, using sequences designed and validated by the Voigt lab for the yeast strain BY4741 [89]. Figure 6 outlines the proof-of-concept experimental design for integrating one GOI cassette into the *ADE2* locus via PCR amplification of a YIp containing one set of TINS, based on our clone-less *in vivo* HR-based assembly method.

In summary, the development of a two-step clone-less *in vivo* DNA assembly and integration approach, with components designed and validated in my fourth research objective, promises a more streamlined and less labour-intensive method for multiplexing in yeast.

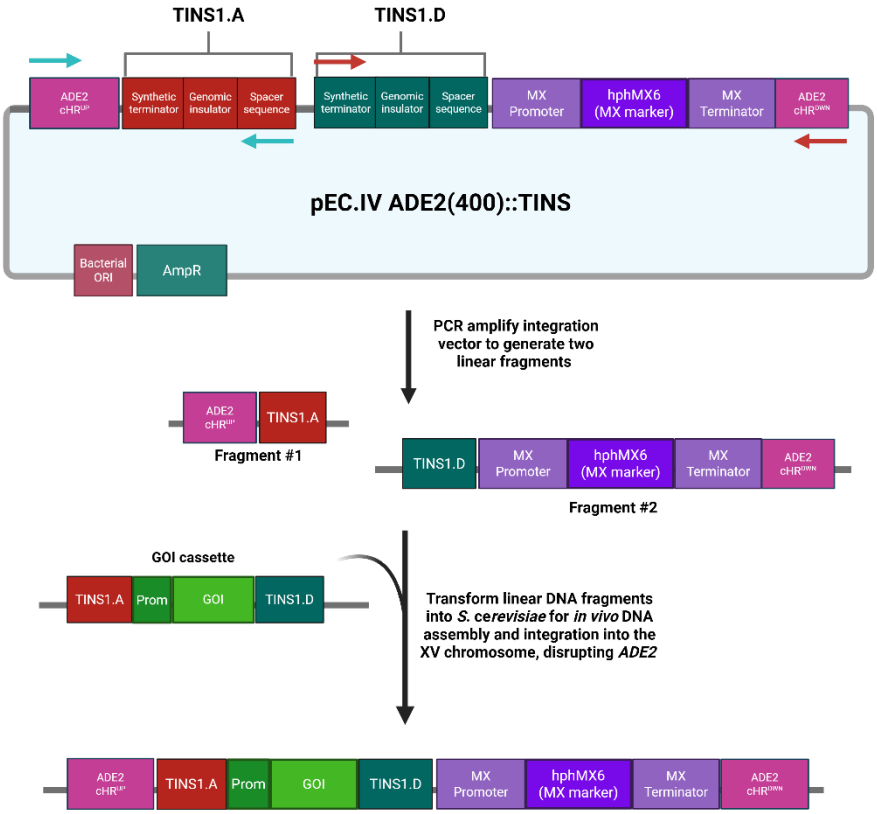

Figure 6. Implementing designed, unique regions of homology as assembly junctions for the integration of a gene of interest cassette into the *S. cerevisiae ADE2* locus. pEC,IV ADE2(400)::TINS is a YIp that can be PCR amplified to enable the clone-less *in vivo* assembly and integration of a GOI cassette into the *ADE2* locus with a *hphMX6* selection marker and unique assembly junctions annotated as TINS1.A and TINS1.D. TINS are terminator insulator regions that are designed to contain unique synthetic terminator, genomic insulator, and spacer sequences. In this figure, TINS1.A and .D are unique from each other and originate from our first set of TINS. Figure created with BioRender.com.

Chapter 2: Materials and Methods

2.1 EasyClone Plasmid Isolation

The EasyClone 2.0 (Addgene kit # 1000000073) and EasyClone-MarkerFree Vector Set (Addgene kit #1000000098) were gifts from Irina Borodina. Each toolkit was delivered in a 96-well format containing each vector as a bacterial glycerol stocks in *E. coli* DH5α. The plasmids used in my research (Table 2) were isolated by streaking onto Luria-Bertani (LB) plates with ampicillin (amp) antibiotic [100 ng/µL] to grow the bacteria at 37 °C for 18 hours then selecting and inoculating single colonies in 5 mL of LB + Amp [100 ng/µL] liquid media at 37 °C, 250 rpm for 18 hours. Plasmid extraction was accomplished using BioBasic's EZ-10 spin column plasmid DNA miniprep kit (catalogue # BS614).

Table 2. Overview of plasmids used from the EasyClone 2.0 and MarkerFree toolkits. This table provides a comprehensive list of plasmids sourced from the EasyClone 2.0 [75] and MarkerFree [76] toolkits, including their names, descriptions, and specific applications relevant to this research. These toolkits, available through Addgene, are supplied as bacterial glycerol stocks, with each plasmid maintained in the high-copy *E. coli* strain DH5α. Hyperlinks to plasmid details are based on information accessible via Addgene's database.

Toolkit	Plasmid Name	Description	Selection	Use in Study
EasyClone 2.0 [75]	pCfB2194	• YIp for integration into the X-4 locus	Features a loxP-flanked *hphMX6* marker for hygromycin selection in yeast and *AmpR* for ampicillin resistance in *E. coli.*	Objectives 1 and 2
	pCfB2513	• YIp for integration into the X-2 locus		Objective 2
	pCfB2195	• YIp for integration into the XI-3 locus		
	pCfB2198	• YIp for integration into the XII-4 locus		
	pCfB2337	• YIp for integration into the XII-5 locus		
EasyClone MarkerFree [76]	pCfB2312	• YRp carrying SpCas9 endonuclease under the transcriptional control of the *TEF1* promoter and *CYC1* terminator	Features a *kanMX* marker for geneticin (G418) selection in yeast and *AmpR* for ampicillin resistance in *E. coli.*	Objectives 1- 4
	pCfB2904	• YIp for integrating into the XI-3 locus	Selection-free YIps featuring *AmpR* for	Objective 2

	pCfB2909	• YIp for integrating into the XII-5 locus	ampicillin resistance in *E. coli*	
	pCfB3042	• YEp gRNA vector targeting Cas9 to the X-4 locus	Features a *natMX6* marker for nourseothricin (Nat) selection in yeast and *AmpR* for ampicillin resistance in *E. coli.*	Objectives 1 and 2
	pCfB3020	• YEp gRNA vector targeting Cas9 to the X-2 locus		Objective 2
	pCfB3045	• YEp gRNA vector targeting Cas9 to the XI-3 locus		
	pCfB3049	• YEp gRNA vector targeting Cas9 to the XII-4 locus		
	pCfB3050	• YEp gRNA vector targeting Cas9 to the XII-5 locus		
	pCfB3052	• YEp gRNA vector targeting Cas9 to the X-4, XI-3, and XII-5 loci • Used for multiplexing		

2.2 Plasmid Construction

Plasmid construction was achieved using the Gibson Assembly method [90]. Table 3 contains a list of the plasmids made for this study with a description of each plasmid's purpose and plasmid-specific construction details. The sequences of the inserts were obtained from available online databases and repositories, as detailed in Table 3. The plasmids that contain *ADE2* cHRs were designed to be 200-400 bp (depending on the plasmid) upstream and downstream of the 20 bp *ADE2* targeting gRNA sequence in pCfB.XV. The sequence for the *ADE2* gene was obtained from the *Saccharomyces* Genome Database (SGD) [91]. The gRNA sequence in pCfB.XV was chosen using Benchling's CRISPR guide design tool to find a Cas9-compatible 20 bp guiding sequence to target the *ADE2* locus with a high efficiency score for *S. cerevisiae* using the scoring method determined by [92]. The gRNA sequence chosen (refer to Appendix A, Table 1) is at position 1388 of the *ADE2* gene with a PAM sequence of 5'-AGG-3'. To create pCfB.MOCK, the *ADE2* targeting gRNA sequence was then scrambled and aligned with the *S. cerevisiae* genome to ensure that it cannot target any site. The sequences that make up the TINS (refer to Appendix A, Table 1) were designed by Dr. Mads Kaern (based on analysis of the Voigt's lab study on genetic circuit design [89]) by identifying combinations of

terminator/ribozyme/spacer sequences that facilitate HR while acting as genetic insulators and terminators.

DNA fragments for assembly were generated via PCR using Thermo Fisher Scientific Phusion High-Fidelity PCR Master Mix (catalogue # F548L), which includes Phusion Flash II DNA Polymerase (high-fidelity enzyme with blunt-end amplification), deoxynucleotide triphosphates (dNTPs), and an optimized reaction buffer containing $MgCl_2$ [93]. Assembly primers were designed to incorporate 15-30 bp of homologous overlapping sequences to the ends of the PCR amplified fragments following the guidelines of containing around 50% GC content, GC clamps, and melting temperature (Tm) of 60-70°C [94]. Gibson assembly designs were verified using the NEBuilder Assembly Tool [95] prior to ordering the custom primers from Integrated DNA Technologies (IDT) as 25 nmol DNA oligonucleotides.

The Gibson Assembly reactions were performed by mixing PCR amplified DNA fragments in a 1:2 vector to insert ratio, with 50 ng of vector added, and the required insert DNA mass calculated using NEBioCalulator Ligation Calculator tool [96]. Depending on reagent availability, Gibson Assembly was performed using the 2X isothermal DNA assembly mix from the Genome Editing and Molecular Biology (GEM) facility at uOttawa [97], or, alternatively, the Gibson Assembly Cloning Kit from New England Biolabs (NEB, catalogue # E5510S). The reactions were incubated at 50°C for 1 hour in a thermal cycler.

After assembly, 5 µl of the reaction was transformed into 50 µl of chemically competent *E. coli* cells by heat shock, following a standard protocol (30 minutes on ice, 45 seconds at 42 °C, 5 minutes on ice, then 1 hour at 37 °C in LB) [98]. For all plasmids listed in Table 3, except pCfB.XV and MOCK, lab-made chemically competent (following [99]) E. *coli* 10- beta cells

were used. For pCfB.XV and MOCK assemblies, the NEB 5-alpha competent *E. coli* strain (NEB catalogue # C2987H) was used.

After the *E. coli* transformation, 100-200 µL of the cells suspended in LB liquid medium were plated on LB agar plates containing the 100 ng/µL of ampicillin (Fisher scientific catalogue # BP1760-5) or 50 ng/µL of kanamycin (Bio Basic, catalogue # KB0286) where appropriate. These plates were left in a 37°C incubator for 16-18 hours. The resultant colonies were screened by colony PCR with insert-specific primers, and positive clones were confirmed by agarose gel electrophoresis using a 1% (w/v) agarose gel stained with SYBR Safe DNA gel stain. Electrophoresis was performed at a constant voltage of 105 V for 60 minutes. Positive clones were then cultured in LB broth with antibiotic and plasmid DNA was extracted using BioBasic's EZ-10 spin column plasmid DNA miniprep kit. The DNA concentration of the purified plasmids was determined by measuring the absorbance of DNA at 260 nm using a Thermo Scientific NanoDrop 2000 spectrophotometer. The purified clones of pCfB.XV and MOCK were further validated using Sanger Sequencing performed at the National Research Council of Canada (NRC) facilities using the sequencing primer listed in Appendix A, Table 1.

Table 3. List of plasmids designed and constructed for this study. The description of each plasmid is provided along with details on the method used for construction, references for sequences, and the specific research objective for which the plasmid was used.

Plasmid Name	Description	Construction	Sequence	Objective (s)
pECIAK-GFP	• Bacterial plasmid with kanamycin resistance marker containing GFP cassette (with *TDH3* promotor and an enhanced *GFP* gene sequence) between upstream EasyClone AJ (*ADH1*	• Gibson Assembly • Primers were designed to integrate GOI between the EasyClone AJs	• **Vector:** Synthesized by Twist • **Insert:** Enhanced *GFP* (GenBank: AAB02572)	1-4

	terminator, 226 bp) and downstream EasyClone AJ (*CYC1* terminator, 207 bp)			
pCfB2194-GFP	• EasyClone 2.0 YIp for integrating a GFP cassette (containing *TDH3* promotor and an enhanced *GFP* gene sequence) into the X-4 locus with hygromycin selection marker	• Gibson Assembly • Primers were designed to integrate GOI cassette between the EasyClone AJs of *ADH1* and *CYC1* terminators.	• **Vector:** pCfB2194 (Addgene plasmid #67545) • **Insert**: Enhanced *GFP* (GenBank: AAB02572)	1 and 2
pCfB2902-URA3	• EasyClone MarkerFree YIp for integrating a *URA3* cassette into the XI-3 site		• **Vector:** pCfB2904 (Addgene plasmid #73276) • **Insert:** *URA3* promoter and gene from pRS316 (provided by the Downey Lab)	2
pCfB2909-LEU2	• EasyClone MarkerFree YIp for integrating a *LEU2* cassette into the XII-5 site		• **Vector:** pCfB2909 (Addgene plasmid # 73281) • **Insert:** *LEU2* promoter and gene from pRS415 (provided by the Downey Lab)	2
pCfB.XV	• *ADE2* targeting gRNA in an EasyClone MarkerFree YEp	• Gibson Assembly • The X-4 gRNA targeting sequence in the vector was replaced by the appropriate targeting sequence using a 70 bp PCR primer (designed to include a 20 bp gRNA targeting sequence with 25 bp sequences at the 5' and 3' ends for	• **Vector:** pCfB3042 (Addgene plasmid # 73284) • **Insert:** Sequence and assembly primers provided in Appendix A, Table 1	3 and 4
pCfB.MOCK	• Mock gRNA (does not target anything in the yeast genome) in an EasyClone MarkerFree YEp		• **Vector:** pCfB3042 (Addgene plasmid # 73284) • **Insert:** Sequence and assembly primers provided in Appendix A, Table 1	

		homology to the vector)		
pEC.IV ADE2(400):: HphMX	• YIp for integrating a GOI cassette into the *ADE2* locus (400 bp cHRs) with EasyClone AJs and a *hphMX6* marker for hygromycin selection in yeast and *AmpR* for ampicillin resistance in *E. coli*	• Gibson Assembly • Primers were designed to integrate elements from an EasyClone YIp into a synthesized vector with 400 bp *ADE2* cHRs	• **Vector:** Synthetic DNA containing 400bp *ADE2* cHRs ordered in a pTwist Amp High Copy cloning vector • **Insert:** EasyClone AJs (*ADH1* and *CYC1* terminators) and *hphMX6* cassette from pCfB2194 (Addgene plasmid #67545)	3
pEC.IV (XV.CL.MX)	• One-step linearizable YIp that liberates cargo linkers (CL) when digested with SapI restriction enzyme	• Synthesized by Twist Bioscience into a pTwist Amp High Copy cloning vector	• Includes 200 bp *ADE2* cHRs, EasyClone AJs (*ADH1* and *CYC1* terminators), and MX cassette homology (*TEF* promoter and terminator)	4
pEC.IV ADE2(400):: TINS	• YIp with TINS (unique AJs) allowing for the integration of one GOI into the *ADE2* locus	• Gibson Assembly • Primers were designed to integrate elements from an EasyClone YIp into a synthesized vector with 400 bp *ADE2* cHRs	• **Vector:** Synthetic DNA containing TINS1.A and .D (sequences provided in Appendix A, Table 1) and 400bp *ADE2* cHRs ordered in a pTwist Amp High Copy cloning vector • **Insert:** *hphMX6* cassette from pCfB2194 (Addgene plasmid #67545)	4
pEC.TINS DNR-GFP	• YIp used to add TINS to a GFP cassette (containing TDH3 promotor and an enhanced *gfp* gene sequence	• Gibson Assembly • Primers were designed to integrate the GFP cassette between TINS1.A and .D	• **Vector:** Synthetic DNA containing TINS1.A and . D (sequences provided in Appendix A, Table #1) ordered in a pTwist Amp High Copy cloning vector • **Insert:** Enhanced GFP (GenBank: AAB02572)	4

2.3 Obtaining Linear DNA Fragments

Linear DNA fragments were generated using the two methods of Polymerase Chain Reaction (PCR) or restriction enzyme digestion, where appropriate.

PCR was the principal method used to generate specific linear DNA fragments for yeast transformations. Amplifications were performed using Phusion Flash High-Fidelity PCR Master Mix (Thermo Fisher Scientific, catalogue # F548L). PCR reactions were performed according to the master mix manufacturer's instructions, with a final primer concentration of 0.5 µM. Template DNA amounts were 10 ng for 20 µL reactions and 50 ng for 50 µL reactions. The PCR cycling protocol using Phusion DNA polymerase consisted of an initial denaturation at 98°C for 10 seconds, 35 cycles of: denaturation at 98°C for 5 seconds, annealing at a primer-specific temperature for 5 seconds, and extension at 72°C for 15 seconds per kilobase of expected amplicon size. A final extension was performed at 72°C for 1 minute. Table 4 details the primer sequences, purpose, and specific cycling conditions used to obtain linear DNA fragments for yeast transformation. For each primer set, Table 4 details the optimized PCR conditions that resulted in a single, clean band when analyzed by 1% (w/v) agarose gel electrophoresis with SYBR Safe staining.

Restriction enzyme digestion was also used to obtain linear DNA fragments, particularly in the experiments related to Objective #1 and Objective #2, which focused on replicating and implementing the EasyClone system's *in vitro* assembly and *in vivo* integration method in both single integration and multiplex experiments. For these objectives, the assembled plasmids pCfB2194-GFP, pCfB2902-URA3, and pCfB2909-LEU2 (Table 3) were linearized using the NotI restriction enzyme (New England Biolabs, catalogue # R3189S). To increase the concentration of the digested product, the NotI digestion reactions were each performed in a total

volume of 80 µL, containing 5 ng of plasmid DNA,10 µL of rCutSmart Buffer, 1 µL of NotI, and nuclease-free water. The digest reactions were incubated for 10 hours at 37°C in a thermocycler since NEB reports that NotI is active for over 8 hours and can digest 1 ug of DNA in 2 hours when 0.13 units of enzyme are added [100]. The NotI digested reactions were then heat-inactivated in a thermocycler at 65°C for 20 minutes.

In Objective #4, the plasmid pEC.IV (XV.CL.MX) was also linearized with a restriction enzyme. SapI (NEB, catalogue # R0569S) was used to release the cargo linker (CL) fragments in a single digest. The digest reaction was set up to optimize the final concentration of linearized DNA based on trial-and-error experiments. This resulted in the following optimal reaction set up and conditions: 80 µL reaction (5 ng of plasmid DNA,10 µL of rCutSmart Buffer, 2 µL of SapI, and nuclease-free water) incubated in a thermocycler for 10 hours at 37°C, then heat-inactivated at 65°C for 20 minutes.

Check gel analysis was done using 1% agarose gel stained with ethidium bromide (EtBr) as it provides optimal sensitivity for detecting DNA fragments resulting from restriction enzyme digests. Analysis of the check gels revealed the expected number of bands: two for the Objective #1 and 2 digests (corresponding to the bacterial backbone and the insert), and four for the Objective #4 digest (the bacterial backbone and the three released CL fragments).

Table 4. The PCR primers used to generate linear DNA fragments for yeast transformation. For each primer set, the following information is provided: the forward (FWD) and reverse (REV) primer names, their sequences (presented in the 5' to 3' direction), the melting temperature (Tm) as determined by Benchling using the SantaLucia 1998 thermodynamic parameters for DNA, and the experimentally determined optimal annealing temperature and extension time used for PCR amplification to achieve replicable results. The symbol '~' indicates approximate values.

Primer set #	Name	Sequence (5' to 3')	Tm (°C)	PCR cycling conditions	Purpose	Object-ive(s)
1	ECH-UP FWD	cggccgcgctgaggg	63.3	62°C annealing, 15 sec extension, ~790 bp fragment	Universal primer for amplifying fragment #1 (contains upstream cHR and AJ) from EasyClone YIps	1 and 2
	IA-UP.REV	atcgcacgcattccgttgg	61.7			
2	IA-DWN.FWD	cgcgtgcattcatccgc	60.0	62°C annealing, 45 sec extension, ~2700 bp fragment	Universal primer for amplifying fragment #2 (contains *hphMX6* cassette, downstream cHR and AJ) from EasyClone YIps	
	ECH-DWN.REV	cggccgcgctgaggtc	63.5			
3	IA-UP.FWD	gcgatgagcgacctcatgc	61.6	62°C annealing, 45 sec extension, 1918 bp fragment	Amplifying GFP cassette with ~200 bp EasyClone AJs	1-3
	IA-DWN.REV	gcgtcccaaaaccttctcaagc	62.5			
4	ADE2(30) -UP. FWD	tgcggaaatagcatatgctga catcctatg	65.2	62°C annealing, 15 sec extension, 281 bp fragment	Amplifying fragment #1 containing 30 bp upstream cHR to *ADE2* locus and EasyClone AJ	3
	IA-UP.REV	atcgcacgcattccgttgg	61.7			
5	IA-DWN.FWD	cgcgtgcattcatccgc	60.0	62°C annealing, 40 sec extension, 2186 bp fragment	Amplifying fragment #2 containing 30 bp downstream cHR to *ADE2* locus, EasyClone AJ, and *hphMX6* cassette	
	ADE2(30)-DWN. REV	gtgacaatagtctctgctcata gaactcca	63.9			
6	ADE2(50)-UP. FWD	gttttaattccacgcttgcttgcg	62.4	62°C annealing, 15 sec extension, 301 bp fragment	Amplifying fragment #1 containing 50 bp upstream cHR to *ADE2* locus and EasyClone AJ	
	IA-UP.REV	atcgcacgcattccgttgg	61.7			
7	IA-DWN.FWD	cgcgtgcattcatccgc	60.0	61°C annealing, 40 sec	Amplifying fragment #2 containing 50 bp	

	ADE2(50)-DWN. REV	attttggcgttccatttgaagtgac	61.2	extension, 2206 bp fragment	downstream cHR to *ADE2* locus, EasyClone AJ, and *hphMX6* cassette	
8	ADE2(200)-UP. FWD	ggaacacctctaggcatttgcac	62.0	62°C annealing, 15 sec extension, 451 bp fragment	Amplifying fragment #1 containing 200 bp upstream cHR to *ADE2* locus and EasyClone AJ	
	IA-UP.REV	atcgcacgcattccgttgg	61.7			
9	IA-DWN.FWD	cgcgtgcattcatccgc	60.0	59°C annealing, 40 sec extension, 2356 bp fragment	Amplifying fragment #2 containing 200 bp downstream cHR to *ADE2* locus, EasyClone AJ, and *hphMX6* cassette	
	ADE2(200)-DWN. REV	actacattacaggtagaactgat attcc	58.4			
10	ADE2(400)-UP. FWD	ataaacttatatattacttgttttc tagataagcttcgtaac	61.4	61°C annealing, 15 sec extension, 651 bp fragment	Amplifying fragment #1 containing 400 bp upstream cHR to *ADE2* locus and EasyClone AJ	
	IA-UP.REV	atcgcacgcattccgttgg	61.7			
11	IA-DWN.FWD	cgcgtgcattcatccgc	60.0	61°C annealing, 45 sec extension, 2556 bp fragment	Amplifying fragment #2 containing 400 bp downstream cHR to *ADE2* locus, EasyClone AJ, and *hphMX6* cassette	
	ADE2(400)-DWN. REV	caccattacaacgaacgcca ttatg	61.2			
12	ADE2(200).UP-D2.FWD	ggaacacctctaggcatttgcac aattgaatgtaaagaatctac	69.5	73°C annealing, 15 sec extension, 481 bp fragment	Amplifying fragment #1 containing 200 bp upstream cHR to *ADE2* locus and 60 bp EasyClone AJ	
	F1(UP)+eGFP(UP) -30HR. REV	attctactgataagccaaaggtg acggggtatcgcacgcattccgt tg	76.5			
13	eGFP(DWN)+F2 (DWN)-30HR. FWD	gcagaagtgacatctggacgct aagaccgacgcgtgcattcatc cgctc	79.4	75°C annealing, 40 sec extension, 2386 bp fragment	Amplifying fragment #2 containing 200 bp downstream cHR to *ADE2* locus, 60 bp EasyClone AJ, and *hphMX6* cassette	
	ADE2(200).DWN-D2.REV	actacattacaggtagaactgat attccaatcaaaatctctgtcgct c	69.8			
14	CC(eGFP)-UP.FWD	accccgtcacctttggcttatc	62.6	62°C annealing, 25 sec extension, 1505 bp fragment	Amplifying GFP cassette with no EasyClone AJ homology	
	CC(eGFP)-DWN. REV	tcggtcttagcgtccagatgtc	61.8			

15	F1(UP)+eGFP(UP)-30HR. FWD	caacgtatctaccaacggaatgcgtgcgataccccgtcacctttggcttatc	77.7	78°C annealing, 25 sec extension, 1565 bp fragment	Amplifying GFP cassette with 30 bp EasyClone AJ homology added by designing the primers with 30 bp overhangs	3 and 4
	eGFP(DWN)+F2(DWN)-30HR. REV	cttttcggttagagcggatgaatgcacgcgtcggtcttagcgtccagatgtc	78.6			
17	ADE2(400)-UP. FWD	ataaacttatatattacttgttttctagataagcttcgtaac	61.4	59°C annealing, 15 sec extension, 600 bp fragment	Amplifying fragment #1 containing 400 bp upstream cHR to *ADE2* locus and TINS1.A	4
	TINS1.A-DWN. REV	gtaaggatccttatatatagtctggttc	56.6			
18	TINS1.A-UP. FWD	aatcggatgatgtatatacgaaaag	55.6	60°C annealing, 30 sec extension, 2181 bp fragment	Amplifying fragment #2 containing 400 bp downstream cHR to *ADE2* locus, TINS1.D, and *hphMX6* cassette	
	ADE2(400)-DWN. REV	caccattacaacgaacgccattatg	61.2			
19	TINS1.A-UP.FWD	aatcggatgatgtatatacgaaaag	55.2	55°C annealing, 30 sec extension, 1828 bp fragment	Amplifying GFP cassette with no TINS1.A and TINS1.D as AJs	
	TINS1.D-DWN.REV	catcattatctaaaccgaacgc	55.7			

2.4 Yeast Transformation

Yeast transformations were performed using a protocol from the Downey lab derived from [101] to integrate DNA into *S. cerevisiae* lab strain BY4741 obtained from the Baetz Lab. BY4741 is a common yeast lab strain derived from S288C with the genotype of MATa his3Δ1 leu2Δ0 met15Δ0 ura3Δ0 [102]. Yeast transformation was performed by first growing a BY4741 single colony overnight in 10 mL YPD at 30°C (200-250 rpm), then diluting 1:50 into 50 mL YPD and growing to OD600 of 0.8-1.0. Cells were pelleted, washed with water, and resuspended in 0.1 M LiAc. For each transformation, 50 µL of cells were pelleted and resuspended with 240 µL 50% PEG, 36 µL 1 M LiAc, 10 µL denatured ssDNA (10 mg/mL), and transforming DNA. After vortexing and 30 min incubation at 30°C, cells were heat-shocked at 42°C for 15 min, pelleted, washed with water.

The volume of sterile water used to resuspend the transformed yeast cells before plating onto Yeast extract Peptone Dextrose (YPD) agar plates was adjusted to achieve the desired plating density. For undiluted plating (equivalent to a 1:1 dilution in the context of the final resuspension volume), the cell pellet was resuspended in 200 µL of water, and the entire volume was plated. To achieve a 1:2 dilution, the pellet was resuspended in 400 µL of water, and 200 µL were plated. For higher dilutions, such as a 1:32 dilution, a serial dilution approach was used. First, a 1:2 dilution was made (resuspending in 400 µL and taking 200 µL). Then, to achieve an approximate 1:32 dilution from the initial 200 µL resuspension, 6.25 µL of the resuspended cells were added to 193.75 µL of sterile water to bring the final volume to 200 µL for plating.

Following overnight incubation at 30°C on YPD, recovered yeast cells were replica plated onto selective media agar using a sterile velvet pad to transfer the colony pattern. These selective plates were then incubated at 30°C for 2-3 days to select for transformants.

YPD plates were made following Cold Spring Harbor Protocols [103]. When appropriate, yeast drop out Synthetic Complete (SC) media was used when detecting auxotrophic markers. SC agar plates were made following Sigma-Aldrich's protocol [104] using yeast synthetic dropout supplements without histidine, leucine, tryptophan, and uracil (Sigma, Y2001-20G), which were added based on the needs of the experiment.

The BY4741 Cas9-expressing strain was created by transforming 500 ng of pCfB2312 (YRp with a *KanMX* marker carrying SpCas9 endonuclease gene under the transcriptional control of the *TEF1* promoter and *CYC1* terminator). Post-transformation, the cells were plated onto YPD agar then replica plating after overnight incubation onto YPD + G418 [200 ng/µL]. Liquid overnight cultures in YPD + G418 [200 ng/µL] were made for single colonies that

successfully integrated the Cas9 expressing YRp and were stored as glycerol stocks at -80°C for downstream applications.

The amount of transforming DNA varied based on its type: 1 picomole (pmol) for PCR fragments, 1000 ng for restriction enzyme-digested products, and 500 ng for plasmids (YEp or YRp). The required mass of a DNA fragment (in ng) was calculated using the formula:

$$Weight\ of\ fragment\ (ng) = \frac{pmol \times Length\ of\ fragment\ (bp) \times 650\ daltons}{1000}$$

where 650 daltons represents the approximate average mass of one base pair (bp) of DNA (calculation is based on information provided by NEB [105]). The volume of DNA to transform (µL) was determined using this calculation:

$$Volume\ of\ DNA\ (\mu L) = \frac{Weight\ of\ fragment\ (ng)}{DNA\ concentation\ (\frac{ng}{\mu L})}$$

where the DNA concentration was obtained by measuring absorbance of DNA at 260 nm using a Thermo Scientific NanoDrop 2000 spectrophotometer.

2.5 Data Analysis

Plate images were captured using a brightfield imaging box (made by Dr. Kaern) and an *in vivo* imaging system (IVIS) at the NRC when fluorescent measurements were required to detect green fluorescent protein (GFP) integrations. The IVIS settings were as follows: 0.50 s exposure time, small binning, C field of view, 480 nm excitation filter, 520 nm emission filter.

Colony counting was performed by uploading plate images to the ImageJ FIJI software [106], with parameters set to optimally distinguish individual colonies based on size and circularity (protocol detailed in Appendix A).

Transformation efficiency was calculated as the number of colony-forming units (CFUs) obtained per picomole (pmol) of DNA transformed using the following equation [107]:

$$Transformation\ Efficiency = \left(\frac{Number\ of\ Colonies\ Counted}{pmol\ of\ DNA\ Transformed}\right)\left(\frac{Final\ Volume\ at\ Recovery\ (mL)}{Volume\ Plated\ (mL)}\right)$$

where the final volume at recovery/ volume plated allows for the normalization of the data by the dilution factor that the transformed yeast cells were plated onto YPD only plates for overnight recovery.

For experiments involving selection media and screening of one gene as a reporter (example GFP), the precision of integration can be determined following this calculation [108]:

$$Precision = \frac{Number\ of\ True\ Positive\ Colonies}{Number\ of\ True\ Positive\ Colonies\ +\ Number\ of\ False\ Positive\ Colonies}$$

where the proportion of colonies that truly have the desired integration (true positives) can be determined out of all the colonies that grew on the selection media.

For applications in which an understanding of integration efficiency is need, the following calculation was used:

$$Integration\ Efficiency = \left(\frac{Number\ of\ True\ Positive\ Colonies}{Total\ Number\ of\ Colonies\ Counted}\right) \times\ 100\%$$

where the number of true positive colonies represents the number of colonies with confirmed integrations of desired GOIs while the total number of colonies counted represents all the true/false positive/negative colonies observed that grew on the selection media.

For the multiplexing experiment in Objective #2, the assessment of simultaneous integration at three distinct sites was achieved using visual and selectable markers (antibiotic, *hphMX6*, and auxotrophic, *URA3* and *LEU2*). This approach aims to bypass the often

challenging and time-consuming need for yeast colony PCR validation [109], as proper transformants can be readily identified by growth on selective media and the presence of GFP expression via IVIS imaging. Furthermore, since we are using the well-established EasyClone system's multiplexing design with its pre-validated integration sites [73], further locus-specific validation was unnecessary for this study.

Chapter 3: Results

3.1 Establishing an Efficient Clone-less *in vivo* DNA Assembly and Integration Method in *S. cerevisiae*

To assess the feasibility of our clone-less *in vivo* DNA assembly and integration method, we tested four conditions to integrate a *GFP* cassette with a hygromycin selection marker into the X-4 chromosomal site of *S. cerevisiae* BY4741. The integrated DNA comprised: an upstream X-4 chromosomal homology region (cHR, 522 bp), an upstream EasyClone assembly junction (AJ) element (*ADH1* terminator, 226 bp), a *TDH3* promoter-driven *GFP* cassette, a downstream EasyClone AJ element (*CYC1* terminator, 207 bp), a hygromycin resistance cassette, and a downstream X-4 cHR (446 bp). Both *in vitro* and *in vivo* DNA assembly methods were evaluated for this integration (Figure 2).

The first condition involved an *in vitro* assembly of a linear YIp (pCfB2194-GFP) followed by yeast transformation using 1000 ng of DNA. The second condition combined the *in vitro* assembly with CRISPR-Cas9-assisted integration. The third condition explored an *in vivo* DNA assembly through the co-transformation of three linear PCR fragments, derived from an EasyClone YIp (pCfB2194) and a *GFP* donor plasmid (pECIAK-GFP) at a 1:1:1 pmol ratio. Finally, the fourth condition integrated our clone-less *in vivo* assembly method with a CRISPR-mediated double-strand break. For conditions 2 and 4, transformations were performed in a Cas9-expressing yeast strain (Chapter 2.4) with 500 ng of X-4 targeting gRNA (pCfB3042) co-transformed with the linear DNA fragments.

Each condition was tested in technical triplicates (n=3). After transformation, yeast recovery mixtures were plated on YPD (diluted 1:4 for conditions without Cas9, 1:32 for those

with Cas9), followed by replica plating onto YPD + Hygromycin B [200 ng/µL]. Successful transformants were identified by hygromycin resistance and GFP expression, assessed by IVIS imaging and quantified using FIJI (Appendix A). Colony counts were normalized for DNA amount and dilution factor (Chapter 2.5) to determine GFP-positive colony-forming units (CFU) per pmol of DNA transformed (Figure 7).

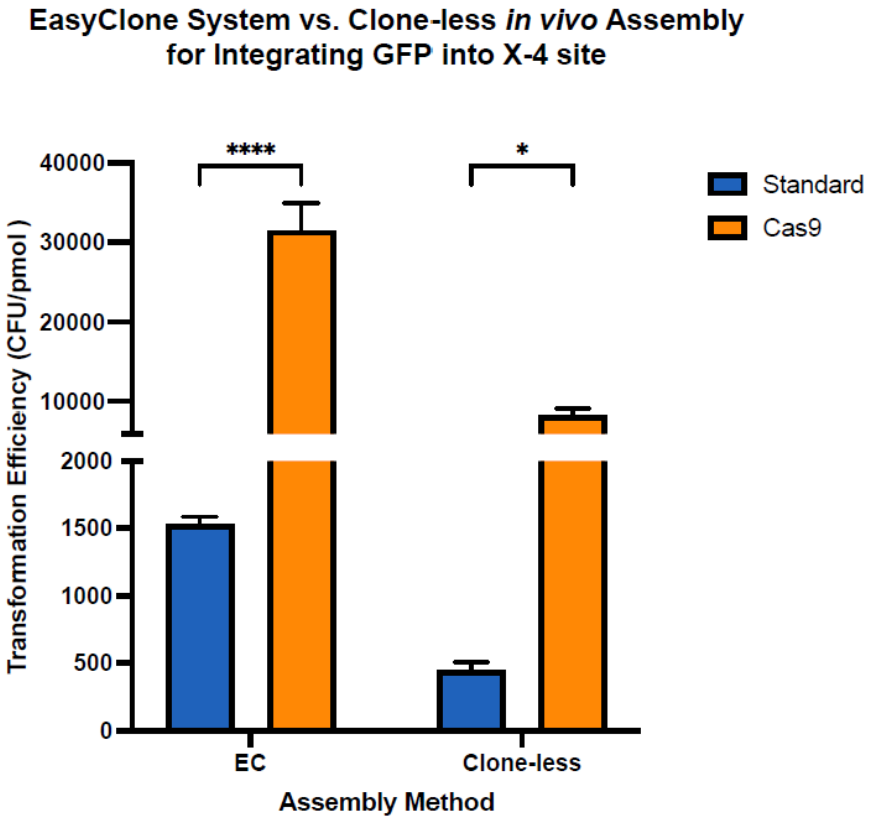

Figure 7. Transformation efficiency for GFP integration at the X-4 locus using the EasyClone (EC) system versus our clone-less *in vivo* assembly method. This was assessed under conditions without (standard) or with Cas9-mediated double-stranded DNA break. Transformation efficiency was calculated by normalizing the number of colonies counted on YPD+ Hygromycin B [200 ng/µL] selection plates to determine the GFP-positive colony-forming units (CFU) per pmol of DNA transformed (0.514 pmol for EC and 1 pmol of each fragment for clone-less). Values represent the mean and standard error (error bars) of triplicate (n=3) transformations in BY4741 yeast. Statistical significance was determined by two-way ANOVA using Šídák's multiple comparisons test (* $p<0.05$, **** $p<0.0001$). Figure and analysis generated using GraphPad Prism.

The transformation efficiency for integrating *GFP* at the X-4 locus was evaluated in Figure 7 for the EasyClone (EC) system and clone-less *in vivo* assembly method, both with and without Cas9-mediated DSBs. Under standard conditions (no Cas9), the EasyClone system achieved approximately 1500 GFP-positive CFU/pmol, which was higher than the 450 GFP-positive CFU/pmol observed with our clone-less method. However, the introduction of Cas9 significantly enhanced the integration efficiency for both methods. For the EC system, a roughly 20-fold increase with approximately 31500 GFP-positive CFU/pmol was observed. The clone-less method showed a similar improvement with an approximately 20-fold increase to around 8300 GFP-positive CFU/pmol.

Two-way ANOVA with Šídák's multiple comparisons test confirmed that Cas9 significantly enhanced transformation efficiency for both EasyClone (****, $p<0.0001$) and clone-less (*, $p<0.05$) methods. This analysis assessed the impact of both the assembly method (EasyClone vs. Clone-less) and the presence of Cas9 on transformation efficiency. The p-values indicate that the presence of Cas9 had a statistically significant positive effect on transformation efficiency for both approaches, supporting the conclusion that targeted DNA cleavage by Cas9 is a key factor in improving DNA integration efficiency, regardless of the assembly strategy employed.

Appendix B, Figure 1 presents the raw counts of hygromycin-resistant colonies from transformations using the EasyClone system or our clone-less method, with and without Cas9-mediated DSB. Colonies exhibiting GFP fluorescence on selective media were true positives, indicating successful integration and expression. Colonies resistant to hygromycin but lacking GFP were false positives. The precision (Chapter 2.5), defined as the proportion of GFP-positive

colonies among all hygromycin-resistant colonies, was high for EasyClone (0.987 standard, 0.988 with Cas9) but slightly lower for the clone-less method (0.914 standard, 0.861 with Cas9).

3.2 Identifying Compatible Genomic Integration Sites Using EasyClone Toolkits

To identify suitable genomic integration sites for multiplexing, five EasyClone chromosomal sites (X-2, X-4, XI-3, XII-4, XII-5) with corresponding EasyClone 2.0 YIps (carrying *hphMX6*) and compatible MarkerFree gRNAs were screened. Using our clone-less *in vivo* DNA assembly and integration method (Figure 2), *GFP* was targeted to each site both without (standard) and with Cas9-mediated DSB.

For each site, three linear DNA fragments were co-transformed: fragment 1 (upstream cHR and *ADH1* terminator EasyClone AJ, primers set 1, Table 4), fragment 2 (*CYC1* terminator EasyClone AJ, *hphMX6* cassette, and downstream cHR, primer set 2, Table 4), and the *GFP* cassette flanked by EasyClone AJs (primer set 3 in Table 4). Standard transformations (no Cas9) involved a 1:1:1 pmol ratio of the three PCR-amplified fragments into BY4741, with a 1:4 dilution of the reaction mixture plated on YPD for overnight recovery. For Cas9-assisted integration, 500 ng of the site-specific gRNA YEp was co-transformed with the DNA fragments (1:1:1 pmol ratio) into a Cas9-expressing BY4741 strain, followed by a 1:32 dilution plating. The YPD recovery plates were replica plated onto YPD + Hygromycin B [200 ng/µL] to select for colonies with the *hphMX6* cassette integrated. Successful GFP integration was assessed by imaging whole plates using an IVIS to identify fluorescent colonies. Figure 8 presents the normalized GFP-positive CFUs (Chapter 2). All experiments were performed in technical triplicates (n=3).

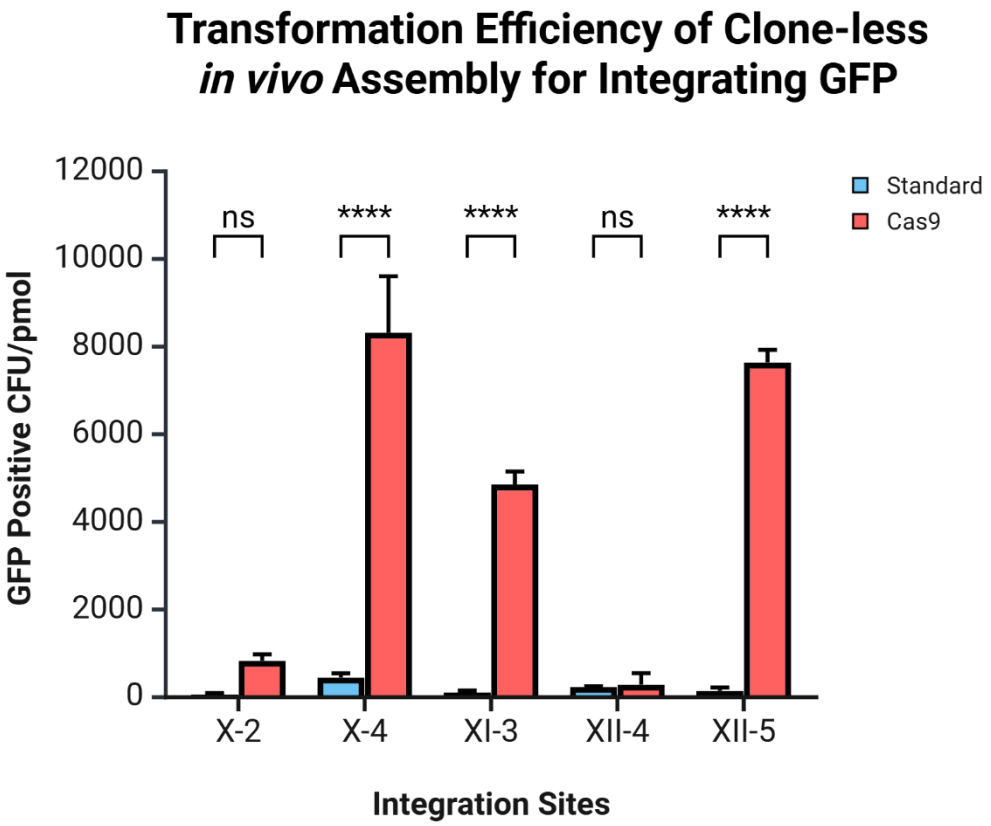

Figure 8. Transformation efficiency of GFP integration at EasyClone *S. cerevisiae* chromosomal sites using our clone-less *in vivo* DNA assembly and integration method with and without Cas9- mediated double-stranded DNA breaks. The normalized GFP-positive colony-forming units (CFU) per pmol of DNA transformed for clone-less integration of GFP at five genomic loci (X-2, X-4, XI-3, XII-4, XII-5) without (standard) and with Cas9 are plotted. Data represent the mean and standard deviation (error bars) of technical triplicates (n=3). Statistical significance was determined by two-way ANOVA with Bonferroni's multiple comparisons test. Figure generated using BioRender.com.

Figure 8 illustrates the efficiency of clone-less *in vivo* assembly for integrating GFP at five different genomic loci, with and without Cas9-assisted targeting. It is apparent that Cas9-mediated DSB increases the transformation efficiency 13-fold at X-2, 18-fold at X-4, 45-fold at XI-3, 1-fold at XII-4, and 53-fold at XII-5 chromosomal integration site. Therefore, it is evident that while integration was detectable at all sites with and without Cas9-assisted conditions, the efficiency varied considerably between loci. The X-4, XI-3, and XII-5 sites exhibited the highest normalized integration efficiencies with Cas9, reaching approximately 8300, 4800, and 7600 GFP-positive CFU/pmol, respectively. In contrast, the standard (no Cas9) conditions generally

resulted in much lower integration efficiencies, although a low level of integration was observed at the X-4 site even without Cas9 (450 GFP-positive CFU/pmol).

The statistical analysis of a two-way ANOVA with Bonferroni multiple comparisons test revealed a significant impact of both the integration site and experimental methods on GFP-positive CFU/pmol ($p < 0.0001$ for both factors), highlighting their combined influence on the dependent variable. Further pairwise comparisons identified statistically significant differences between specific standard and Cas9 conditions, notably in X-4, XI-3, and XII-5 (****, $p < 0.0001$), whereas X-2 and XII-4 showed no significant differences.

The resultant analysis is that the X-4, XI-3, and XII-5 are the most appropriate sites to target in multiplexing experiments with or without Cas9.

3.3 Demonstrating the EasyClone System's Multiplexing Capability by Integrating Four Genes into Three Distinct Loci

To establish a positive control for multiplex genome editing, we aimed to simultaneously integrate three DNA cargos (cloned into three EasyClone YIps) into three distinct genomic loci of *S. cerevisiae* BY4741, using CRISPR-Cas9. Specifically, *GFP* with hygromycin resistance (*hphMX6*) was targeted to the X-4 locus, *URA3* (selectable on SC media lacking uracil) to the XI-3 locus, and *LEU2* (selectable on SC -leucine) to the XII-5 locus. This experiment, employed a multi-site targeting gRNA YEp from the EasyClone MarkerFree toolkit (pCfB3052) to simultaneously guide Cas9 to the X-4, XI-3, and XII-5 chromosomal sites.

Technical triplicates (n=3) were performed with a Cas9-expressing yeast strain (BY4741) to assess targeted integration at loci X-4, XI-3, and XII-5. For each replicate, 1000 ng of linear DNA fragments (linearized YIp with GOI) were co-transformed with 500 ng of either a

multiplexing gRNA plasmid or a mock gRNA (pCfB.MOCK). Following transformation, cells were plated on YPD (diluted 1:1 for mock, 1:2 for multiplexing). Integration was assessed via replica plating onto selective media (SC -Ura -Leu + Hygromycin for mock; YPD + Hygromycin, SC -Ura -Leu + Hygromycin, SC -Ura + Hygromycin, and SC -Leu + Hygromycin for multiplexing). GFP integration was further evaluated by fluorescence visualization.

The efficiency of multiplexed integration was further assessed by examining raw colony counts on various selection plates (Appendix B, Figure 2). Compared to the number of GFP-positive colonies growing on the triple selection media (SC -Ura -Leu + Hygromycin), a 2-fold increase was observed on YPD + Hygromycin (selecting for X-4 integration), a 1.5-fold increase on SC -Ura + Hygromycin (selecting for X-4 and XII-3 integration), and a 0.5-fold decrease on SC -Leu + Hygromycin (selecting for X-4 and XII-5 integration). To evaluate the precision of the multiplexing approach, colonies growing on the triple selection plates (SC -Ura -Leu + Hygromycin) were analyzed, with GFP-positive colonies considered true positives for integration at all three targeted loci. The calculated precision was 0.86, indicating that approximately 14% of the colonies selected for integration at all three loci did not exhibit GFP expression, suggesting incomplete integration of all four genes in those clones.

Figure 9 presents the normalized transformation efficiency (CFU/pmol) from counting GFP-positive colonies growing on the triple selection media (SC -Ura -Leu + Hygromycin) for the simultaneous integration of four genes into three different loci using the EasyClone system, comparing a mock gRNA control to conditions with a multiplex gRNA simultaneously targeting the X-4, XI-3, and XII-5 loci. The bar graph shows a clear trend of higher transformation efficiency in the multiplexing condition compared to the mock gRNA control.

An unpaired t-test revealed a statistically significant difference in transformation efficiency between the mock and multiplex conditions (**, p = 0.0047). The mean transformation efficiency in the multiplex condition (1037 CFU/pmol) was higher than in the mock condition (2.00 CFU/pmol), with a mean difference of 1035 CFU/pmol. This substantial difference demonstrates a strong positive effect of multiplexed gRNA targeting on integration efficiency.

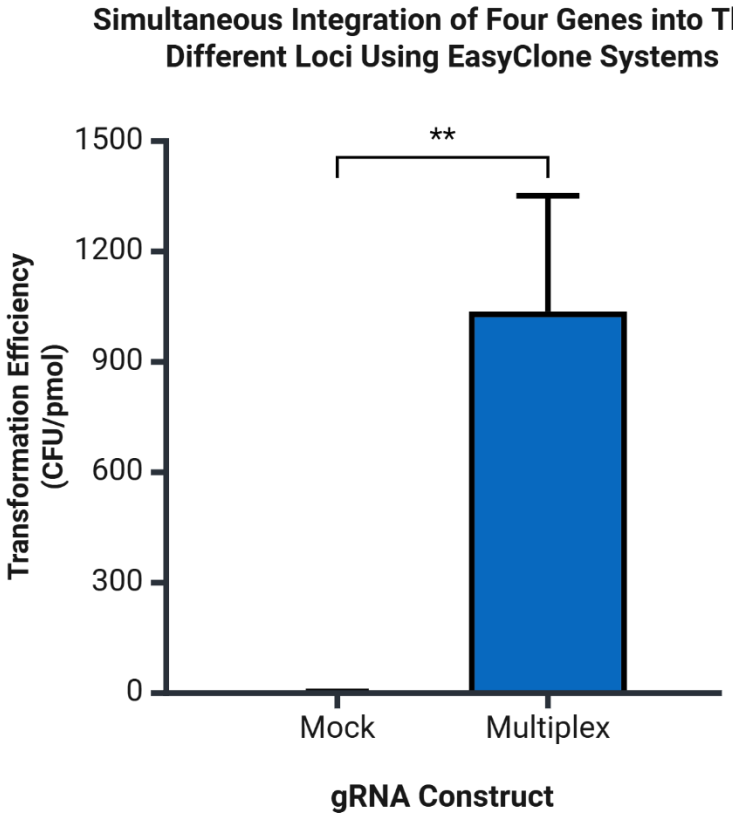

Figure 9. The transformation efficiency of successful colonies containing four genes that were simultaneously integrated into three different loci using EasyClone systems. The four genes and three integration locations are: *GFP* and *hphMX6* into X-4, *URA3* into XII-3, and *LEU2* into XII-5. These genes were integrated into EasyClone YIps, linearized, and co-transformed with mock or multiplex (targeting the three integration sites) gRNAs into a BY4741 yeast strain expressing Cas9. Successful integrations were determined by counting colonies on plates with triple selection (SC –Ura -Leu + Hygromycin B [200ng/uL]) and imaged using IVIS to detect GFP-positive colonies. Data represent the mean and standard deviation (error bars) of technical triplicates (n=3). Statistical significance was determined by an unpaired t-test. Figure generated using BioRender.com.

3.4 Determining the Impact of Varying Homology Region Lengths on *in vivo* DNA Assembly Targeting the *ADE2* Locus

To enhance our understanding of yeast's endogenous homologous recombination (HR) capabilities, I investigated the impact of varying the length of chromosomal homology regions (cHRs) and assembly junctions (AJs) in our three-fragment clone-less DNA assembly method, targeting the *ADE2* locus. The *ADE2* gene provides a colorimetric readout, where disruption leads to pink yeast colonies, aiding in identifying successful gene of interest (GOI) integrations.

Our pEC.IV ade2(400)::HphMX YIp is designed to integrate a GOI with a *hphMX6* marker in the *ADE2* locus on chromosome XV (Figure 4). This YIp was PCR-amplified (Table 4) to generate fragments #1 (upstream *ADE2* cHR, *ADH1* terminator AJ) and #2 (*CYC1* terminator AJ, *hphMX6*, downstream *ADE2* cHR). For each condition (varying cHR/AJ lengths), linear fragments (including a *GFP* GOI) were co-transformed in a 1:1:1 pmol ratio with 500 ng of either a mock gRNA (pCfB.MOCK) or an *ADE2*-targeting gRNA (pCfB.XV) into a Cas9-expressing BY4741 strain. Transformants with proper *hphMX6* integration were selected by replica plating onto YPD with hygromycin plates.

First, I tested *ADE2* cHR lengths of 30, 50, 200, and 400 bp for integrating a *GFP* cassette with about 200 bp EasyClone AJs. Figure 10 presents the transformation efficiency (CFU/pmol) from counting GFP-positive colonies growing on YPD + Hygromycin [200 ng/µL] plates imaged using an IVIS. With the *ADE2*-targeting gRNA, successful integration was observed across all tested cHR lengths. The highest efficiency was achieved with the 400 bp cHRs, showing approximately 6300 pink GFP-positive CFU/pmol. A substantial level of integration was also seen with 200 bp cHRs (around 4000 CFU/pmol). Shorter cHRs of 30 bp and 50 bp resulted in lower, but still detectable, integration efficiencies (approximately 1700 and

1000 CFU/pmol, respectively). In contrast, the mock gRNA results generally showed minimal integration, indicating high target specificity. However, a notable exception was observed with the 400 bp cHRs, where the mock gRNA condition yielded an approximately 870 pink GFP-positive CFU/pmol, suggesting increased random or non-Cas9 mediated integration with longer homology arms.

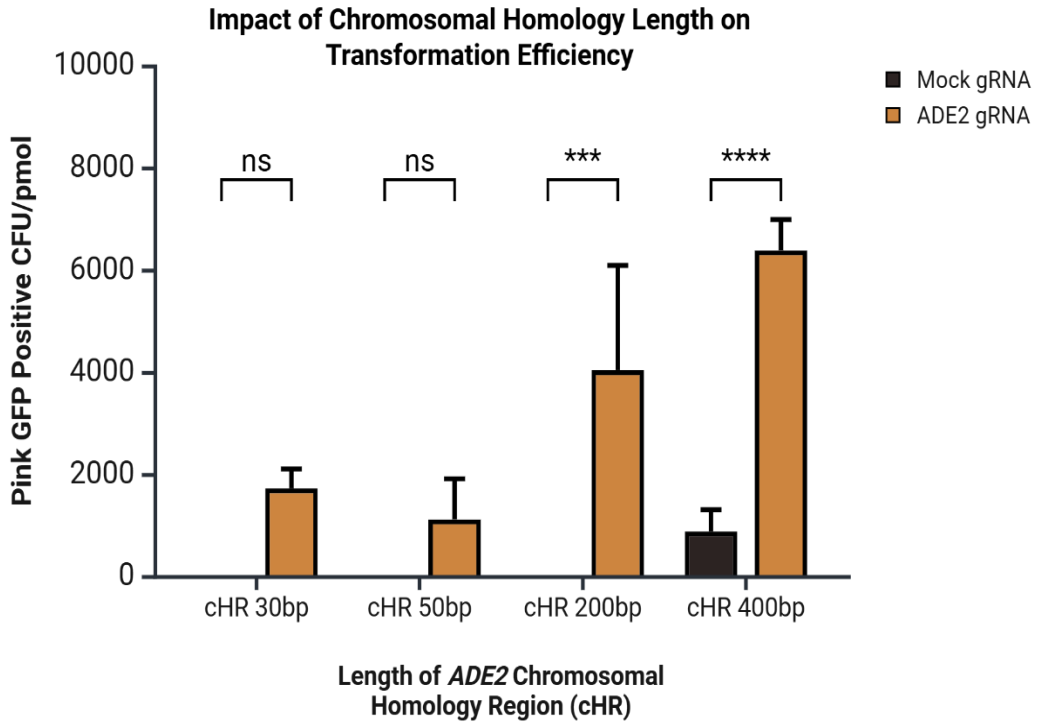

Figure 10. The impact of varying chromosomal homology region lengths from 30-400 bp on transformation efficiency using our Cas9-mediated clone-less *in vivo* DNA assembly method to integrate *GFP* in the *ADE2* locus. Linear products were PCR amplified from the same YIp, with modifications being made only to the length of cHRs. These fragments were transformed into yeast strain BY4741 containing Cas9 in a 1:1:1 pmol ratio with 500 ng of *ADE2* targeting or mock gRNA. Post- transformation, the reaction mixtures were plated on YPD only agar plates in a 1:32 dilution and then replica plated onto YPD + Hygromycin B [200ng/µL] plates after 20 hours. Normalized values for the pink GFP-positive colony forming units (CFU) per pmol of DNA transformed are plotted. The pink, GFP-positive colonies were counted by analyzing brightfield and fluorescent (using IVIS) images of the plates on FIJI. Data represent the mean and standard deviation (error bars) of technical triplicates (n=3). Statistical significance was determined by two-way ANOVA with Bonferroni multiple comparisons. Figure generated using BioRender.com.

The data in Figure 10 was statistically analyzed using a two-way ANOVA with Bonferroni's multiple comparisons test, which revealed significant main effects of both cHR

length ($p < 0.0001$) and the gRNA used ($p < 0.0001$) on the normalized transformation efficiency (pink GFP-positive CFU/pmol). A significant interaction between cHR length and gRNA was also observed ($p = 0.00097$), indicating that the effect of cHR length on integration efficiency depends on whether a targeting or mock gRNA was used. A significantly higher CFU/pmol was detected with the *ADE2*-targeting gRNA compared to the mock gRNA at cHR lengths of 200 bp (***, $p = 0.0006$) and 400 bp (mean difference = -5504 CFU/pmol, ****, $p < 0.0001$). In contrast, no significant differences were found between mock and *ADE2* gRNA conditions for the shorter cHR lengths (30 bp and 50 bp).

Furthermore, the integration efficiency, calculated as the percentage of correctly integrated colonies out of all colonies on the selection plate (Chapter 2.5), can be determined using Appendix B, Figure 3. For the *ADE2* gRNA condition, the integration efficiency was 75.3% for 30 bp cHRs, 86.4% for 50 bp cHRs, 94.3% for 200 bp cHRs, and 93.6% for 400 bp cHRs, indicating a trend of higher sensitivity with increasing cHR length. In the mock gRNA condition, the integration efficiency was zero for cHR lengths of 30, 50, and 200 bp (no true positive colonies observed). However, with the 400 bp cHR and mock gRNA, the integration efficiency was 59.6%, indicating that even without Cas9-induced cleavage, longer homology regions can promote detectible levels of proper integration.

The second factor tested to better understand yeast's HR capabilities is the effect of AJ length (30, 60, and 200 bp, with a 0 bp control) on the efficiency of integrating a *GFP* GOI cassette, using 200 bp cHRs (Figure 4). Figure 11 presents the transformation efficiency (CFU/pmol) that was normalized from counting GFP-positive colonies growing on YPD with hygromycin plates by the dilution factor plated and amount of DNA transformed. The graph reveals that the highest integration efficiency was achieved with 200 bp AJs, while shorter AJs

(30 bp and 60 bp) also resulted in successful integration at lower efficiencies. Notably, the mock gRNA conditions showed minimal integration across all AJ lengths, indicating a high degree of target specificity. The absence of an assembly junction (0 bp AJ) resulted in no integration.

Statistical analysis of the data presented in Figure 11 was conducted using a two-way ANOVA with Bonferroni's multiple comparisons test. This revealed that there were significant main effects of both AJ length ($p = 0.00048$), and the gRNA used ($p < 0.0001$), along with a significant interaction between the two factors ($p = 0.00049$). Furthermore, there is a significantly higher CFU/pmol observed with the *ADE2*-targeting gRNA compared to the mock gRNA at AJ lengths of 60 bp (*, $p = 0.026$) and 200 bp (****, $p < 0.0001$).

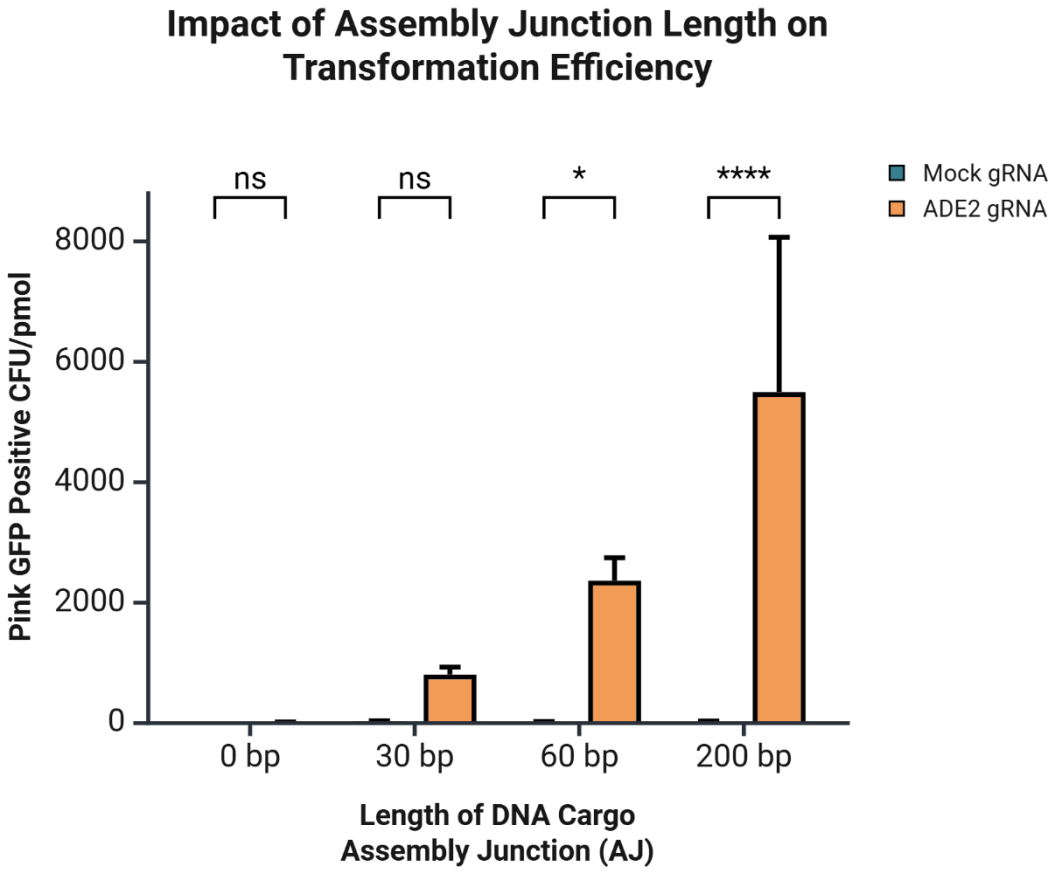

Figure 11. The impact of varying assembly junction lengths from 0-200 bp on transformation efficiency using our Cas9-mediated clone-less *in vivo* DNA assembly and integration method to integrate *GFP* in the *ADE2* locus. Linear products were PCR amplified from the same plasmids, with modifications being made only to the

length of AJs. These fragments were transformed into yeast strain BY4741 containing Cas9 in a 1:1:1 pmol ratio with 500 ng of *ADE2* targeting or mock gRNA. Post-transformation, reaction mixtures were plated on YPD agar at dilutions of 1:1 (all mock samples and 0 bp AJs), 1:2 (30 and 60 bp AJs), or 1:32 (200 bp AJs) to obtain countable colony numbers, followed by replica plating onto YPD + Hygromycin B [200 ng/µL] after 20 hours. Normalized values for the pink GFP-positive colony forming units (CFU) per pmol of DNA transformed are plotted. The pink, GFP-positive colonies were counted by analyzing brightfield and fluorescent (using IVIS) images of the plates on FIJI. Data represent the mean and standard deviation (error bars) of technical triplicates (n=3). Statistical significance was determined by two-way ANOVA with Bonferroni multiple comparisons. Figure generated using BioRender.com.

3.5 One-Step Clone-less Yeast Transformation for Simultaneous Integration of Two Genes into the *ADE2* Locus Using a Cargo Linker Liberating YIp

pEC.IV(XV.CL.MX) is a YIp designed to integrate two genes (a DNA cassette and an MX selection marker) in a simultaneous yeast transformation reaction into the *ADE2* loci. The plasmid has SapI restriction enzyme cut sites at locations that enable the liberation of the cargo linker (CL) fragments essential for our clone-less *in vivo* DNA assembly and integration approach (Figure 5). We investigated the transformation efficiency of co-transforming 1000 ng of the SapI-digested reaction of pEC.IV(XV.CL.MX) with 1 pmol of a PCR amplified *GFP* cassette that has 30 bp AJs and 1 pmol of a *hphMX6* cassette with its *TEF* promoter (372 bp) and terminator (203 bp) as AJs into a Cas9-expressing BY4741 strain.

Figure 12 presents the transformation efficiency, measured as pink and GFP-positive colony-forming units per pmol (CFU/pmol), when simultaneously integrating two genes (*GFP* and *hphMX6*) into the *ADE2* locus using a linearized YIp. The graph compares a mock gRNA control to an *ADE2*-targeting gRNA. A Welch's t-test revealed a statistically significant effect of the gRNA target on transformation efficiency (*, $p = 0.036$). The mean CFU/pmol in the *ADE2*-targeting condition (198 pink GFP+ CFU/pmol) was noticeably higher than in the mock gRNA condition (0 pink GFP+ CFU/pmol), with a mean difference of 198. This indicates that targeting

the *ADE2* locus with a specific gRNA significantly enhanced the integration efficiency of the two genes compared to the non-targeting mock gRNA.

Appendix B, Figure 4 presents the raw number of colonies observed on YPD + Hygromycin B [200 ng/µL] for the data reported in Figure 12. In the mock gRNA condition, an average of 692 white and GFP-negative colonies grew on the selective media, indicating integration of the resistance marker without the intended *ADE2* disruption or GFP integration. In the *ADE2* gRNA condition, where pink colonies indicate *ADE2* disruption, the integration efficiency for achieving a pink, GFP-positive phenotype (true positive) out of all the colonies observed (pink/ white and GFP-positive/negative) was calculated to be 27.2%. The precision for the *ADE2* gRNA condition, representing the likelihood that a pink colony also contained GFP, was 0.538. This suggests that among the colonies exhibiting *ADE2* disruption (pink), approximately 53.8% also showed GFP expression. Conversely, this implies that about 46.2% of the pink colonies selected on hygromycin did not contain the *GFP* insert.

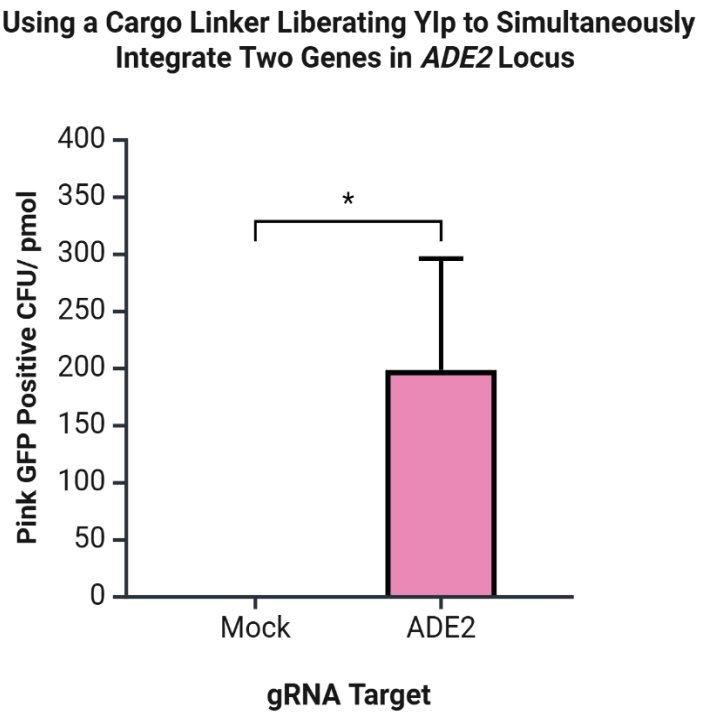

Figure 12. The transformation efficiency, represented as pink and GFP-positive colony forming units/pmol, when simultaneously integrating two genes into the *ADE2* locus. pEC.IV(XV.CL.MX) YIp was digested with SapI to release the linear fragments that would enable the integration of a PCR amplified *GFP* and *hphmx6* cassettes into the *ADE2* locus. These linear fragments were co-transformed (1 pmol of each of *GFP* and *hphMX6* cassettes, 1000 ng of digest) with an *ADE2* targeting or mock gRNA (500 ng) into a BY4741 yeast strain expressing Cas9. The normalized pink GFP-positive colony forming units (CFU) that grew on YPD + Hygromycin [200 ng/µL] are plotted. Data represent the mean and standard deviation (error bars) of technical triplicates (n=3). Statistical significance was determined by an unpaired t-test. Figure generated using BioRender.com.

3.6 Using Terminator Insulator Spacer Sequences as Unique Assembly Junctions for Integrating One Gene into the *ADE2* Locus

pEC.IV ADE2(400)::TINS is a YIp that provides unique assembly junctions (AJs), rather than the previously used EasyClone AJs, for our clone-less *in vivo* DNA assembly and integration method. Using primer sets 17-19 (Table 4), the YIp was PCR amplified to provide fragments #1 (contains 400 bp upstream *ADE2* cHR and TINS1.A) and 2 (TINS1.D, *hphMX6* cassette, and 400 bp downstream *ADE2* cHR) for the integration of a *GFP* cassette with TINS1.A and TINS1.D functioning as AJs. The normalized (by amount of DNA transformed and dilution

factor plated) data generated from co-transforming the linear fragments (1:1:1 pmol ratio) using *ADE2*-targeting or mock gRNAs (500 ng) are presented in Figure 13.

An unpaired t-test indicated no statistically significant difference in transformation efficiency between the mock and *ADE2* gRNA conditions ($p = 0.195$). The mean pink GFP-positive CFU/pmol for the mock gRNA condition was 800, while the *ADE2* gRNA condition showed a lower mean of 522, with a mean difference of -277.

Analysis of the raw colony counts presented in Appendix B, Figure 5, provides insights into the efficiency and precision of using TINS as unique AJs for targeted integration of a GOI cassette at the *ADE2* locus with 400 bp cHRs. A higher number of true positive colonies (pink GFP-positive colonies with hygromycin resistance) was observed on the mock gRNA plates (average of 25) compared to the *ADE2*-targeting gRNA plates (average of 16), an approximate 1.5-fold increase in the non-targeted condition. This suggests that while the selection for DNA uptake was effective, more colonies were observed with both *ADE2* disruption and *GFP* integration when integration was not specifically directed. The calculated integration efficiency indicates that with the *ADE2* gRNA 72.7% and with the mock gRNA 67.6% of colonies observed on the selection plate are true positives. The precision values reveal that the likelihood that a pink colony (showing *ADE2* disruption) also contained GFP was 0.800 for the *ADE2* gRNA and 0.862 for the mock gRNA condition.

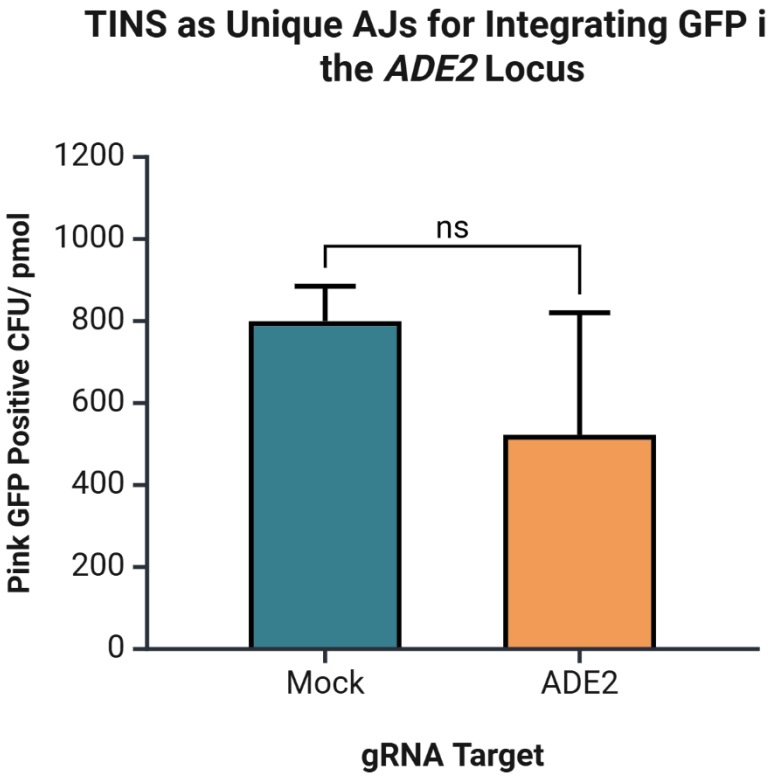

Figure 13. The transformation efficiency, represented as pink and GFP-positive colony forming units/pmol, when using terminator insulator spacer sequences as unique assembly junctions for integrating GFP into the *ADE2* locus. pEC.IV ADE2(400)::TINS YIp was PCR amplified to provide fragments #1 (contains 400 bp upstream *ADE2* cHR and TINS1.A) and 2 (TINS1.D, hphMX6 cassette, and 400 bp downstream *ADE2* cHR) for the clone-less *in vivo* DNA assembly and integration of a GFP cassette with TINS1.A and TINS1.D functioning as AJs. These linear DNA fragments were co-transformed in a 1:1:1 pmol ratio with an *ADE2* targeting or mock gRNA (500 ng) into a BY4741 yeast strain expressing Cas9. The normalized pink GFP-positive colony forming units (CFU) that grew on YPD + Hygromycin [200 ng/µL] are plotted. Data represent the mean and standard deviation (error bars) of technical triplicates (n=3). Statistical significance was determined by an unpaired t-test. Figure generated using BioRender.com.

Chapter 4: Discussion

The central hypothesis of my research is that we can design a novel yeast integrating plasmid (YIp) capable of one-step, simultaneous multi-loci integration and *in vivo* assembly of linear DNA fragments in *S. cerevisiae*, driven by homologous recombination (HR). This YIp was conceptualized as an expansion of the EasyClone system [74], [75], [76] for enhanced multiplexing by simplifying experimental steps. To support this hypothesis, my thesis aimed to make incremental improvements to existing yeast genetic engineering systems while building a foundational understanding of key genetic elements and processes that focus on efficient genome modification in *S. cerevisiae*. This involved exploring several interconnected aspects: yeast's HR capabilities, the enhancement of HR efficiency through CRISPR-Cas9-induced double-strand breaks (DSBs), the utility of yeast as a whole-cell reporter system (utilizing *ADE2*, GFP, antibiotic, and auxotrophic selection), the inherent challenges of multiplexed genetic engineering compared to single-target modifications, the development of a cargo linker liberating YIp for clone-less integration, and the design of unique assembly junctions (TINS).

4.1 Clone-less *in vivo* DNA Assembly

My first research objective was to establish an efficient clone-less *in vivo* DNA assembly and integration method in *S. cerevisiae*, leveraging its endogenous HR capabilities. Yeast possesses a remarkable ability to assemble DNA *in vivo* through its efficient HR-based DNA repair pathway [31], [32]. This inherent HR proficiency has enabled impressive *in vivo* assemblies, such as the simultaneous joining of up to 38 linear DNA fragments with 20–200 bp long homologies, as demonstrated in prominent research conducted by Daniel G. Gibson [85].

Yeast's capacity to efficiently assemble DNA *in vivo*, bypassing the need for traditional *in vitro* cloning steps, forms the foundational principle motivating the development and exploration of our streamlined clone-less DNA assembly and integration method presented in this thesis.

We hypothesized that this streamlined approach could offer an alternative to the multi-step *in vitro* cloning-based systems, such as those highlighted in Table 1. To achieve this, we chose to use elements of the well-characterized and easily accessible EasyClone system. My study was designed to mimic the EasyClone system's *in vitro* cloning requirements (DNA amplification, plasmid assembly, bacterial transformation, colony inoculation, and plasmid purification and validation) while presenting a clone-less alternative. This was achieved by PCR amplifying fragments from an EasyClone YIp to enable the *in vivo* assembly of a gene of interest (GOI) under standard and Cas9-mediated DSBs conditions (Figure 2). Our results, presented in Figure 7, demonstrate the feasibility of this clone-less method for genomic integration of *GFP* with a hygromycin resistance gene at the X-4 locus.

Under standard conditions (without CRISPR-Cas9), the traditional EasyClone system demonstrated a higher transformation efficiency (1500 GFP positive CFU/pmol) compared to our clone-less approach (450 GFP positive CFU/pmol). This difference in efficiency could arise because the EasyClone method transforms a single, pre-assembled, and linearized fragment of DNA, which may present a more readily available substrate for the yeast's HR machinery to incorporate. In contrast, our clone-less method requires the initial *in vivo* assembly of multiple linear DNA fragments before HR can lead to integration, a process that can be less efficient than direct integration of a single linearized molecule [110].

To enhance our clone-less integration method for scalability and high-throughput, we incorporated CRISPR-Cas9, a well-established tool for efficient, targeted genome editing [20]. The EasyClone MarkerFree system [76] leverages the CRISPR-Cas9 system for targeted genome editing in *S. cerevisiae*. CRISPR-Cas9 has been a pillar in the field of genetic engineering due to its simple two-component system (Cas9 protein and a gRNA), well-characterized mechanism of creating blunt-end DSBs, and the availability of various well-validated toolkits (Table 1) for its use in *S. cerevisiae* [76], [111].

The introduction of CRISPR-Cas9-mediated DSB at the X-4 locus significantly enhanced the integration efficiency for both methods tested (Figure 7). This observation aligns with the well-established principle that DSBs stimulate HR in yeast [71], [76], [81]. The approximately 20-fold increase in GFP-positive CFUs/pmol for both EasyClone and our clone-less method in the presence of Cas9 highlights the influential effect of targeted DNA cleavage on genomic integration efficiency. The statistical significance of this enhancement, confirmed by two-way ANOVA where $p<0.00001$ and <0.05 was obtained for the EasyClone and clone-less approach respectively, demonstrates the crucial role of Cas9 in improving the outcome of both assembly strategies.

Interestingly, while Cas9 significantly enhanced transformation efficiencies for both methods, the precision, defined as the proportion of GFP-positive colonies among hygromycin-resistant colonies, was slightly lower for the clone-less method, particularly in the presence of Cas9 (about 5% decrease). This suggests that while the overall number of transformants increased with CRISPR-Cas9, the clone-less approach might have a higher background of non-specific integration or incomplete assembly events leading to hygromycin resistance but lacking the complete *GFP* cassette. This observation represents a potential trade-off for the significant

reduction in the need for tedious *in vitro* molecular cloning steps, a simplification that was a primary aim of this study.

Furthermore, the raw colony counts (Appendix B, Figure 1) suggest similar transformation outcomes between EasyClone and our clone-less approach, however, the normalized efficiency data in Figure 7 provides a more insightful comparison by accounting for the different amounts of input DNA and plating dilutions. Notably, even with the requirement for *in vivo* assembly from multiple fragments, the clone-less method still yielded a substantial number of normalized transformants, indicating a viable pathway for genomic integration that bypasses traditional cloning.

In summary, this combined system (clone-less with CRISPR-mediated DSBs) holds significant potential for future studies, particularly in expanding the multiplexing capabilities of the EasyClone system without the need for extensive *in vitro* cloning steps.

4.2 Multiplexing Using the EasyClone System

The EasyClone system provides YIps that enable integration of GOIs into pre-characterized intergenic loci in the *S. cerevisiae* genome for stable DNA integration, high gene expression, and minimal impact on cell growth [73], [75]. These sites are typically referred to by their chromosome number and a sequential identifier [73], [75]. These well-characterized chromosomal integration sites have been widely adopted by other researchers [51], [81], making them a valuable component for yeast genetic engineering.

The second objective of my study was to characterize multiplexing in yeast using the EasyClone system. My first aim was to identify EasyClone integration sites that are compatible

with the design of our clone-less DNA assembly and integration approach. These sites will then be used to achieve the second aim of my second objective of demonstrating the potential for multiplexing in a proof-of-concept experiment by simultaneously integrating multiple GOIs into distinct chromosomal loci using the EasyClone system.

My initial experiments focused on identifying compatible integration sites using five pre-validated EasyClone loci (X-2, X-4, XI-3, XII-4, XII-5). These loci were selected to adhere to the Borodina lab's recommendation for multiplexing of targeting sites that are positioned on different chromosomes to avoid the potential genome instability that may arise if they were closely positioned [76]. By targeting *GFP* to each of these sites using our clone-less assembly method, both with and without Cas9-mediated DSBs, varying integration efficiencies across the loci was observed (Figure 8). As anticipated, Cas9-assisted integration significantly enhanced transformation efficiencies at most sites, highlighting the benefit of targeted DNA cleavage for genome integration. Notably, the X-4, XI-3, and XII-5 sites exhibited the highest normalized integration efficiencies with Cas9, suggesting that these loci are particularly suitable for efficient genetic manipulation using our combined approach. While detectable integration occurred without Cas9, the efficiencies were considerably lower, highlighting the importance of DSBs for robust integration of linear DNA fragments generated via PCR in our clone-less strategy.

The significantly lower transformation efficiencies observed at the X-2 and XII-4 sites, under both standard and Cas9 conditions, is inconsistent with the higher efficiencies reported in the EasyClone MarkerFree paper's validation data [76]. While potential genomic variations in our BY4741 strain compared to the CEN.PK 117-7D strain used by the EasyClone MarkerFree authors could explain this discrepancy, the primary aim of this objective was to identify three

sites compatible with an EasyClone system multi-loci targeting gRNA. Therefore, we proceeded with the more efficient sites rather than pursuing this variation further.

Having identified X-4, XI-3, and XII-5 as promising integration sites, I proceeded to my second aim of characterizing the EasyClone system's multiplexing capability using their three-loci targeting gRNA (pCfB3052 [X-4, XI-3, XII-5]). The design of this multiplexing experiment in detailed in Figure 14, where *GFP* and *hphMX6* were targeted to the X-4 locus (using pCfB2194), *URA3* to XI-3 (using pCfB2195 for selection on -Ura), and *LEU2* to XII-5 (using pCfB2337 for selection on -Leu), allowing for the assessment of simultaneous integration at three distinct sites using visual and selectable markers.

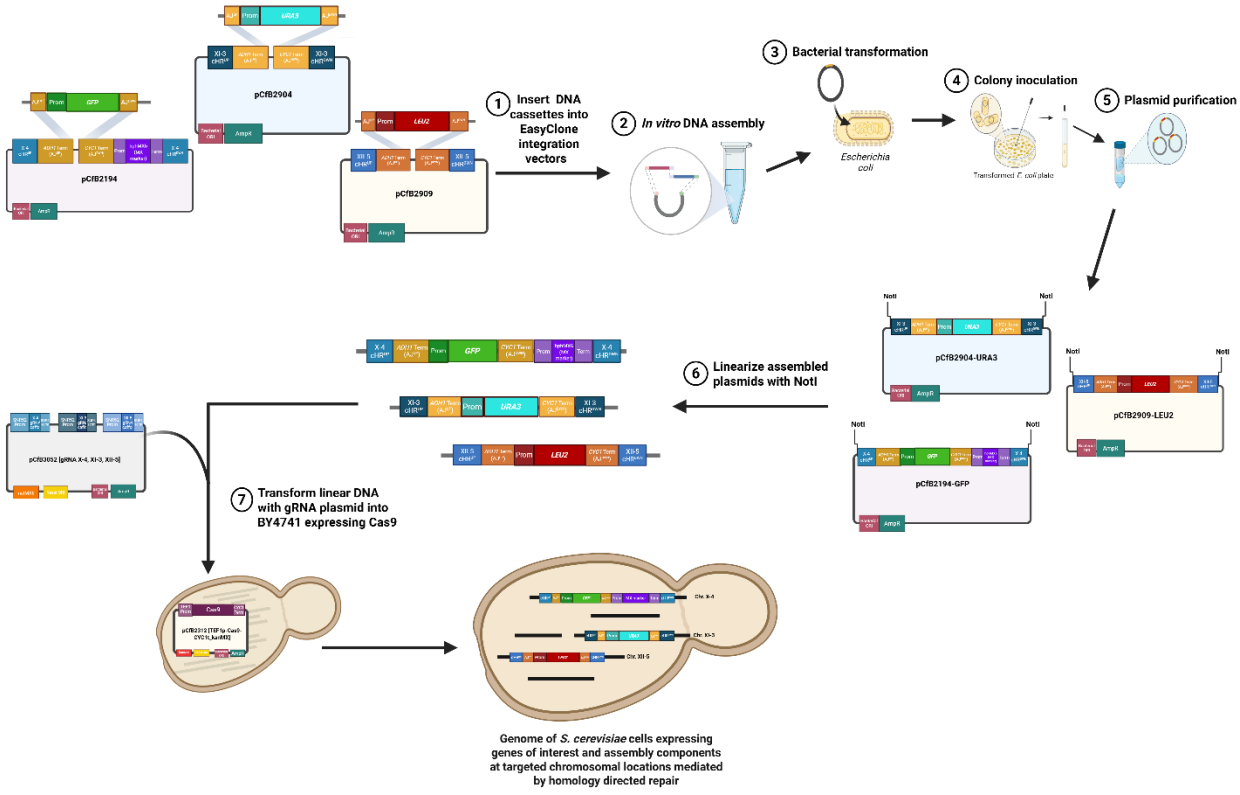

Figure 14. Using the EasyClone system to simultaneously integrate *GFP* and a hygromycin resistance cassette into the X-4 site, *URA3* into the XI-3 site, and *LEU2* into the XII-5 site in the genome of *S. cerevisiae*. Components from the EasyClone 2.0 (pCfB2194) and MakerFree (pCfB2904, pCfB2909, pCfB3052, and pCfB2312) toolkits were used to replicate the system's multiplexing design, where *in vitro* assembly of genes of interest (GOIs) into YIps is required prior to integration into yeast. Figure generated using BioRender.com.

We successfully demonstrated the simultaneous integration of four genes (*GFP*, *hphMX6*, *URA3*, and *LEU2*) into three distinct loci using a multiplexing gRNA (Figure 9). The statistically significant increase in transformation efficiency compared to the mock control confirms the system's capacity for multi-site targeting and integration. However, precision analysis of colonies selected for integration at all three loci revealed that approximately 14% did not exhibit GFP expression, resulting in a precision of 0.86. This is lower than the 0.988 precision achieved in our single-gene, single-locus integration following the EasyClone system's design (Figure 7). This observation aligns the EasyClone-MarkerFree study's analysis which notes targeting efficiencies of 90-100% for single insertions and 60-70% for triple insertions [76], suggesting that the complexity of multiplexing can impact the reliability of complete co-integration.

This proof-of-concept experiment, intended to establish a baseline efficiency for my research on multiplexing with the EasyClone system, highlighted a significant limitation: the requirement for extensive *in vitro* cloning. Due to the EasyClone system's uniform assembly junction (AJ) sequences (*ADH1* terminator upstream, *CYC1* terminator downstream) across all YIps, our clone-less approach was not directly applicable, necessitating traditional cloning steps. Nevertheless, this experiment (Figure 14) successfully provided an understanding of the capabilities and limitations of using the EasyClone system for multiplexing.

4.3 Exploiting Yeast Homologous Recombination

My next research objective focused on leveraging yeast's efficient HR machinery to streamline and reduce the cost of genetic engineering workflows. By minimizing reliance on *in vitro* cloning, this approach can enable YIp design with shorter cHRs and direct integration of pre-synthesized GOIs or DNA fragments using PCR-added homology overhangs (AJs).

A key challenge in this objective is the lack of definitive and quantifiable information regarding the minimal length of homology required for robust and accurate *in vivo* DNA assembly and integration. This variability might be due to factors such as AT/GC content, DNA fragment structure, or potential unintended complementarity to other regions of the yeast genome [84], [85]. Therefore, determining the shortest effective homology length could significantly advance our understanding of yeast's HR capabilities, potentially supporting literature speculations that surprisingly short homology regions of 20-30 bp can be sufficient [84], [85], [112]. To investigate the impact of homology length, we used the *ADE2* locus as a visual reporter system since its disruption leads to pink colonies, providing a direct readout of successful homologous directed repair (HDR) at a CRISPR-induced DSB [87].

The first aim I investigated was to determine the shortest chromosomal homology length for predictable and efficient genomic integration using our clone-less approach. To achieve this, we designed a YIp, pEC.IV ade2(400)::HphMX, based on an EasyClone YIp backbone (maintaining the *ADH1* and *CYC1* terminator AJs and the hygromycin selection cassette), but targeting the *ADE2* locus with 400 bp upstream and downstream homologies. We then used CRISPR-Cas9 to target the *ADE2* locus on chromosome XV and tested the integration efficiency of a GFP expression and *hphMX6* cassette with varying chromosomal homology region (cHR) lengths (30, 50, 200, and 400 bp), while keeping the EasyClone AJ lengths consistent at approximately 200 bp. Linear DNA fragments were co-transformed with either an *ADE2*-targeting gRNA or a mock gRNA into a Cas9-expressing yeast strain.

Figure 10 shows successful *GFP* integration across all tested cHR lengths using the *ADE2*-targeting gRNA, with 400 bp cHRs being the most efficient (6378 CFU/pmol, 93.6% integration efficiency), yet 30 bp also showed integration (1700 CFU/pmol, 75.3% integration

efficiency). Without the *ADE2*-targeting gRNA, integration was only observed with 400 bp cHRs (874 CFU/pmol, 59.6% efficiency), likely from inherent yeast HR, similar to our Cas9-independent results at the X-4 locus with 400 bp cHRs (Figure 7, 450 CFU/pmol). The significantly higher efficiency with the *ADE2* gRNA emphasizes CRISPR-Cas9's role in enhancing targeted integration. Furthermore, the 200 bp cHR length also demonstrated high transformation and integration efficiencies with the *ADE2*-targeting gRNA (4000 CFU/pmol, 94.3% integration efficiency) and, importantly, showed no integration in the mock gRNA condition, suggesting it could be a favourable length balancing efficiency and specificity.

In my second aim of this research objective, I explored the impact of assembly junction (AJ) length (30, 60, and 200 bp, and a 0 bp control) while using 200 bp cHRs (Figure 11). The highest transformation efficiency was achieved with 200 bp AJs, but even shorter AJs (30 and 60 bp) facilitated integration. As expected, no integration was observed in the absence of any assembly junction (0 bp AJ). Similar to the cHR experiments, the mock gRNA conditions showed minimal integration across all AJ lengths, highlighting the specificity conferred by the gRNA-Cas9 system.

These results suggest that a more streamlined and cost-effective genetic engineering workflow is achievable. Specifically, future YIp designs can incorporate 200 bp cHRs (based on their high efficiency and specificity), while any GOI cassette can be prepared with 30 bp AJs added via PCR overhangs. This strategy, leveraging direct DNA synthesis or PCR, promises a more cost-effective and rapid workflow for multiplexed yeast genetic engineering.

4.4 Designing and Validating a One-Step Cargo Linker Liberating YIp

Building upon our exploration of yeast's HR capabilities for streamlined genetic engineering, my next research objective aimed to simplify the process of multiplexing. Current methods for multi-gene integration, such as those using the EasyClone system, often require the construction and individual preparation of multiple integrative plasmids (YIps), which can be time-consuming. To address this, we designed and validated a YIp, pEC.IV(XV.CL.MX), intended to streamline the simultaneous integration of two gene cassettes at the *ADE2* locus through a single restriction enzyme digest reaction (Figure 5).

The design of pEC.IV(XV.CL.MX) incorporates SapI restriction enzyme recognition sites strategically positioned to liberate the necessary cargo linker (CL) fragments for our clone-less *in vivo* DNA assembly and integration approach with a single digest reaction (Figure 5). SapI, a Type IIS restriction enzyme, was chosen for its ability to cut outside of its recognition sequence, allowing us to precisely define the ends of the DNA fragments released [113], [114]. This is crucial for generating CLs with the AJs and cHRs needed for efficient *in vivo* HR-mediated integration of the *GFP* cassette and the *hphMX6* selection marker at the *ADE2* locus.

The results presented in Figure 12 demonstrate that co-transforming yeast with the SapI-digested pEC.IV(XV.CL.MX) and PCR-amplified *GFP* and *hphMX6* cassettes, along with an *ADE2*-targeting gRNA, resulted in a statistically significant increase in pink, GFP-positive colonies compared to the mock gRNA control. The presence of a significant number of white, GFP-negative colonies in the mock condition represents the background integration of the resistance marker, likely due to non-specific plasmid integration or incomplete integration

events, which highlights the importance of the CRISPR-Cas9-mediated DSBs for targeted integration using this experimental design.

The integration efficiency for achieving the desired pink, GFP-positive phenotype (27.2%) and the precision (53.8% of pink colonies were also GFP positive) suggest that further optimization may be needed to enhance the reliability of co-integration. Overall, this indicates that our one-step linearizable YIp design, coupled with the clone-less approach, can facilitate the simultaneous integration of multiple genes at a targeted genomic locus.

In summary, this proof-of-concept study demonstrates the potential of using a one-step linearizable YIp to simplify multiplexing by reducing the need for multiple *in vitro* plasmid constructions. However, the observed imbalance in co-integration (having pink but GFP-negative colonies) suggests a potential bias in the integration efficiency of the selection marker (*hphMX6*) versus the gene of interest (*GFP*). We hypothesize that the longer homology regions part of PCR amplified *hphMX6* cassette (173 bp upstream and 200 bp downstream) may facilitate its integration at a higher rate than the added *GFP* cassette, which only had 30 bp AJs. To address this, future work will involve testing this hypothesis by designing PCR primers to amplify the *hphMX6* cassette with only 30 bp homology to the linearized YIp CL fragments. By making the homology lengths equal for both the selection marker and the GOI, we aim to improve the efficiency and precision of simultaneous multi-gene integration using this one-step YIp approach.

4.5 Establishing Unique Terminator Insulator Spacer (TINS) Sequences as Assembly Junctions

When looking to expand our clone-less *in vivo* DNA assembly and integration approach for multiplexing across multiple genomic loci, we recognized a limitation of the EasyClone system. Each EasyClone YIp contains identical AJs (*ADH1* terminator upstream and *CYC1* terminator downstream). This means that we cannot use the EasyClone AJs to simultaneously direct the *in vivo* assembly of multiple DNA constructs in one yeast transformation reaction.

To address the limitations of the EasyClone system's identical assembly junctions across its YIps, we aimed to create novel AJs with unique homology regions. Inspired by the Voigt lab's work on genetic circuits [89], which included the analysis of sequences for the creation of insulated gates with synthetic promoters, strong terminators, insulators (ribozymes and terminators), and spacers to prevent interference and unwanted HR, we designed Terminator Insulator Spacer (TINS) sets as unique AJs. We then constructed the pEC.IV ADE2(400)::TINS YIp (Table 3) to test the integration of a single GOI into the *ADE2* locus using one of these TINS sets, with the TINS sequences designed based on an analysis of the Voigt lab's results [89] (Appendix A, Table 1).

The results of my evaluation of TINS as unique AJs presented in Figure 13 showed no significant difference (un-paired t-test) in transformation efficiency between the *ADE2*-targeting (522 CFU/pmol) and mock (800 CFU/pmol) gRNA conditions for obtaining colonies with proper integrations (pink, GFP-positive, and hygromycin resistant). The mock condition yielded more true positive colonies than the *ADE2*-targeting (average 25 vs. 16). While the calculated integration efficiencies (67.6% mock, 72.7% *ADE2* gRNA) for true positive colonies and

precision values (0.862 mock, 0.800 *ADE2* gRNA) for the chance that a pink colony is also GFP positive are high in both conditions, the lack of CRISPR-Cas9 enhancement is notable.

The higher number of true positives in the mock condition implies that the TINS sequences might be promoting a significant level of Cas9-independent integration. This could be attributed to the 400 bp of *ADE2* cHRs used, which, as seen in our earlier experiments (Figure 10), can facilitate HR even without a DSB.

Moreover, the presence of terminators after gene sequences in DNA cargos used for yeast integration is crucial for ensuring proper expression of the GOI [88]. Transcriptional terminators are composed of efficiency elements (like TATATA variants) that enhance termination strength, positioning elements (often A-rich sequences resembling AAUAAA) that guide RNA cleavage, and polyadenylation sites where the poly(A) tail is added for mRNA stability [115]. If a terminator does not function correctly, it can lead to transcriptional read-through into downstream sequences, potentially disrupting the expression of other genes, and result in unstable or incorrectly processed mRNA, ultimately leading to reduced or abnormal expression of the intended gene [115], [116]. Therefore, we hypothesize that the TINS are not functioning as expected due to inefficient termination of transcription, resulting in lower and less targeted expression of the *GFP* gene in pink, *ADE2* disrupted colonies.

A potential solution is to replace the terminator sequences in the TINS with ones characterized by MacPherson and colleagues [117]. MacPherson's study designed and validated a set of short, orthogonal synthetic terminators to prevent HR-mediated rearrangements caused by repeated use of standard terminators during yeast multigene assembly, achieving a range of termination efficiencies, some highly effective [117]. We can further enhance our redesigned TINS by adding adaptor sequences after the spacers with a proven ability to facilitate modular

genetic assembly in *S. cerevisiae* [72]. These are VEGAS (versatile genetic assembly system) adaptors characterized by the Boeke lab as 57 bp sequences made from an in-house collection of sequences that are distinct from the yeast genome to prevent unintended HR [72].

In summary, while our initial evaluation demonstrated that TINS could function as unique assembly junctions for gene integration, the lack of CRISPR-Cas9-dependent enhancement and the lower overall efficiency compared to EasyClone AJs suggest limitations in their current design. We hypothesize that inefficient transcriptional termination within the TINS may contribute to reduced and less targeted GFP expression. To address this, future efforts will focus on redesigning the TINS to create TINAs (Terminator Insulator spacer Adaptor sequences), potentially by incorporating highly effective synthetic terminators identified by MacPherson [117] and including VEGAS adaptors [72] after the spacers to, aiming to create more robust and efficient unique AJs for multiplexed genome engineering.

4.6 Future Outlook: Designing an EasyClone Expansion Pack for Streamlined Multiplexing

My thesis lays the foundation for a more streamlined and versatile approach to multiplexed genetic engineering in yeast, which we envision as an EasyClone Expansion Pack. Figure 15 provides a comparative overview contrasting the current multi-step EasyClone system with our proposed two-step Expansion Pack for the simultaneous genomic integration of multiple genes of interest (GOIs) into several chromosomal sites.

The current EasyClone system (Figure 15a) requires the individual cloning of each GOI into separate YIp, which must be linearized before co-transformation with a multiplexing gRNA plasmid into a Cas9-expressing yeast strain. While effective (Figure 9), this multi-step process,

particularly the *in vitro* cloning, can be time-consuming and labour-intensive. In contrast, our proposed EasyClone Expansion Pack (Figure 15b) aims to simplify this workflow. We envision a single, yeast integrative vector, pEC.IV [EC EP], containing 200 bp chromosomal homology regions (cHRs) for multiple pre-defined integration sites (such as X-4, XI-3, XII-5). Crucially, this vector would incorporate our uniquely designed terminator, insulator, spacer, and adaptor regions (TINAs) as unique AJ sequences. A single restriction digest using SapI would linearize this vector, releasing cargo linkers (CLs) as integrative fragments for yeast transformation.

The EasyClone Expansion Pack workflow would involve co-transforming these CLs with linear GOI cassettes or MX selection marker cassettes. These cassettes would be designed to contain short (30 bp) homology arms complementary to the TINA sequences on the linearized vector fragments. This design would leverage our findings on efficient integration with short AJ lengths of 30 bp, allowing for the direct use of PCR-amplified GOIs or synthesized DNA fragments, further minimizing the need for *in vitro* cloning. Combined with a multiplexing gRNA plasmid, this two-step approach promises to enable the simultaneous integration of multiple genes into targeted chromosomal locations.

The anticipated outcome of both the traditional EasyClone system and our proposed Expansion Pack (Figure 15c) is the precise integration of GOIs and selection markers at the desired genomic loci in *S. cerevisiae*. Future work will focus on constructing and validating the pEC.IV [EC EP] vector and optimizing the efficiency of the TINA-mediated assembly and integration of multiple DNA fragments simultaneously.

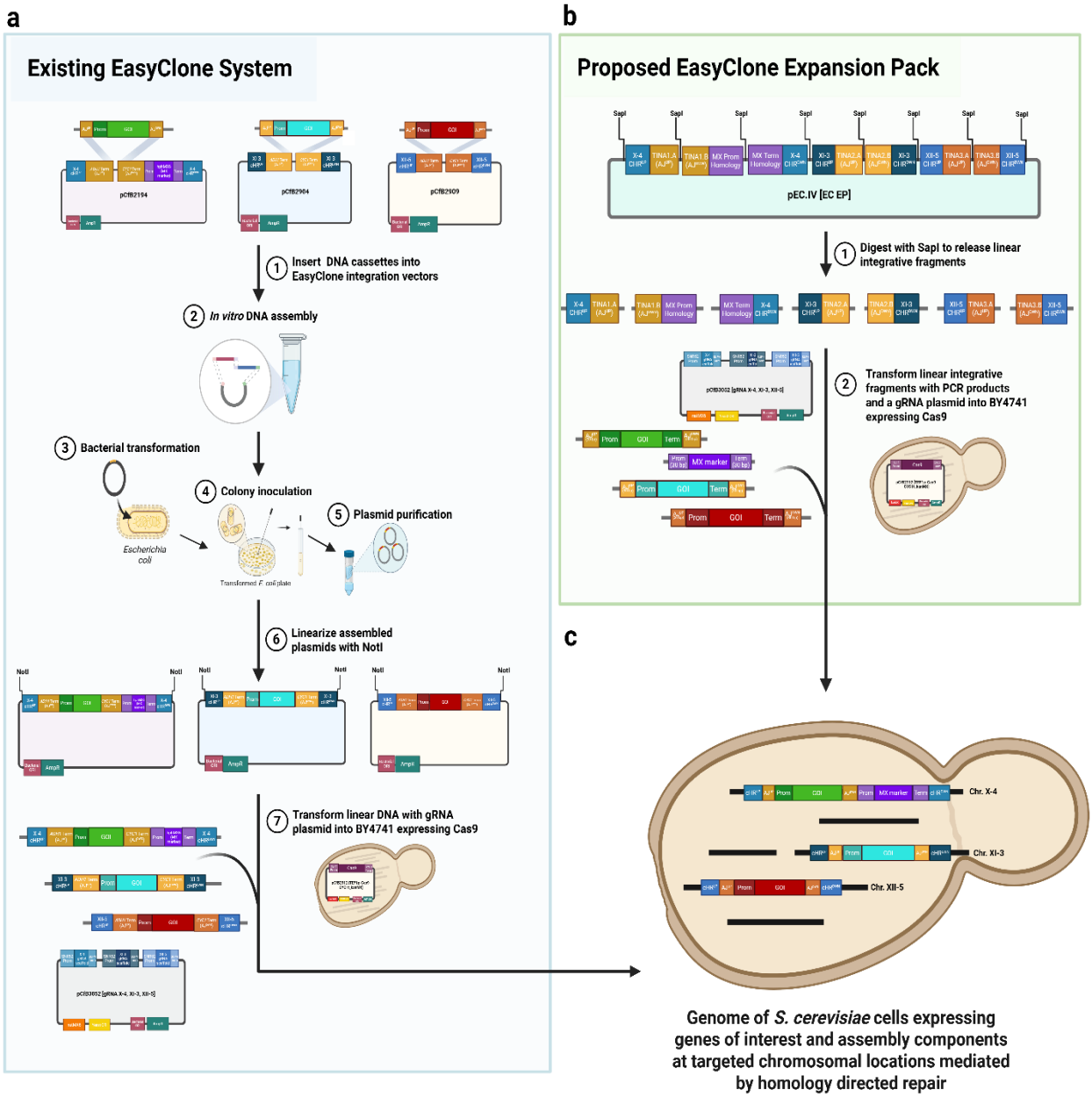

Figure 15. Comparative overview of the multi-step EasyClone system versus our streamlined two-step EasyClone Expansion Pack (EC EP) approach. Both systems allow for the simultaneous genomic integration of multiple genes of interest (GOIs) into three chromosomal sites (X-4, XI-3, and XII-5) in *Saccharomyces cerevisiae*. This figure was created using BioRender.com.

Chapter 5: Conclusion

This thesis advanced yeast genetic engineering research through the exploration and development of streamlined, clone-less DNA integration methods enhanced by CRISPR-Cas9. Yeast's endogenous homologous recombination (HR) machinery was explored, resulting in efficient *in vivo* DNA assemblies occurring when yeast integrating plasmids (YIps) contain 200 bp of chromosomal homology (cHR) with 30 bp of homologous overhangs (AJs) added to genes of interest by PCR. To simplify multiplexing, a novel one-step cargo linker liberating YIp was designed and validated for the clone-less simultaneous integration of multiple genes at a single locus. Furthermore, the potential of unique Terminator Insulator Spacer (TINS) sequences as assembly junctions for scalable, multi-locus integration was explored, although initial findings suggest a need for further development to achieve efficiency that is comparable to existing systems.

These advancements collectively contribute valuable tools and insights towards supporting my hypothesis that a novel YIp, presented as our EasyClone Expansion Pack, could be designed for the two-step, simultaneous multi-loci integration and *in vivo* assembly of linear DNA fragments in *S. cerevisiae*, leveraging HR. This paves the way for the use of low-cost and streamlined yeast genetic engineering in applications such as complex metabolic pathway construction for biofuel and vaccine production [46], [50], rapidly engineering industrial yeast strains with multiple enhanced traits [45], [48], and prototyping gene interactions for mammalian cell studies [118].

Appendix

Appendix A: Materials and Methods Supplemental Information

Table 1. Supplemental sequence information for the DNA constructs used in this study.

Purpose	Name	Sequence (5' to 3')
To create pCfB.XV (*ADE2* gRNA)	20 bp *ADE2* targeting gRNA sequence	CTGCTCATAGAACTCCACAT
	70 bp oligonucleotide ordered to integrate *ADE2* targeting gRNA sequence into an EasyClone gRNA YEp	tctccgcagtgaaagataaatgatcCTGCTCATAGAACTCCACATgttttagagctagaaatagcaagtt
To create pCfB.MOCK	20 bp mock gRNA sequence	GCCTATCATCTCGAATCACA
	70 bp oligonucleotide ordered to integrate mock gRNA sequence into an EasyClone gRNA YEp	tctccgcagtgaaagataaatgatcGCCTATCATCTCGAATCACAgttttagagctagaaatagcaagtt
Sequencing primer to validate pCfB.XV and pCfB.MOCK plasmid assemblies	gRNA-ORI.REV	gggggcggagcctatg
Unique regions of homology created using Terminator Insulator Spacer (TINS) elements with sequences evaluated in [89]	TINS1.A	CCTATGAATCGGatgatGtATATAcgAAAAGTATTAAAAACATCTTACCATtcAAACTACGAGCGCTGTCTGTACTTGTATCAGTACACTGACGAGTCCCTAAAGGACGAAACACCGTGATTTGATCGTAACTTATTCACCCGGTCTGTGTTATTTTTTAGATACTGATGATATTTTAGAACCAGACTATATATAaggatCCTTAC
	TINS1.D	CAGTGGacAGCTTTTGATTAAGCCTTCTTCCAAAAAACACTTTTGGTCAaTCCTGAAGCCCCATAGGGTGGTGTGTACCACCCCTGATGAGTCCAAAAGGACGAAATGGGGGCCATGTTGGTATGGTCAATGCGCGGGGCGGCCACGCGCATCTATGGCGATTAAGCCCTGGAGGGGCAAGGGTGTGGAAGGCCCTCGGCGTTCGGTTTAgataatgatgTCATTATTaatatatataTATATATAttgtaCCATCC

Protocol followed for counting colonies using ImageJ, FIJI [106]**:**

1. Open the Image J software (Fiji Downloads (imagej.net)) and upload image of plate
2. Convert image to 8-bit:
    a. Image → Type → 8-bit
3. Crop image to only include the plate
4. Image → Adjust → Threshold → Slide to select which colonies get counted → Apply
5. Process → Binary → Make binary
6. Process → Binary → Watershed. This separates any clumps of colonies
7. Define colony size
    a. Analyze → Analyze particles. Set size to 10–25000 pixel units and circularity to 0.60 – 1.00. Show overlay

Appendix B: Results Supplemental Information

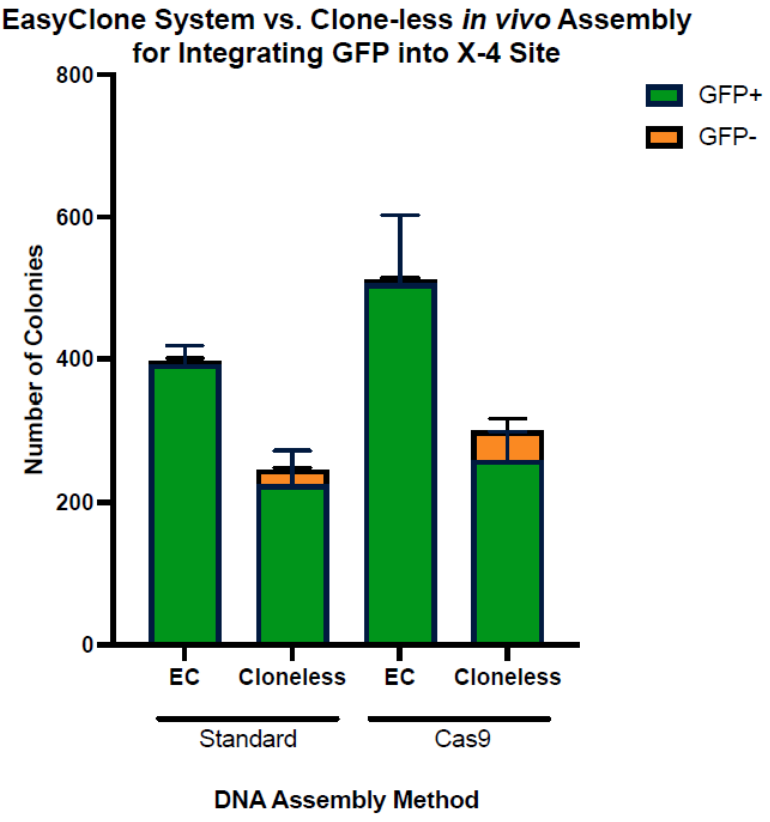

Figure 1. The number of GFP-positive and negative colonies obtained for *GFP* integration at the X-4 locus using the EasyClone (EC) system versus our clone-less *in vivo* assembly method. This was assessed under conditions without (standard) or with Cas9-mediated double-stranded DNA break. Bars represent the total number of colonies, with the green portion indicating GFP-positive colonies and the orange portion indicating GFP-negative colonies. This data was not normalized by the amount of DNA transformed and instead represents the raw colony counts on YPD + Hygromycin B [200 ng/µL] plates using IVIS for imaging and FIJI for standardized counting. The standard plates are from 1:4 dilutions and Cas9 from 1:32 dilutions of the yeast transformation mixture plated onto

YPD for recovery. Error bars represent the standard error of triplicate (n=3) transformations in BY4741 yeast. Figure created using GraphPad Prism.

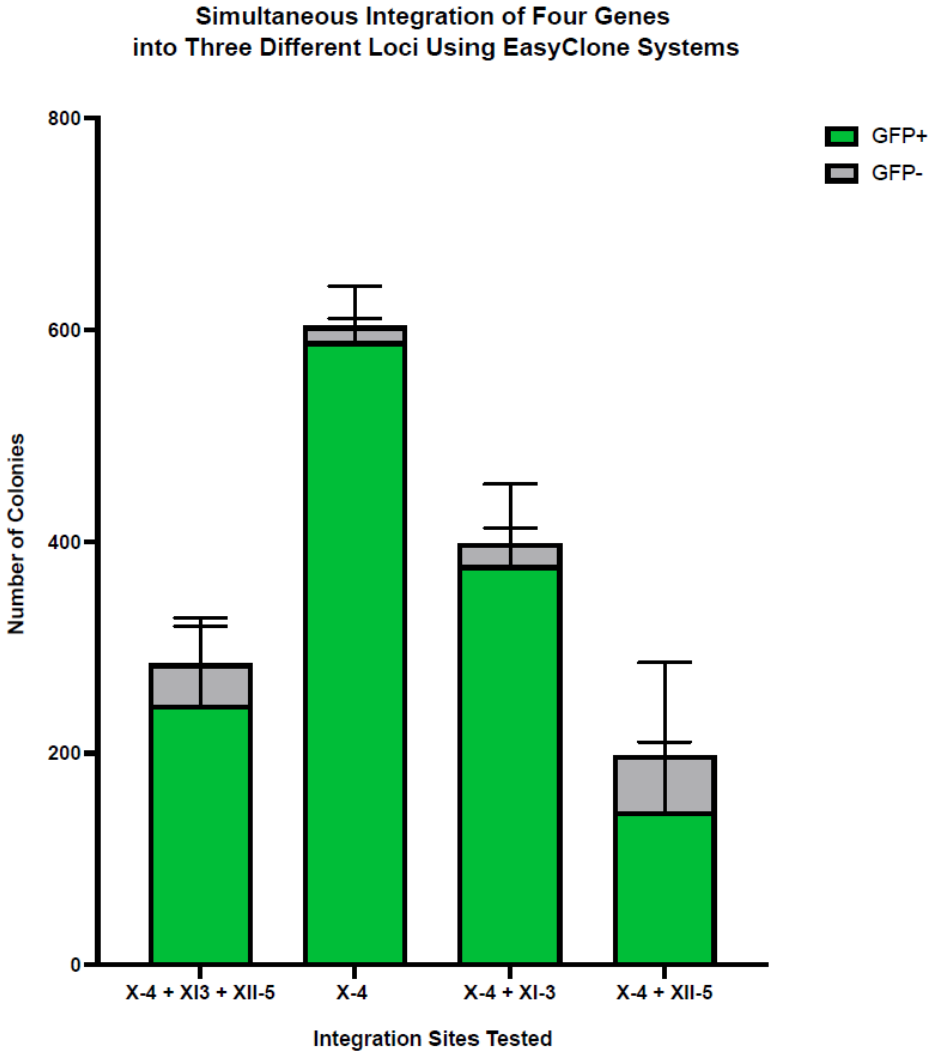

Figure 2. The number of colonies counted on different selection plates for the simultaneous integration of four genes into three different loci using EasyClone systems and a multiplexing gRNA. The four genes and three integration locations are: *GFP* and *hphMX6* into X-4, *URA3* into XII-3, and *LEU2* into XII-5. These genes were integrated into EasyClone YIps, linearized, and co-transformed with mock or multiplex (targeting the three integration sites) gRNAs into BY4741 yeast expressing Cas9. Colonies that were integrated into the X-4 locus were counted on YPD + Hygromycin plates, X-4 and XI-3 loci on SC -Ura +Hygromycin plates, X-4 and XII-5 loci on SC -Leu + Hygromycin plates, and all three loci (X-4 + XI-3 + XII-5) on SC –Ura -Leu + Hygromycin. IVIS was used to image plates and detect GFP-positive/ negative colonies. Data represent the mean and standard error (error bars) of technical triplicates (n=3). Figure generated using GraphPad Prism.

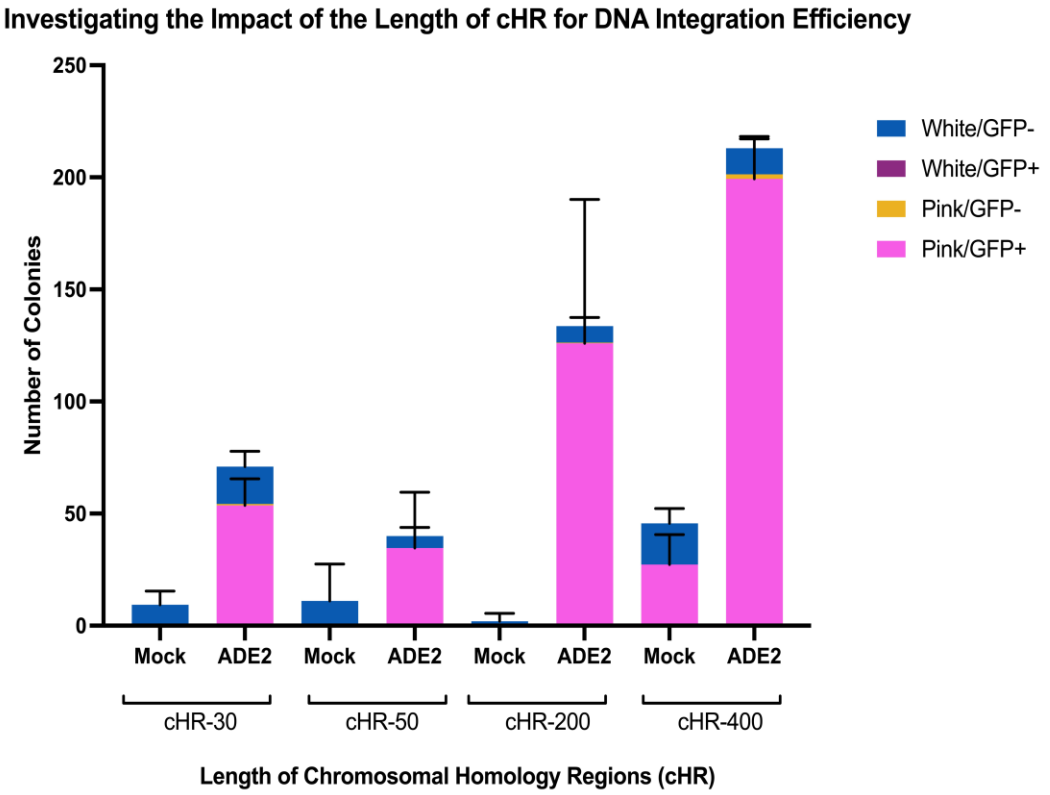

Figure 3. The impact of varying chromosomal homology region lengths from 30-400 bp on integration efficiency using our Cas9-mediated clone-less *in vivo* DNA assembly and integration method to integrate *GFP* in the *ADE2* locus. Linear products were PCR amplified from the same plasmids, with modifications being made only to the length of chromosomal homology regions (cHRs). These fragments were transformed into yeast strain BY4741 containing Cas9 in a 1:1:1 pmol ratio with 500 ng of *ADE2*-targeting or mock gRNA. Post-transformation, the reaction mixtures were plated on YPD only agar plates in a 1:32 dilution and then replica plated onto YPD + Hygromycin B [200ng/µL] plates after 20 hours. The pink, GFP-positive colonies were counted by analyzing brightfield and fluorescent (using IVIS) images of the plates on FIJI. Data represent the mean and standard error (error bars) of technical triplicates (n=3). Figure generated using GraphPad Prism.

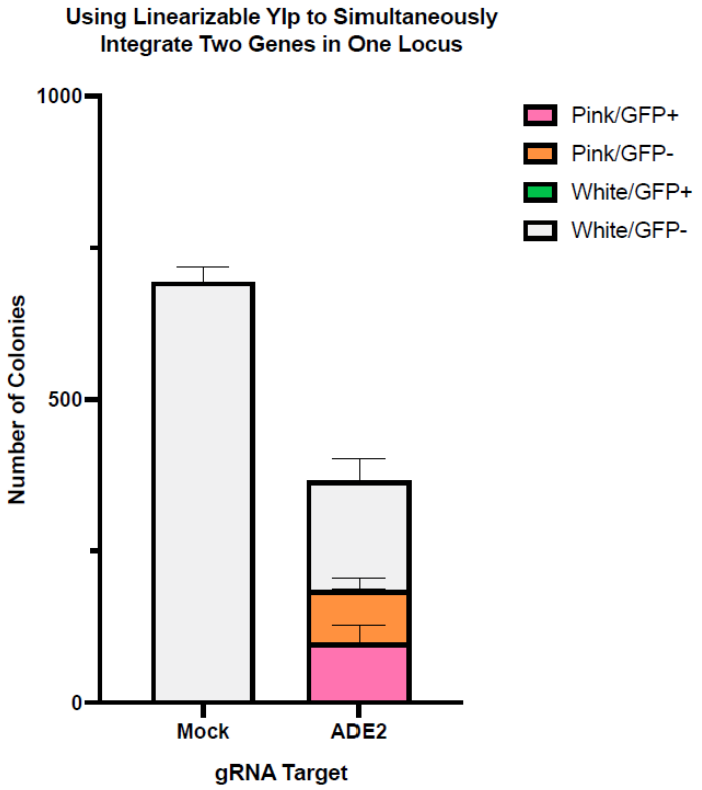

Figure 4. The number of colonies observed when simultaneously integrating two genes into the *ADE2* locus. pEC.IV(XV.CL.MX) YIp was digested with SapI to release the linear fragments that would enable the integration of a PCR amplified *GFP* cassette and *hphMX6* cassette into the *ADE2* locus. These linear fragments were co-transformed (1 pmol of each of *GFP* and *hphMX6* cassettes, 1000 ng of digest) with an *ADE2*-targeting or mock gRNA (500 ng) into a BY4741 yeast strain expressing Cas9. Post-transformation, 1:1 dilution (for the mock samples) and 1:2 dilution (for the *ADE2* gRNA samples) of the transformed yeast cells were plated on YPD prior to replica plating onto YPD+ Hygromycin B [200 ng/µL]. The number of colonies observed on the YPD + Hygromycin plate imaged using brightfield (to observe pink colonies) and IVIS (to detect GFP) are plotted. Data represent the mean and standard error (error bars) of technical triplicates (n=3). Figure generated using GraphPad Prism.

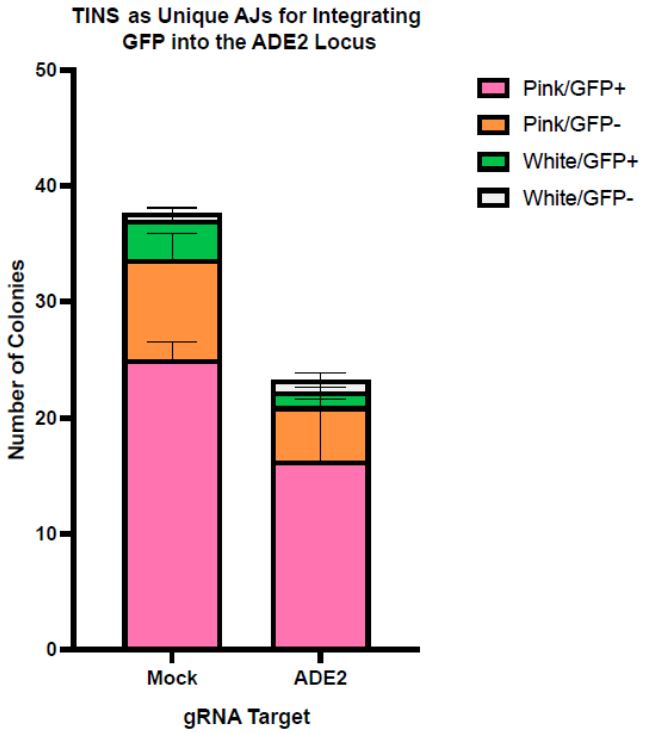

Figure 5. The number of colonies observed when using terminator insulator spacer sequences as unique assembly junctions for integrating *GFP* into the *ADE2* locus. pEC.IV ADE2(400)::TINS YIp was PCR amplified to provide fragments #1 (contains 400 bp upstream ADE2 cHR and TINS1.A) and 2 (TINS1.D, hphMX6 cassette, and 400 bp downstream *ADE2* cHR) for the clone-less *in vivo* DNA assembly and integration of a *GFP* cassette with TINS1.A and TINS1.D functioning as AJs. These linear DNA fragments were co-transformed in a 1:1:1 pmol ratio an *ADE2*-targeting or mock gRNA (500 ng) into a BY4741 yeast strain expressing Cas9. Post-transformation, 1:32 dilutions of transformed yeast cells were plated on YPD only prior to replica plating onto YPD+ Hygromycin B [200 ng/µL]. The number of colonies observed on the YPD + Hygromycin plate imaged using brightfield (to observe pink colonies) and IVIS (to detect GFP) are plotted. Data represent the mean and standard error (error bars) of technical triplicates (n=3). Figure generated using GraphPad Prism.

Bibliography

[1] T. M. Lanigan, H. C. Kopera, and T. L. Saunders, "Principles of Genetic Engineering," *Genes (Basel)*, vol. 11, no. 3, p. 291, Mar. 2020, doi: 10.3390/GENES11030291.

[2] Y. Zheng, Y. Li, K. Zhou, T. Li, N. J. VanDusen, and Y. Hua, "Precise genome-editing in human diseases: mechanisms, strategies and applications," *Signal Transduction and Targeted Therapy 2024 9:1*, vol. 9, no. 1, pp. 1–21, Feb. 2024, doi: 10.1038/s41392-024-01750-2.

[3] A. M. Khalil, "The genome editing revolution: review," *Journal of Genetic Engineering and Biotechnology*, vol. 18, no. 1, pp. 1–16, Dec. 2020, doi: 10.1186/S43141-020-00078-Y/FIGURES/7.

[4] L. Krenning, J. van den Berg, and R. H. Medema, "Life or Death after a Break: What Determines the Choice?," *Mol Cell*, vol. 76, no. 2, pp. 346–358, Oct. 2019, doi: 10.1016/J.MOLCEL.2019.08.023.

[5] D. P. Mathiasen and M. Lisby, "Cell cycle regulation of homologous recombination in Saccharomyces cerevisiae," *FEMS Microbiol Rev*, vol. 38, no. 2, pp. 172–184, Mar. 2014, doi: 10.1111/1574-6976.12066.

[6] X. Li and W. D. Heyer, "Homologous recombination in DNA repair and DNA damage tolerance," *Cell Res*, vol. 18, no. 1, p. 99, Jan. 2008, doi: 10.1038/CR.2008.1.

[7] X. Zhao *et al.*, "Cell cycle-dependent control of homologous recombination," *Acta Biochim Biophys Sin (Shanghai)*, vol. 49, no. 8, pp. 655–668, Aug. 2017, doi: 10.1093/ABBS/GMX055.

[8] W. D. Wright, S. S. Shah, and W. D. Heyer, "Homologous recombination and the repair of DNA double-strand breaks," *J Biol Chem*, vol. 293, no. 27, p. 10524, Jul. 2018, doi: 10.1074/JBC.TM118.000372.

[9] H. Li, Y. Yang, W. Hong, M. Huang, M. Wu, and X. Zhao, "Applications of genome editing technology in the targeted therapy of human diseases: mechanisms, advances and prospects," *Signal Transduction and Targeted Therapy 2020 5:1*, vol. 5, no. 1, pp. 1–23, Jan. 2020, doi: 10.1038/s41392-019-0089-y.

[10] A. J. Davis and D. J. Chen, "DNA double strand break repair via non-homologous end-joining," *Transl Cancer Res*, vol. 2, no. 3, p. 130, Jun. 2013, doi: 10.3978/J.ISSN.2218-676X.2013.04.02.

[11] D. L. Court, J. A. Sawitzke, and L. C. Thomason, "Genetic engineering using homologous recombination," *Annu Rev Genet*, vol. 36, pp. 361–388, 2002, doi: 10.1146/ANNUREV.GENET.36.061102.093104.

[12] A. J. Ellington and C. R. Reisch, "Efficient and iterative retron-mediated in vivo recombineering in Escherichia coli," *Synth Biol*, vol. 7, no. 1, Dec. 2022, doi: 10.1093/SYNBIO/YSAC007.

[13] D. Yu, H. M. Ellis, E. C. Lee, N. A. Jenkins, N. G. Copeland, and D. L. Court, “An efficient recombination system for chromosome engineering in Escherichia coli,” *Proc Natl Acad Sci U S A*, vol. 97, no. 11, pp. 5978–5983, May 2000, doi: 10.1073/PNAS.100127597/ASSET/F69FA843-F371-4F59-9B29-04753CD272E5/ASSETS/GRAPHIC/PQ1001275005.JPEG.

[14] J. A. Mosberg, C. J. Gregg, M. J. Lajoie, H. H. Wang, and G. M. Church, “Improving Lambda Red Genome Engineering in Escherichia coli via Rational Removal of Endogenous Nucleases,” *PLoS One*, vol. 7, no. 9, p. e44638, Sep. 2012, doi: 10.1371/JOURNAL.PONE.0044638.

[15] D. Carroll, “Genome Engineering With Zinc-Finger Nucleases,” *Genetics*, vol. 188, no. 4, p. 773, Aug. 2011, doi: 10.1534/GENETICS.111.131433.

[16] J. K. Joung and J. D. Sander, “TALENs: a widely applicable technology for targeted genome editing,” *Nature Reviews Molecular Cell Biology 2012 14:1*, vol. 14, no. 1, pp. 49–55, Nov. 2012, doi: 10.1038/nrm3486.

[17] T. Gaj, C. A. Gersbach, and C. F. Barbas, “ZFN, TALEN and CRISPR/Cas-based methods for genome engineering,” *Trends Biotechnol*, vol. 31, no. 7, p. 397, Jul. 2013, doi: 10.1016/J.TIBTECH.2013.04.004.

[18] T. Li *et al.*, “CRISPR/Cas9 therapeutics: progress and prospects,” *Signal Transduction and Targeted Therapy 2023 8:1*, vol. 8, no. 1, pp. 1–23, Jan. 2023, doi: 10.1038/s41392-023-01309-7.

[19] C. Xue and E. C. Greene, “DNA repair pathway choices in CRISPR-Cas9 mediated genome editing,” *Trends Genet*, vol. 37, no. 7, p. 639, Jul. 2021, doi: 10.1016/J.TIG.2021.02.008.

[20] H. Liao, J. Wu, N. J. VanDusen, Y. Li, and Y. Zheng, “CRISPR-Cas9-mediated homology-directed repair for precise gene editing,” *Mol Ther Nucleic Acids*, vol. 35, no. 4, p. 102344, Dec. 2024, doi: 10.1016/J.OMTN.2024.102344.

[21] A. Rasheed *et al.*, “A Critical Review: Recent Advancements in the Use of CRISPR/Cas9 Technology to Enhance Crops and Alleviate Global Food Crises,” *Curr Issues Mol Biol*, vol. 43, no. 3, p. 1950, Dec. 2021, doi: 10.3390/CIMB43030135.

[22] A. Mayorga-Ramos, J. Zúñiga-Miranda, S. E. Carrera-Pacheco, C. Barba-Ostria, and L. P. Guamán, “CRISPR-Cas-Based Antimicrobials: Design, Challenges, and Bacterial Mechanisms of Resistance,” *ACS Infect Dis*, vol. 9, no. 7, p. 1283, Jul. 2023, doi: 10.1021/ACSINFECDIS.2C00649.

[23] J. Kanter *et al.*, “Biologic and Clinical Efficacy of LentiGlobin for Sickle Cell Disease,” *N Engl J Med*, vol. 386, no. 7, pp. 617–628, Feb. 2022, doi: 10.1056/NEJMOA2117175.

[24] A. Dimitri, F. Herbst, and J. A. Fraietta, “Engineering the next-generation of CAR T-cells with CRISPR-Cas9 gene editing,” *Molecular Cancer 2022 21:1*, vol. 21, no. 1, pp. 1–13, Mar. 2022, doi: 10.1186/S12943-022-01559-Z.

[25] C. J. Bashor, I. B. Hilton, H. Bandukwala, D. M. Smith, and O. Veiseh, “Engineering the next generation of cell-based therapeutics,” *Nat Rev Drug Discov*, vol. 21, no. 9, p. 655, Sep. 2022, doi: 10.1038/S41573-022-00476-6.

[26] J. K. K. Mark, C. S. Y. Lim, F. Nordin, and G. J. Tye, “Expression of mammalian proteins for diagnostics and therapeutics: a review,” *Mol Biol Rep*, vol. 49, no. 11, p. 10593, Nov. 2022, doi: 10.1007/S11033-022-07651-3.

[27] H. Yang *et al.*, “Methods Favoring Homology-Directed Repair Choice in Response to CRISPR/Cas9 Induced-Double Strand Breaks,” *Int J Mol Sci*, vol. 21, no. 18, pp. 1–20, Sep. 2020, doi: 10.3390/IJMS21186461.

[28] L. Serrano *et al.*, “Homologous Recombination Conserves DNA Sequence Integrity Throughout the Cell Cycle in Embryonic Stem Cells,” *Stem Cells Dev*, vol. 20, no. 2, p. 363, Feb. 2010, doi: 10.1089/SCD.2010.0159.

[29] M. Parapouli, A. Vasileiadis, A. S. Afendra, and E. Hatziloukas, “Saccharomyces cerevisiae and its industrial applications,” *AIMS Microbiol*, vol. 6, no. 1, p. 1, 2020, doi: 10.3934/MICROBIOL.2020001.

[30] A. A. Duina, M. E. Miller, and J. B. Keeney, “Budding Yeast for Budding Geneticists: A Primer on the Saccharomyces cerevisiae Model System,” *Genetics*, vol. 197, no. 1, p. 33, 2014, doi: 10.1534/GENETICS.114.163188.

[31] G. C. Finnigan and J. Thorner, “Complex in vivo Ligation Using Homologous Recombination and High-efficiency Plasmid Rescue from Saccharomyces cerevisiae,” *Bio Protoc*, vol. 5, no. 13, p. e1521, 2015, doi: 10.21769/BIOPROTOC.1521.

[32] A. K. Löbs, C. Schwartz, and I. Wheeldon, “Genome and metabolic engineering in non-conventional yeasts: Current advances and applications,” *Synth Syst Biotechnol*, vol. 2, no. 3, pp. 198–207, Sep. 2017, doi: 10.1016/J.SYNBIO.2017.08.002.

[33] A. Goffeau *et al.*, “Life with 6000 genes,” *Science*, vol. 274, no. 5287, pp. 546–567, 1996, doi: 10.1126/SCIENCE.274.5287.546.

[34] M. G. Fraczek, S. Naseeb, and D. Delneri, “History of genome editing in yeast,” *Yeast*, vol. 35, no. 5, p. 361, May 2018, doi: 10.1002/YEA.3308.

[35] L. Vanderwaeren, R. Dok, K. Voordeckers, S. Nuyts, and K. J. Verstrepen, “Saccharomyces cerevisiae as a Model System for Eukaryotic Cell Biology, from Cell Cycle Control to DNA Damage Response,” *Int J Mol Sci*, vol. 23, no. 19, Oct. 2022, doi: 10.3390/IJMS231911665.

[36] M. Valencia-Burton, M. Oki, J. Johnson, T. A. Seier, R. Kamakaka, and J. E. Haber, “Different Mating-Type-Regulated Genes Affect the DNA Repair Defects of Saccharomyces RAD51, RAD52 and RAD55 Mutants,” *Genetics*, vol. 174, no. 1, pp. 41–55, Sep. 2006, doi: 10.1534/GENETICS.106.058685.

[37] J. E. Haber, “Mating-Type Genes and MAT Switching in Saccharomyces cerevisiae,” *Genetics*, vol. 191, no. 1, pp. 33–64, May 2012, doi: 10.1534/GENETICS.111.134577.

[38] S. J. Hanson and K. H. Wolfe, “An Evolutionary Perspective on Yeast Mating-Type Switching,” *Genetics*, vol. 206, no. 1, p. 9, May 2017, doi: 10.1534/GENETICS.117.202036.

[39] A. Brückner, C. Polge, N. Lentze, D. Auerbach, and U. Schlattner, “Yeast Two-Hybrid, a Powerful Tool for Systems Biology,” *Int J Mol Sci*, vol. 10, no. 6, p. 2763, Jun. 2009, doi: 10.3390/IJMS10062763.

[40] T. Stellberger, R. Häuser, P. Uetz, and A. Von Brunn, “Yeast Two-Hybrid Screens: Improvement of Array-Based Screening Results by N- and C-terminally Tagged Fusion Proteins,” *Functional Genomics*, vol. 815, p. 277, 2011, doi: 10.1007/978-1-61779-424-7_21.

[41] P. Uetz *et al.*, “A comprehensive analysis of protein-protein interactions in Saccharomyces cerevisiae,” *Nature*, vol. 403, no. 6770, pp. 623–627, Feb. 2000, doi: 10.1038/35001009.

[42] R. König *et al.*, “Global analysis of host-pathogen interactions that regulate early stage HIV-1 replication,” *Cell*, vol. 135, no. 1, p. 49, Oct. 2008, doi: 10.1016/J.CELL.2008.07.032.

[43] J. N. Conde, “Yeast Two-Hybrid System for Mapping Novel Dengue Protein Interactions,” *Methods Mol Biol*, vol. 2409, pp. 119–132, 2022, doi: 10.1007/978-1-0716-1879-0_9.

[44] Y. Zhou *et al.*, “A comprehensive SARS-CoV-2–human protein–protein interactome reveals COVID-19 pathobiology and potential host therapeutic targets,” *Nature Biotechnology 2022 41:1*, vol. 41, no. 1, pp. 128–139, Oct. 2022, doi: 10.1038/s41587-022-01474-0.

[45] J. Nielsen, “Yeast Systems Biology: Model Organism and Cell Factory,” *Biotechnol J*, vol. 14, no. 9, p. 1800421, Sep. 2019, doi: 10.1002/BIOT.201800421.

[46] Z. Liu, H. Moradi, S. Shi, and F. Darvishi, “Yeasts as microbial cell factories for sustainable production of biofuels,” *Renewable and Sustainable Energy Reviews*, vol. 143, p. 110907, Jun. 2021, doi: 10.1016/J.RSER.2021.110907.

[47] J. K. Ko and S. M. Lee, “Advances in cellulosic conversion to fuels: engineering yeasts for cellulosic bioethanol and biodiesel production,” *Curr Opin Biotechnol*, vol. 50, pp. 72–80, Apr. 2018, doi: 10.1016/J.COPBIO.2017.11.007.

[48] Z. Que *et al.*, “The powerful function of *Saccharomyces cerevisiae* in food science and other fields a critical review,” *Food Innovation and Advances 2024 2:*, vol. 3, no. 2, pp. 167–180, 2024, doi: 10.48130/FIA-0024-0016.

[49] G. L. Armstrong and S. T. Goldstein, “Hepatitis B: Global Epidemiology, Diagnosis, and Prevention,” *Immigrant Medicine: Text with CD-ROM*, pp. 321–341, Oct. 2007, doi: 10.1016/B978-0-323-03454-8.50026-7.

[50] S. Kalyoncu *et al.*, “Process development for an effective COVID-19 vaccine candidate harboring recombinant SARS-CoV-2 delta plus receptor binding domain produced by Pichia pastoris,” *Scientific Reports 2023 13:1*, vol. 13, no. 1, pp. 1–14, Mar. 2023, doi: 10.1038/s41598-023-32021-9.

[51] K. Malcl *et al.*, “Standardization of Synthetic Biology Tools and Assembly Methods for Saccharomyces cerevisiae and Emerging Yeast Species,” *ACS Synth Biol*, vol. 11, no. 8, pp. 2527–2547, Aug. 2022, doi: 10.1021/ACSSYNBIO.1C00442/ASSET/IMAGES/LARGE/SB1C00442_0011.JPEG.

[52] B. Alberts, A. Johnson, J. Lewis, M. Raff, K. Roberts, and P. Walter, *Isolating, Cloning, and Sequencing DNA*, 4th ed. Garland Science, 2002. Accessed: Apr. 22, 2025. [Online]. Available: https://www.ncbi.nlm.nih.gov/books/NBK26837/

[53] R. J. Roberts, “How restriction enzymes became the workhorses of molecular biology,” *Proc Natl Acad Sci U S A*, vol. 102, no. 17, pp. 5905–5908, Apr. 2005, doi: 10.1073/PNAS.0500923102/ASSET/B4C43D74-1725-42C2-9867-1F63232C3852/ASSETS/GRAPHIC/ZPQ0150578910004.JPEG.

[54] P. Rai and H. Arya, “Molecular cloning,” *The Design and Development of Novel Drugs and Vaccines: Principles and Protocols*, pp. 135–163, Jan. 2021, doi: 10.1016/B978-0-12-821471-8.00011-8.

[55] N. Khehra, I. S. Padda, and C. J. Swift, “Polymerase Chain Reaction (PCR),” *StatPearls*, Mar. 2023, Accessed: Apr. 22, 2025. [Online]. Available: https://www.ncbi.nlm.nih.gov/books/NBK589663/

[56] K. Kadri and K. Kadri, “Polymerase Chain Reaction (PCR): Principle and Applications,” *Synthetic Biology - New Interdisciplinary Science*, Jun. 2019, doi: 10.5772/INTECHOPEN.86491.

[57] A. E. Tomkinson and J. A. Della-Maria, “DNA Ligases: Mechanism and Functions,” *Encyclopedia of Biological Chemistry: Second Edition*, pp. 28–32, Feb. 2013, doi: 10.1016/B978-0-12-378630-2.00303-0.

[58] R. Chao, Y. Yuan, and H. Zhao, “Recent advances in DNA assembly technologies,” *FEMS Yeast Res*, vol. 15, no. 1, p. 1, 2015, doi: 10.1111/1567-1364.12171.

[59] R. P. Shetty, D. Endy, and T. F. Knight, “Engineering BioBrick vectors from BioBrick parts,” *J Biol Eng*, vol. 2, no. 1, pp. 1–12, Apr. 2008, doi: 10.1186/1754-1611-2-5/TABLES/4.

[60] C. Engler and S. Marillonnet, “Golden Gate cloning,” *Methods Mol Biol*, vol. 1116, pp. 119–131, 2014, doi: 10.1007/978-1-62703-764-8_9.

[61] N. B. Hansen, M. Lübeck, and P. S. Lübeck, “Advancing USER cloning into simpleUSER and nicking cloning,” *J Microbiol Methods*, vol. 96, no. 1, pp. 42–49, Jan. 2014, doi: 10.1016/J.MIMET.2013.10.018.

[62] M. D. Nelson and D. H. A. Fitch, “Overlap extension PCR: an efficient method for transgene construction,” *Methods Mol Biol*, vol. 772, pp. 459–470, 2011, doi: 10.1007/978-1-61779-228-1_27.

[63] A. Reynolds, V. Lundblad, D. Dorris, and M. Keaveney, “Yeast vectors and assays for expression of cloned genes,” *Curr Protoc Mol Biol*, vol. Chapter 13, no. 1, Jul. 2001, doi: 10.1002/0471142727.MB1306S39.

[64] A. J. van Brabant, W. L. Fangman, and B. J. Brewer, “Active Role of a Human Genomic Insert in Replication of a Yeast Artificial Chromosome,” *Mol Cell Biol*, vol. 19, no. 6, p. 4231, Jun. 1999, doi: 10.1128/MCB.19.6.4231.

[65] R. Gnügge and F. Rudolf, “Saccharomyces cerevisiae Shuttle vectors,” *Yeast*, vol. 34, no. 5, pp. 205–221, May 2017, doi: 10.1002/YEA.3228.

[66] N. A. Da Silva and S. Srikrishnan, “Introduction and expression of genes for metabolic engineering applications in Saccharomyces cerevisiae,” *FEMS Yeast Res*, vol. 12, no. 2, pp. 197–214, Mar. 2012, doi: 10.1111/J.1567-1364.2011.00769.X.

[67] V. Lundblad, “Yeast Cloning Vectors and Genes,” *Curr Protoc Mol Biol*, vol. 21, no. 1, pp. 13.4.1-13.4.10, Jan. 1993, doi: 10.1002/0471142727.MB1304S21.

[68] N. Kouprina and V. Larionov, “Exploiting the yeast Saccharomyces cerevisiae for the study of the organization and evolution of complex genomes,” *FEMS Microbiol Rev*, vol. 27, no. 5, pp. 629–649, Dec. 2003, doi: 10.1016/S0168-6445(03)00070-6.

[69] E. Weber, C. Engler, R. Gruetzner, S. Werner, and S. Marillonnet, “A Modular Cloning System for Standardized Assembly of Multigene Constructs,” *PLoS One*, vol. 6, no. 2, p. e16765, 2011, doi: 10.1371/JOURNAL.PONE.0016765.

[70] W. M. Shaw, A. S. Khalil, and T. Ellis, “A Multiplex MoClo Toolkit for Extensive and Flexible Engineering of Saccharomyces cerevisiae,” *ACS Synth Biol*, vol. 12, no. 11, pp. 3393–3405, Nov. 2023, doi: 10.1021/ACSSYNBIO.3C00423,.

[71] K. Malcl *et al.*, “ACtivE: Assembly and CRISPR-Targeted in Vivo Editing for Yeast Genome Engineering Using Minimum Reagents and Time,” *ACS Synth Biol*, vol. 11, no. 11, pp. 3629–3643, Nov. 2022, doi: 10.1021/ACSSYNBIO.2C00175/ASSET/IMAGES/LARGE/SB2C00175_0007.JPEG.

[72] L. A. Mitchell *et al.*, “Versatile genetic assembly system (VEGAS) to assemble pathways for expression in S. cerevisiae,” *Nucleic Acids Res*, vol. 43, no. 13, pp. 6620–6630, Apr. 2015, doi: 10.1093/NAR/GKV466,.

[73] M. D. Mikkelsen *et al.*, “Microbial production of indolylglucosinolate through engineering of a multi-gene pathway in a versatile yeast expression platform,” *Metab Eng*, vol. 14, no. 2, pp. 104–111, Mar. 2012, doi: 10.1016/j.ymben.2012.01.006.

[74] N. B. Jensen *et al.*, “EasyClone: Method for iterative chromosomal integration of multiple genes in Saccharomyces cerevisiae,” *FEMS Yeast Res*, vol. 14, no. 2, pp. 238–248, 2014, doi: 10.1111/1567-1364.12118,.

[75] V. Stovicek, G. M. Borja, J. Forster, and I. Borodina, “EasyClone 2.0: expanded toolkit of integrative vectors for stable gene expression in industrial Saccharomyces cerevisiae strains,” *J Ind Microbiol Biotechnol*, vol. 42, no. 11, p. 1519, Nov. 2015, doi: 10.1007/S10295-015-1684-8.

[76] M. M. Jessop-Fabre *et al.*, “EasyClone-MarkerFree: A vector toolkit for marker-less integration of genes into Saccharomyces cerevisiae via CRISPR-Cas9,” *Biotechnol J*, vol. 11, no. 8, pp. 1110–1117, Aug. 2016, doi: 10.1002/BIOT.201600147,.

[77] N. Milne, L. R. R. Tramontin, and I. Borodina, “A teaching protocol demonstrating the use of EasyClone and CRISPR/Cas9 for metabolic engineering of Saccharomyces cerevisiae and Yarrowia lipolytica,” *FEMS Yeast Res*, vol. 20, no. 2, p. 62, Mar. 2020, doi: 10.1093/FEMSYR/FOZ062.

[78] T. Strucko, “Synthetic yeast based cell factories for vanillin-glucoside production,” 2013, *Department of Systems Biology, Technical University of Denmark*. Accessed: Apr. 27, 2025. [Online]. Available: https://orbit.dtu.dk/en/publications/synthetic-yeast-based-cell-factories-for-vanillin-glucoside-produ

[79] C. H. Liu, J. H. Chang, Y. C. Chang, and K. Y. Mou, “Treatment of murine colitis by Saccharomyces boulardii secreting atrial natriuretic peptide,” *J Mol Med*, vol. 98, no. 12, pp. 1675–1687, Dec. 2020, doi: 10.1007/S00109-020-01987-8/FIGURES/6.

[80] “Canada’s first Genome Foundry is using robots to build synthetic genomes - Concordia University.” Accessed: Apr. 27, 2025. [Online]. Available: https://www.concordia.ca/news/stories/2018/08/06/canadas-first-genome-foundry-is-using-robots-to-build-synthetic-genomes.html

[81] B. D. M. Bean, M. Whiteway, and V. J. J. Martin, “The MyLO CRISPR-Cas9 toolkit: a markerless yeast localization and overexpression CRISPR-Cas9 toolkit,” *G3: Genes|Genomes|Genetics*, vol. 12, no. 8, p. jkac154, Aug. 2022, doi: 10.1093/G3JOURNAL/JKAC154.

[82] Z. Shao, H. Zhao, and H. Zhao, “DNA assembler, an in vivo genetic method for rapid construction of biochemical pathways,” *Nucleic Acids Res*, vol. 37, no. 2, p. e16, 2008, doi: 10.1093/NAR/GKN991.

[83] C. Janke *et al.*, “A versatile toolbox for PCR-based tagging of yeast genes: New fluorescent proteins, more markers and promoter substitution cassettes,” *Yeast*, vol. 21, no. 11, pp. 947–962, Aug. 2004, doi: 10.1002/YEA.1142,.

[84] S. bing Hua, M. Qiu, E. Chan, L. Zhu, and Y. Luo, “Minimum length of sequence homology required for in vivo cloning by homologous recombination in yeast,” *Plasmid*, vol. 38, no. 2, pp. 91–96, 1997, doi: 10.1006/plas.1997.1305.

[85] D. G. Gibson, “Synthesis of DNA fragments in yeast by one-step assembly of overlapping oligonucleotides,” *Nucleic Acids Res*, vol. 37, no. 20, pp. 6984–6990, Nov. 2009, doi: 10.1093/NAR/GKP687.

[86] T. Amen and D. Kaganovich, “Integrative modules for efficient genome engineering in yeast,” vol. 4, no. 6, doi: 10.15698/mic2017.06.576.

[87] S. M. Sankaran, J. D. Smith, and K. R. Roy, “CRISPR-Cas9 Gene Editing in Yeast: A Molecular Biology and Bioinformatics Laboratory Module for Undergraduate and High School Students,” *J Microbiol Biol Educ*, vol. 22, no. 2, Sep. 2021, doi: 10.1128/JMBE.00106-21.

[88] K. A. Curran, A. S. Karim, A. Gupta, and H. S. Alper, “Use of expression-enhancing terminators in Saccharomyces cerevisiae to increase mRNA half-life and improve gene expression control for metabolic engineering applications,” *Metab Eng*, vol. 19, pp. 88–97, Sep. 2013, doi: 10.1016/J.YMBEN.2013.07.001.

[89] Y. Chen, S. Zhang, E. M. Young, T. S. Jones, D. Densmore, and C. A. Voigt, “Genetic circuit design automation for yeast,” *Nature Microbiology 2020 5:11*, vol. 5, no. 11, pp. 1349–1360, Aug. 2020, doi: 10.1038/s41564-020-0757-2.

[90] D. G. Gibson, L. Young, R. Y. Chuang, J. C. Venter, C. A. Hutchison, and H. O. Smith, “Enzymatic assembly of DNA molecules up to several hundred kilobases,” *Nat Methods*, vol. 6, no. 5, pp. 343–345, 2009, doi: 10.1038/NMETH.1318,.

[91] “ADE2 | SGD.” Accessed: May 11, 2025. [Online]. Available: https://www.yeastgenome.org/locus/ade2

[92] P. D. Hsu *et al.*, “DNA targeting specificity of RNA-guided Cas9 nucleases,” *Nat Biotechnol*, vol. 31, no. 9, pp. 827–832, Sep. 2013, doi: 10.1038/NBT.2647;SUBJMETA=338,552,61,631;KWRD=SYNTHETIC+BIOLOGY.

[93] “Phusion Flash High-Fidelity PCR Master Mix.” Accessed: May 11, 2025. [Online]. Available: https://www.thermofisher.com/order/catalog/product/F548L

[94] G. Assembly, “INSTRUCTION MANUAL”, Accessed: May 11, 2025. [Online]. Available: http://www.neb.com/TmCalculator.

[95] “NEBuilder.” Accessed: May 11, 2025. [Online]. Available: https://nebuilder.neb.com/#!/

[96] “NEBioCalculator.” Accessed: May 11, 2025. [Online]. Available: https://nebiocalculator.neb.com/#!/ligation

[97] “Genome Editing and Molecular biology (GEM) Facility - GEM | Faculty of Medicine.” Accessed: May 11, 2025. [Online]. Available: https://www.uottawa.ca/faculty-medicine/core-facilities/gem

[98] A. Froger and J. E. Hall, “Transformation of Plasmid DNA into E. coli Using the Heat Shock Method,” *J Vis Exp*, no. 6, p. 253, Jul. 2007, doi: 10.3791/253.

[99] A. Y. Chang, V. W. Chau, J. A. Landas, and Yvonne, “Preparation of calcium competent Escherichia coli and heat-shock transformation,” vol. 1, 2017.

[100] “Restriction Endonucleases - Survival in a Reaction | NEB.” Accessed: May 11, 2025. [Online]. Available: https://www.neb.com/en-ca/tools-and-resources/usage-guidelines/restriction-endonucleases-survival-in-a-reaction

[101] Alison. Adams and Chris. Kaiser, “Methods in yeast genetics : a Cold Spring Harbor Laboratory course manual,” p. 177, 1998.

[102] “BY4741 | SGD.” Accessed: May 22, 2025. [Online]. Available: https://www.yeastgenome.org/strain/by4741

[103] “YPD media,” *Cold Spring Harb Protoc*, vol. 2010, no. 9, p. pdb.rec12315, Sep. 2010, doi: 10.1101/PDB.REC12315.

[104] S.-A. Corp, “Yeast Synthetic Drop-out Media Supplements - Datasheet”, Accessed: May 12, 2025. [Online]. Available: www.sigmaaldrich.com

[105] “NEBuilder® HiFi DNA Assembly Reaction Protocol (NEB #E2621, #E5520, #E2623) | NEB.” Accessed: May 12, 2025. [Online]. Available: https://www.neb.com/en-ca/protocols/2014/11/26/nebuilder-hifi-dna-assembly-reaction-protocol

[106] J. Schindelin *et al.*, “Fiji: An open-source platform for biological-image analysis,” *Nat Methods*, vol. 9, no. 7, pp. 676–682, Jul. 2012, doi: 10.1038/NMETH.2019;SUBJMETA=1647,245,631,794;KWRD=IMAGING,SOFTWARE.

[107] “how to calculate transformation efficiency.” Accessed: May 16, 2025. [Online]. Available: https://www.edvotek.com/how-to-calculate-transformation-efficiency?srsltid=AfmBOooyR9XnIf313qDufdZf1GHMQ1xDI1PmxIV8MLSiBN3Wed9Eq4A_

[108] J. Shreffler and M. R. Huecker, “Diagnostic Testing Accuracy: Sensitivity, Specificity, Predictive Values and Likelihood Ratios,” *StatPearls*, Mar. 2023, Accessed: May 12, 2025. [Online]. Available: https://www.ncbi.nlm.nih.gov/books/NBK557491/

[109] H. Pereira, P. Cé sar Silva, and B. rn Johansson, “Chapter 17 Bacteria and Yeast Colony PCR”, doi: 10.1007/978-1-0716-3358-8_17.

[110] T. L. Orr-Weaver, J. W. Szostak, and R. J. Rothstein, “Yeast transformation: A model system for the study of recombination,” *Proc Natl Acad Sci U S A*, vol. 78, no. 10 I, pp. 6354–6358, 1981, doi: 10.1073/PNAS.78.10.6354,.

[111] P. D. Hsu, E. S. Lander, and F. Zhang, “Development and applications of CRISPR-Cas9 for genome engineering,” *Cell*, vol. 157, no. 6, pp. 1262–1278, Jun. 2014, doi: 10.1016/j.cell.2014.05.010.

[112] F. David and V. Siewers, “Advances in yeast genome engineering,” *FEMS Yeast Res*, vol. 15, no. 1, pp. 1–14, Feb. 2015, doi: 10.1111/1567-1364.12200.

[113] J. C. Samuelson, Z. Zhu, and S. Y. Xu, “The isolation of strand-specific nicking endonucleases from a randomized SapI expression library,” *Nucleic Acids Res*, vol. 32, no. 12, p. 3661, 2004, doi: 10.1093/NAR/GKH674.

[114] “SapI | NEB.” Accessed: May 17, 2025. [Online]. Available: https://www.neb.com/en-ca/products/r0569-sapi?srsltid=AfmBOorjDe8fxrHdAAub3upQycZkwtZr2kpLaHMss31ayrtyEmLL9xwL

[115] X. Ni, Z. Liu, J. Guo, and G. Zhang, “Development of Terminator–Promoter Bifunctional Elements for Application in Saccharomyces cerevisiae Pathway Engineering,” *Int J Mol Sci*, vol. 24, no. 12, p. 9870, Jun. 2023, doi: 10.3390/IJMS24129870/S1.

[116] N. Uwimana, P. Collin, C. Jeronimo, B. Haibe-Kains, and F. Robert, “Bidirectional terminators in Saccharomyces cerevisiae prevent cryptic transcription from invading neighboring genes,” *Nucleic Acids Res*, vol. 45, no. 11, pp. 6417–6426, Jun. 2017, doi: 10.1093/NAR/GKX242,.

[117] M. MacPherson and Y. Saka, “Short synthetic terminators for assembly of transcription units in vitro and stable chromosomal integration in Yeast S. Cerevisiae,” *ACS Synth Biol*, vol. 6, no. 1, pp. 130–138, Jan. 2017, doi: 10.1021/ACSSYNBIO.6B00165,.

[118] C. Voisset, N. García-Rodríguez, A. Birkmire, M. Blondel, and R. E. Wellinger, “Using yeast to model calcium-related diseases: Example of the Hailey–Hailey disease,” *Biochimica et Biophysica Acta (BBA) - Molecular Cell Research*, vol. 1843, no. 10, pp. 2315–2321, Oct. 2014, doi: 10.1016/J.BBAMCR.2014.02.011.